Spring 2024

Exploring Subtype C HIV-1 Tissue Reservoirs and the Impact of Cannabis Use in Virally Suppressed African Individuals

Zhou Liu
University of Nebraska-Lincoln

EXPLORING SUBTYPE C HIV-1 TISSUE RESERVOIRS AND THE IMPACT OF CANNABIS USE IN VIRALLY SUPPRESSED AFRICAN INDIVIDUALS

by

Zhou Liu

A DISSERTATION

Presented to the Faculty of

The Graduate College at the University of Nebraska

In Partial Fulfillment of Requirements

For the Degree of Doctor of Philosophy

Major: Biological Sciences

(Genetics, Cellular, and Molecular Biology)

Under the Supervision of Professors Charles Wood and Peter Angeletti

Lincoln, Nebraska

May, 2024

EXPLORING SUBTYPE C HIV-1 TISSUE RESERVOIRS AND THE IMPACT OF CANNABIS USE IN VIRALLY SUPPRESSED AFRICAN INDIVIDUALS

Zhou Liu, Ph.D.

University of Nebraska, 2024

Advisors: Charles Wood, Peter Angeletti

Antiretroviral therapy (ART) has dramatically prolonged the lives of people living with HIV (PLWH), but it is not curative as it cannot eliminate integrated HIV-1 proviruses in different tissue reservoirs. Even though subtype C HIV-1 accounts for almost half of global HIV-1 infections, few studies had evaluated HIV-1 reservoirs for this subtype. Many co-factors, including the lifestyle factor cannabis use, have been investigated for their potential effects in HIV-1 infection. However, only limited information exists regarding cannabis's effects on HIV-1 infections *in vivo*, and the impact of cannabis use on HIV-1 parenchymal tissue reservoirs is unexplored. This dissertation aims to deepen our understanding of subtype C HIV-1, which is predominant in resource-limited settings and presents unique challenges in management and treatment. Specifically, it explores the landscape of subtype C HIV-1 tissue reservoirs, particularly identifying the human appendix as a novel reservoir, and assessed the effects of cannabis use on these reservoirs.

To map the distribution of subtype C HIV-1 tissue reservoirs, we conducted systematically sample collections from autopsies in Zambia, sub-Saharan Africa (SSA), and employed advanced molecular techniques to map the distribution and viral burden of subtype C HIV-1 within different tissue compartments. We discovered significant viral persistence in the lymphoid and gastrointestinal (GI) tract tissues, but unlike well-

documented subtype B HIV-1, subtype C HIV-1 poorly accessed the brain. Interestingly, subtype C proviruses were readily detected in the appendix, a previously unrecognized tissue reservoir. This finding suggests that the appendix may play a crucial role in the long-term persistence of HIV-1, challenging existing paradigms of reservoir locations.

To evaluate the impact of cannabis use on subtype C HIV-1 tissue reservoirs, we analyzed viral load and immune modulation, via analyses of inflammatory cytokine mRNA expression in cannabis-using and non-using individuals. Results demonstrated that cannabis use is associated with a reduced size of viral reservoirs and altered inflammatory responses, indicating potential therapeutic implications in exploiting lifestyle factors in managing HIV-1.

Overall, this dissertation provides critical insights into the unique characteristics of subtype C HIV-1 reservoirs and the modulatory effects of cannabis. These findings not only contribute to the field of HIV research by identifying new targets for potential eradication strategies but also highlight the importance of considering behavioral factors in the clinical management of HIV. The research underscores the need for a comprehensive approach that includes both molecular characterization of HIV reservoirs and evaluation of lifestyle influences on disease dynamics.

ACKNOWLEDGEMENTS

First and foremost, I would like to extend my deepest gratitude to all the participants of this study and their families, whose generosity has been the cornerstone of this research's success. I am also profoundly thankful for all our project collaborators in Lusaka, Zambia, for their diligent work. Furthermore, I owe special thanks to each member of my committee: Dr. Charles Wood, Dr. Peter Angeletti, Dr. Matthew Wiebe, Dr. Eric Weaver, and Dr. David Steffen, who has provided unwavering support and assistance at every stage of my project.

I am sincerely grateful to my advisor Dr. Wood, and to Dr. West. I consider myself fortunate to have been guided by these two distinguished professors whose scientific guidance has helped shape me into a more competent researcher. I also want to express my appreciation to both past and present members of our lab, especially Guobin Kang, Sara Privatt, Sydney Bennett, Danielle Shea, Dicle Yalcin, and For Yue, for their support and companionship throughout this journey.

Additionally, I am immensely thankful to Dr. Xiaohong Kong for her ongoing concern and valuable career advice. I am also very grateful to Cathy Wood for her care and support, especially when I first came in the United States as an international student.

Lastly, I wish to thank my friends for their support. A special thank you goes to my parents and parents-in-law for their selfless love and care, which have been my enduring source of motivation. Finally, the last thank you is reserved for my wife, Xiaowen, whom I am lucky to have as my life-time partner. Her love, support, and sacrifices have been indispensable to my success.

PREFACE

Chapter 2 of this dissertation research has been published in *JCI Insight* (Liu, et al, "Subtype C HIV-1 reservoirs throughout the body in ART-suppressed individuals" (Published in *JCI Insight*, Oct, 2022).)

Chapter 3 of this dissertation research has been submitted for publication *Journal of the International of AIDS Society* (Liu, et al, "Cellular tropism and viral genetics in appendix tissue reservoirs of subtype C HIV-1 infected aviremic individuals" (Submitted for publication in *JIAS*, Apr, 2024).)

Chapter 4 of this dissertation research has been submitted for publication in *Journal of NeuroVirology* (Liu, et al, "Limited HIV-associated neuropathologies and lack of immune activation in sub-Saharan African individuals with late-stage subtype C HIV-1 infection" (Submitted for publication in *Journal of NeuroVirology*, Mar, 2024).)

Chapter 5 of this dissertation research has been published in *The Journal of Infectious Diseases* (Liu, et al, "Cannabis use associates with reduced proviral burden and inflammatory cytokine expression in tissues from men with clade C HIV-1 on suppressive ART" (Published in *JID*, Jan, 2024).)

In this project, Zhou Liu performed experiments, analyzed the data, achieved data visualization, and wrote the manuscripts. Peter Julius led sample collection and contributed methodology. Victor Mudenda, Cordilia Maria Himwaze and Luchenga

Adam Mucheleng'anga aided with tissue collection and processing and obtaining clinical information. Guobin Kang helped conduct histological and immunological staining. Dicle Yalcin performed phylogenetic analysis. Luis Del Valle provided pathology expertise in chapters 3 and 4. Andrew G. Chapple performed statistical analysis in chapter 5. John T. West supported methodology, data analysis, and manuscript editing. Charles Wood conceived of and led the study, obtained funding, and managed project administration.

TABLE OF CONTENTS

LIST OF TABLES AND FIGURES

CHAPTER 1:

LITERATURE REVIEW

Human Immunodeficiency Virus (HIV)

Precursors to the pandemic

While the exact date of the first case showing symptoms of what would later be defined as human immunodeficiency virus (HIV) infection is difficult to determine retrospectively, the earliest known case of HIV infection was identified from an archival blood sample taken in 1959 from a man in Kinshasa, Democratic Republic of Congo (Zaire) (1). However, it was not until the early 1980s that the medical community recognized a pattern of symptoms associated with a new immunodeficiency syndrome predominantly in the homosexual male population. In a Morbidity and Mortality Weekly Report (MMWR) published on June 5, 1981, the Centers for Disease Control and Prevention (CDC) in the United States described five cases of rare *Pneumocystis carinii* pneumonia (PCP) among previously healthy young men in Los Angeles (2). All those men were described as homosexuals, and two had died by the time of the report. Shortly after the initial MMWR report, a series of cases of an unusually aggressive Kaposi's sarcoma (KS) among homosexual men in New York and California were reported (3). Subsequent reports expanded the recognition of the disease among other populations, including intravenous drug users and transfusion recipients (4). These initial cases were characterized by severe immunodeficiency, which would later be named acquired immunodeficiency syndrome (AIDS), characterized with opportunistic infections and cancers that were otherwise uncommon.

HIV discovery and pandemic

In 1983, Dr. Luc Montagnier et al. at the Pasteur Institute in France isolated a virus from a patient with signs of AIDS, which they named Lymphadenopathy-Associated Virus (LAV) (5). In 1984, Dr. Robert Gallo's team at the National Cancer Institute (NCI) in the United States announced that they had also isolated a virus from AIDS patients, which they named Human T-lymphotropic Virus Type III (HTLV-III) (6-9). Subsequent research confirmed that LAV and HTLV-III were the same virus. In 1986, the International Committee on Taxonomy of Viruses (ICTV) officially named the virus human immunodeficiency virus (HIV) (10).

HIV is an enveloped spherical virus of about 90 nm in diameter, and it is a member of the family Retroviridae and genus Lentivirus. HIV contains a diploid positive-sense single strand (ss)RNA genome surrounded by a capsid and a lipid envelope (11). Since its discovery, HIV has infected more than 90 million people worldwide (The Joint United Nations Programme on HIV/AIDS; UNAIDS) and claimed around 40 million lives (The World Health Organization; WHO), making it one of the most long-lasting and devastating pandemics in human history (12). The early years of the epidemic saw rapid spread and high mortality rates, primarily due to the lack of observance of protected sex practices, ineffective treatments and the profound impact of untreated HIV on the immune system. As of the end of 2023, approximately 39.0 million people were living with HIV worldwide (UNAIDS), with sub-Saharan Africa (SSA) harboring over two-thirds of global infections (13, 14).

Potential origin of HIV

There are two known strains of HIV, HIV-1 and HIV-2. HIV-1 is the most predominate worldwide and accounts for 95% of all HIV infection globally (15), and is believed to have originated from the simian immunodeficiency virus (SIV) found in chimpanzees (*Pan troglodytes troglodytes*), specifically SIVcpz (16, 17). This cross-species transmission event likely happened in Central Africa, with genetic studies suggesting multiple independent transmissions from SIVcpz to humans, leading to several groups of HIV-1, including the main (M), outlier (O), non-M, non-O (N), and pending confirmation (P) groups, with group M being responsible for the global HIV/AIDS pandemic (18, 19). In contrast, HIV-2 is closely related to SIVsmm, a virus found in sooty mangabey monkeys (*Cercocebus atys*). HIV-2 is thought to have crossed over to humans from sooty mangabey monkeys in West Africa (16, 17). There have been at least eight distinct cross-species transmission events from sooty mangabeys to humans, leading to the different groups of HIV-2 (A through H) (20). HIV-2 is primarily found in West Africa and in communities with links to West Africa (e.g., in Portugal and France due to colonial ties) (21, 22). Compared to HIV-1, HIV-2 is less pathogenic, progresses to AIDS more slowly, and is less transmissible (23).

The primary theory for the cross-species transmission of SIV to humans (resulting in HIV) involves the hunting and consumption of bushmeat (16, 17). Chimpanzees and sooty mangabey monkeys, both of which can be infected with SIV, have long been hunted for food in certain parts of Africa. It is hypothesized that SIV could have crossed into humans as a result of cuts or wounds that occurred during the hunting or butchering process, allowing the virus to transmit to humans. Based on molecular clock analyses of

HIV genetic sequences, scientists estimate that HIV-1 group M, crossed into humans in the early 20th century, likely between 1910 and 1930 (24, 25). Similarly, HIV-2 is thought to have crossed into humans in a separate event or events, also believed to have occurred in the 20th century (17). After SIV was introduced into humans and became HIV, the virus began to spread, evolve, and diversify, leading to the various geographically segregated subtypes and strains observed today. The spread of HIV was likely facilitated by factors such as urbanization, increased travel, and social contacts, which allowed the virus to spread beyond rural areas into larger more centralized and globally connected populations.

HIV-1 subtypes

Because HIV was first isolated when molecular biological and nucleic acid sequencing techniques were available, it has been characterized genetically as opposed to serologically, as for many preceding viral organisms. Genetic diversification within group M has led to the segregation of HIV-1 genotypes into multiple subtypes and circulating recombinant forms (CRFs). The HIV-1 subtypes exhibit distinct geographic distribution patterns consistent with variations in the viral genome sequences (**Figure 1.1**) (26). The HIV-1 *env* gene sequences that encode envelope protein can vary by up to 35% across subtypes (26). The genetic variation among these subtypes is a reflection of the rapid replication cycle and high mutation rate of HIV-1, which contributes to its ability to evade the host immune response, develop antiretroviral drugs resistance, and maintain the HIV-1 reservoirs. There are subtypes A, B, C, D, F, G, H, J, and K, with numerous CRFs arising from recombination events between these subtypes (27).

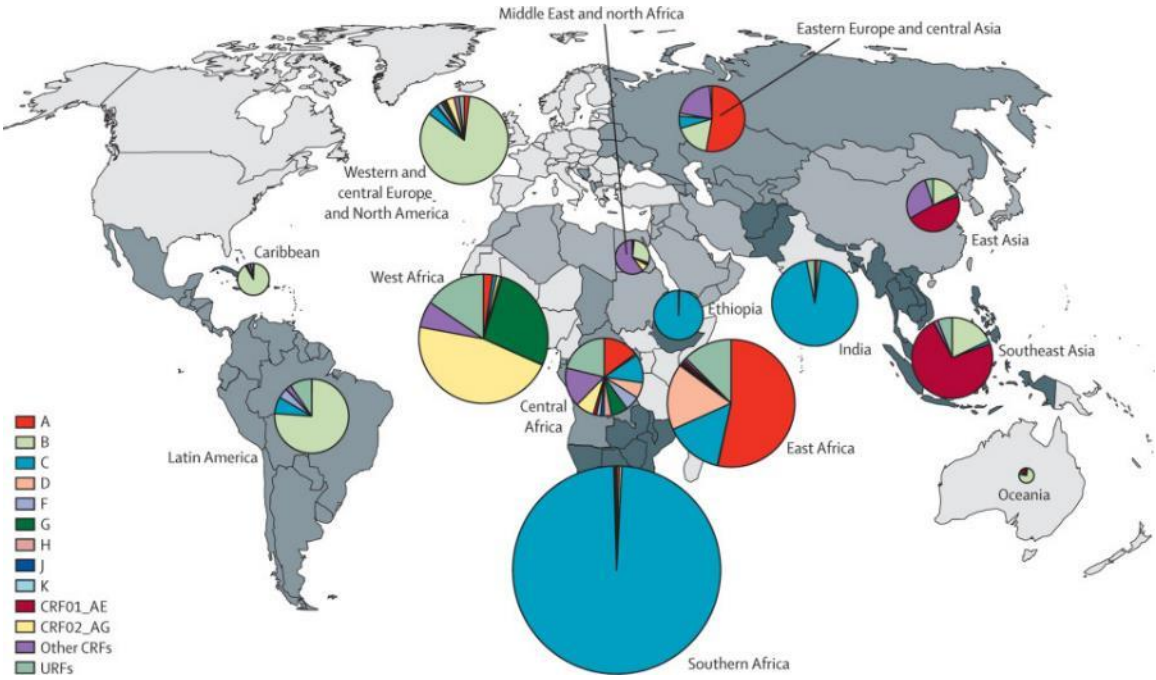

Figure 1.1. Figure from Hemelaar, et al. (26). Global and regional prevalences of different HIV-1 subtypes.

Among different subtypes, HIV-1 subtype B accounts for approximately 12% of HIV infections globally, and it is the most prevalent subtype in North America, Europe, Oceania, and parts of East Asia (26). Because of infection in resource-rich areas, research and development of HIV diagnostic tools, treatments, and vaccines have predominantly focused on subtype B. This focus has provided a deep understanding of virology, pathogenesis, and treatment response of subtype B HIV-1 but has, to date, not provided a prophylactic vaccine or curative treatment.

In contrast, subtype C is the most prevalent HIV subtype and is responsible for about 50% of all HIV infections worldwide. It is especially dominant in resource-limited regions such as sub-Saharan Africa, India, and parts of South America, where it drives local epidemics (26). Despite its global impact, less attention has been given to subtype C in terms of research compared to subtype B. The predominance of subtype C in regions

with constrained healthcare resources and infrastructure is still posing significant challenges in managing the HIV/AIDS epidemic.

As the third most widespread subtype, HIV-1 subtype A accounts for about 10% of all HIV-1 infection, and is notably common in Eastern Europe, Central Asia, and East Africa, demonstrating a wide but specific geographical spread (26). Other HIV-1 subtypes, such as D, F, G, H, J, and K, have more localized distributions. Subtype D is primarily found in East and Central Africa, while F and G are seen in Eastern Europe, South America, and West Africa respectively (26). The distribution of these subtypes underscores early epidemic 'founder effects' and the complex epidemiological landscape of HIV-1.

HIV-1 genome structure

The genome of HIV-1, like that of other retroviruses, is compact and efficiently organized, enabling the virus to encode multiple proteins from a ~10Kb genome. The HIV-1 genome is composed of two identical positive-sense, single-stranded RNA, each approximately 9,700 nucleotides long. Upon entering a host cell, this RNA is reverse-transcribed into double-stranded complementary cDNA, which then inserts into the host's genome through the action of the HIV-1 integrase (IN). This integrated viral DNA is called a provirus. The HIV-1 proviral genome consists of 9 genes; 3 structural genes encoding polyproteins (*gag*, *pol*, *env*) and 6 regulatory genes (*tat*, *rev*, *vif*, *vpr*, *vpu*, and *nef*), all of which are flanked by long terminal repeats (LTRs) (**Figure 1.2**) (28).

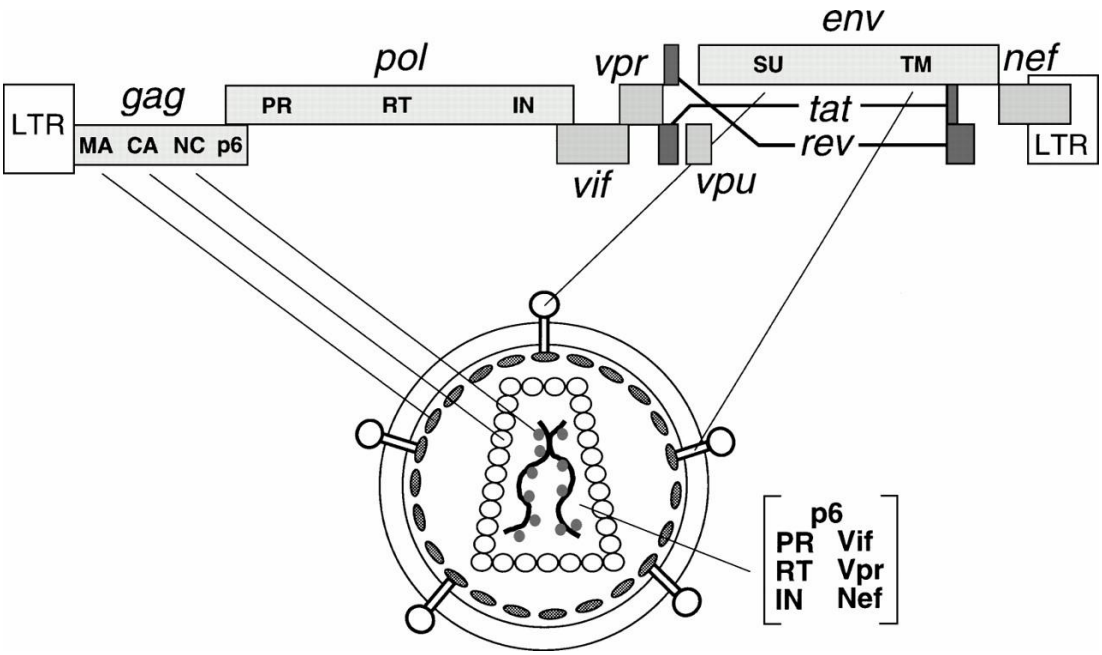

Figure 1.2. Figure from Frankel, et el. (28). HIV-1 genome and encoded viral proteins.

The 5' LTR acts as a promoter and contains cis-regulatory elements that are recognized by both constitutive transcription factors such as Sp1 (specificity protein 1) and Oct-1 (o-binding protein 1) and inducible transcription factors such as NF-κB (nuclear factor-kappa B), AP-1 (activator protein 1), and NFAT (nuclear factor of activated T-cells) that are essential for the transcription of the viral genome. This region includes the U3, R, and U5 regions, with U3 containing promoter and enhancer elements that initiate the transcription process (29). The R region contains the primary binding sites for RNA polymerase II, which is necessary for the initiation of transcription of the viral RNA (**Figure 1.3**). The 3' LTR also contains U3, R, and U5 sections and is essential for terminating transcription and polyadenylation of viral RNA transcripts (30). The 3'LTR contains signals necessary for the proper termination of transcription and the addition of a poly(A) tail to the newly synthesized viral RNA transcripts. This poly(A)

tail is crucial for the export of the mRNA from the nucleus to the cytoplasm and for its stability and translation in the cytoplasm (31, 32).

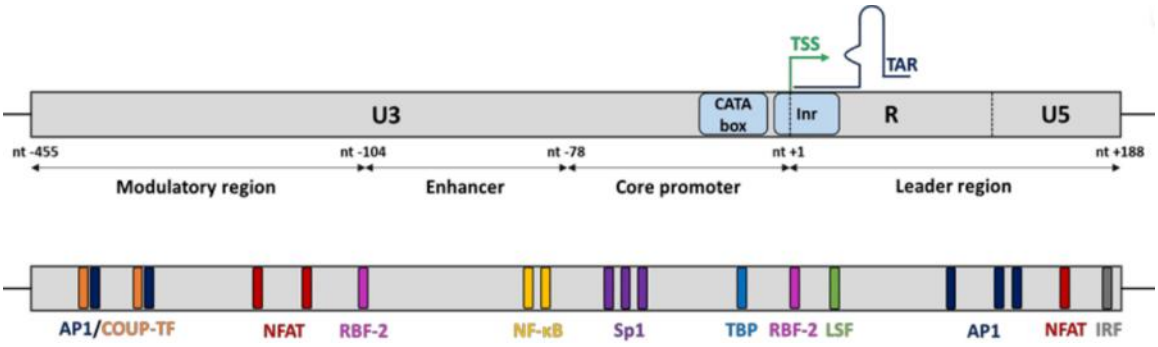

Figure 1.3. Figure from Dutilleul et al (33). The structure of HIV-1 5' LTR.

The *gag* gene encodes a structural polyprotein that is the precursor for the matrix (MA; p17), capsid (CA; p24), nucleocapsid (NC; p7) proteins, and p6 proteins. These proteins are crucial for virus assembly and upon HIV protease (PR) activation, and formation of the mature viral core (34). After the *gag* reading frame, the *pol* gene encodes the viral enzymes protease (PR), reverse transcriptase (RT), RNase H, and integrase (IN). These enzymes are critical for viral replication. The RT synthesizes a complementary DNA copy of the viral RNA genome while RNase H simultaneously digests RNA , but only in hybrid RNA-DNA intermediates produced during reverse transcription, IN integrates double-stranded viral cDNA into the host genome, and PR processes the Gag, and Gag-PR-Pol polyproteins into their mature forms (35). The *env* gene encodes the envelope (Env) glycoprotein precursor gp160 that oligomerizes to a trimer in the ER and is cleaved in the *trans* Golgi to produce gp120 and gp41, the proteins responsible for virus entry into host cells. Gp120 is involved in binding to the CD4 receptor and a co-receptor CCR5 or CXCR4 on the host cell, while gp41 is involved in the fusion of the viral and cellular membranes (36).

HIV-1 regulatory genes encode proteins that modulate various aspects of the viral life cycle and the host immune response. For instance, the trans-activator of transcription (Tat) protein, encoded by the *tat* gene, is a multifunctional protein that plays a pivotal role in the regulation of HIV-1 transcription elongation and the modulation of the host cellular environment, whereas the Rev protein (encoded by *rev*) regulates the export of unspliced and singly-spliced viral mRNA from the nucleus to the cytoplasm (37). Vif (encoded by *vif*) counters the antiviral activity of host factors such as APOBEC3G (38), Vpu (encoded by *vpu*) enhances virus release from the cell (39), Vpr (encoded by *vpr*) affects nuclear import of the viral genome (40), and Nef (encoded by *nef*) modulates several host cell functions, such as downregulation of CD4 and MHC class I to enable HIV-1 immune escape (41).

HIV-1 Life Cycle

Viral entry

The outermost layer of the virus is the highly glycosylated viral envelope, a lipid bilayer derived from the host cell membrane during viral budding. Embedded in this envelope are viral glycoproteins gp120 and gp41. The initial step of infection involves the interaction of gp120 with the CD4 receptor on the surface of target cells, typically CD4+ T lymphocytes. Upon binding to CD4, gp120 undergoes a conformational change that facilitates its interaction with a coreceptor, either CCR5 or CXCR4. This interaction triggers gp41-mediated fusion of the viral envelope with the cell membrane, allowing the viral capsid to enter the cytoplasm (**Figure 1.4**) (42).

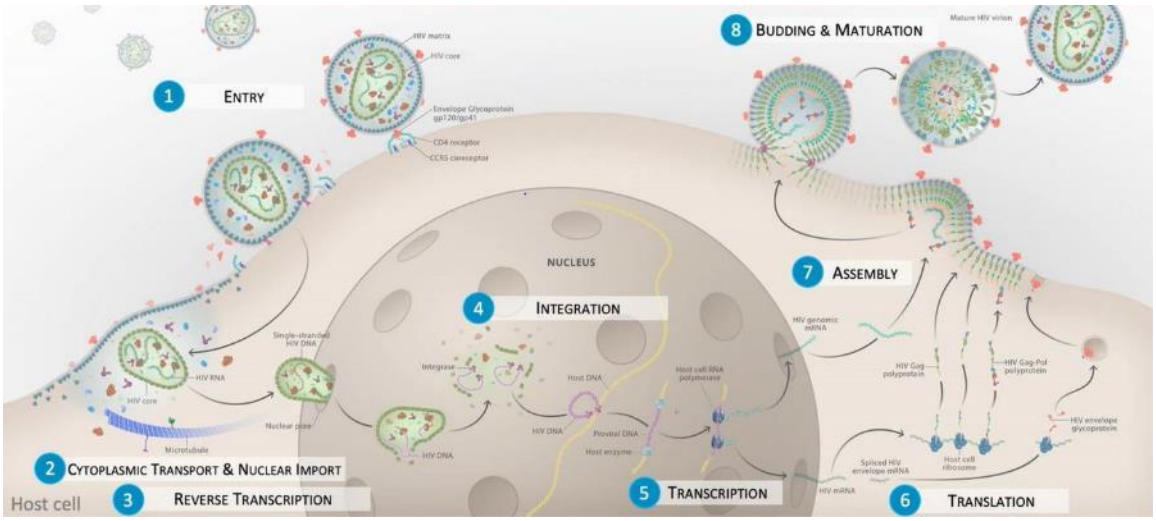

Figure 1.4. Figure from Spach, et al. (42). HIV-1 life cycle.

Reverse transcription and nuclear import

After fusion of the viral and host cell membranes, the conical capsid, containing the viral RNA and RT/RNase H/IN, is released into the cytoplasm. In the cytoplasm, the viral RNA genome starts to be reverse transcribed into DNA by the viral enzyme RT, using host deoxynucleoside triphosphates (dNTPs) and a host tRNA as a primer (43). The viral RT lacks proofreading capabilities, leading to a high mutation rate during reverse transcription. As a result, the DNA copies of the viral genome often contain mutations, deletions, or insertions, that contribute to the genetic diversity of HIV (44).

Concomitant with reverse transcription, the capsid is transported towards the nucleus via the host's microtubule network, (45, 46), a process thought to be mediated by interactions with motor proteins such as dynein (47, 48). This movement is essential for HIV capsid to reach the nuclear pore, where it can enter the nucleus. Recent research has illuminated the sophisticated mechanism by which the HIV capsid interacts with the nuclear pore complex (NPC), resembling the behavior of a transport receptor (49, 50).

Upon reaching the nuclear envelope, the capsid exploits the cellular machinery typically used for the nuclear import of macromolecules but does so without the need for host transport receptors. After entering the nucleus, the capsid undergoes a process known as uncoating, where the capsid protein shell disassembles. The reverse transcription step is then completed in the host nuclear (51).

Integration

The assembly of pre-integration complex (PIC) is a prerequisite for the integration of the newly synthesized viral DNA into the host genome. The PIC consists of the newly formed viral double-stranded cDNA, viral proteins including integrase, and several host proteins, such as lens epithelium-derived growth factor p75 (LEDGF/p75) (52). Following nuclear import, integrases catalyze a series of reactions that covalently insert viral DNA into the host's chromosomal DNA. The integration of the viral DNA into the host genome is a hallmark of retroviral infection and a pivotal moment in the HIV-1 life cycle. The integrated viral DNA is also known as a provirus. Integration results in a permanent genomic alteration of the host cell, enabling the virus to hijack the cellular machinery for its replication and production of new viral particles. The stability and transcriptional activity of the integrated provirus could be influenced by the HIV-1 integration site within the host genome. The integration site within the host genome is somewhat random, which can affect the efficiency of viral gene expression. Integration into transcriptionally active regions would slow down the decay of the integrated HIV-1 in tissue reservoirs due to ongoing low-level viral replication (53). It would also facilitate the transcription of viral genes to provide a favorable environment for the recruitment of RNA polymerase II and other transcription factors (54). Moreover, the specific histone

modifications near the integration site can also impact HIV-1 gene expression. Integration near regions marked with histone modifications associated with active transcription (such as H3K4me3 or H3K36me3) can enhance viral transcription. Conversely, regions with repressive marks (like H3K27me3) may inhibit transcription.

Provirus latency and reactivation

The integrated proviruses can either remain latent, which might be associated with the integration sites and host epigenetic modifications, allowing the infected cell to evade the immune system, or become reactivated reactivation. virions under various stimuli, including some cytokines, such as tumor necrosis factor-alpha (TNF-α) and interleukins like IL-2 and IL-7, and microbial products, like lipopolysaccharides (LPS), can activate immune cells and potentially trigger HIV reactivation. Different latency reversal agents (LRAs) can also reactivate latent proviruses. The production of new infectious virions will bud from the host cell to initiate new rounds of infection. Notably, the error-prone nature of viral RT results that the majority of integrated proviruses are defective and incapable of producing infectious virions, although defective proviruses can produce some viral proteins (55). Only those replication-competent proviruses can give rise to new infectious virions.

HIV-1 transcription and translation involve complex processes that are tightly regulated and essential to produce new viral particles. Transcription of HIV-1 provirus begins with the activation of the HIV-1 promoter located in the 5' long terminal repeat (LTR) of the provirus, and the assembly of general transcription factors and RNA polymerase II at the promoter in the 5' LTR. HIV-1 transcription is strongly enhanced by the viral protein Tat, which binds to a region in the HIV-1 LTR known as the trans-

activation response (TAR) element. The Tat protein recruits positive transcription elongation factor b (P-TEFb), which phosphorylates the C-terminal domain (CTD) of Pol II and other transcription factors, converting Pol II into an actively elongating form (56). This elongation phase is crucial for the synthesis of full-length viral RNA, which serves as genomic RNA for new viruses, as mRNA for translation, or as a template for further processing.

After transcription, in the absence of the HIV-1 Rev protein, the primary HIV-1 RNA transcript undergoes extensive splicing. HIV-1 RNA splicing generates multiple spliced transcripts that encode different viral proteins. Fully spliced RNAs encode the accessory and regulatory proteins Tat, Rev, and Nef. Partially spliced RNAs encode proteins Vif, Vpr, Vpu, and Env (57). Whereas unspliced RNA encodes Gag-Pol protein as well as the viral genome. The selection of splice sites is influenced by host splicing factors and the viral Rev protein. Early in the infection cycle, fully spliced viral mRNAs are predominantly produced. As the concentration of Rev increases in the cell, it binds to the Rev response element (RRE) in unspliced and partially spliced viral RNAs, facilitating their export from the nucleus to the cytoplasm (58). This regulation of splicing allows the expression program to shift from production of regulatory proteins to structural proteins and enzymes needed for viral assembly and release of progeny virions that contain two copies of unspliced RNA as genome.

The translation of viral RNA occurs on ribosomes in the cytoplasm. Notably, the production of the Gag-Pol polyprotein precursor is from the same RNA transcript as Gag, utilizing a translation strategy known as “-1 ribosomal frameshift” (59, 60). The ribosomal frameshift occurs at a specific signal sequence within the viral RNA. This

signal consists of two main elements: a slippery sequence where the frameshift takes place, and a downstream RNA structure, often a stem-loop or pseudoknot. In HIV-1, the slippery sequence is a heptanucleotide motif, such as UUUUUUA (59). This frameshift enables a single viral mRNA to encode both Gag and Gag-Pol precursors by shifting the ribosome reading frame backwards by one nucleotide, thereby changing the downstream amino acid sequence.

Assembly, budding, and maturation

After translation, the assembly of new HIV-1 virions begins with the trafficking of Gag polyproteins to the inner surface of the host cell plasma membrane. Upon reaching the plasma membrane, Gag polyproteins undergo multimerization, which is primarily driven by interactions among the matrix (MA) domain, the capsid (CA) domain, and the nucleocapsid (NC) domain of the Gag molecules. The MA domain plays a crucial role in binding to the plasma membrane, facilitated by the myristylation of its N-terminus, which targets Gag to the membrane. The CA domain contributes to Gag-Gag interactions that are essential for the formation of the viral capsid structure during and after budding. The NC domain binds to the viral RNA, promoting its encapsulation and playing a role in the correct assembly of the virion (34). This specificity is mediated by the nucleocapsid domain of Gag, which recognizes and binds to sequences on the viral RNA known as packaging signals (Psi), within the leader sequence of the unspliced, full-length HIV-1 RNA. Meanwhile, the Env glycoproteins gp120 and gp41 are transported from Golgi apparatus (after cleaved from gp160 in Golgi) to the assembly site and incorporated into the plasma membrane (61).

As Gag-Pol multimers accumulate at the plasma membrane, they induce curvature, leading to the formation of a budding virion. The process is supported by the matrix domain of Gag and involves host cell factors such as the Endosomal Sorting Complex Required for Transport (ESCRT) machinery (34, 62). The p6 domain of Gag also interacts with components of the ESCRT pathway, facilitating membrane fission and release of the virion. After budding, the HIV-1 protease, contained within the Gag-Pol polyprotein, becomes active. The protease cleaves the Gag and Gag-Pol polyproteins into their functional protein components, including the matrix, capsid, nucleocapsid, p6, reverse transcriptase, integrase, and protease itself. Cleavage triggers a structural rearrangement within the virion. The cleavage of Gag leads to the condensation of the capsid protein into a mature, conical core that encapsulates the viral RNA and associated enzymes. The assembly, budding, and maturation processes are critical to produce infectious progeny virions.

HIV Disease Progression

The progression of HIV infection to AIDS is a complex process that varies significantly among people living with HIV (PLWH). Without treatment, HIV gradually weakens the immune system, leading to AIDS and increasing the risk of opportunistic infections and cancers. The course of HIV disease progression includes three stages: acute HIV infection, chronic HIV infection, and late-stage HIV infection (AIDS) (**Figure 1.5**) (63).

The acute phase of HIV-1 infection begins 2 to 4 weeks after the virus is acquired. This stage is marked by high levels of viral replication and a rapid decline in CD4+ T cells, which are critical components of the immune system. The HIV copies in the blood

are very high during acute infection, which makes individuals highly infectious (64). Despite the intense viral activity, symptoms during this phase are often nonspecific, such as fever, headache, rash, lymphadenopathy, and muscle aches (65). These symptoms are the body's intrinsic immune response to the HIV infection and can easily be mistaken as indicative of other viral infections. In this stage, the immune system begins to produce antibodies against HIV, a process known as seroconversion (65).

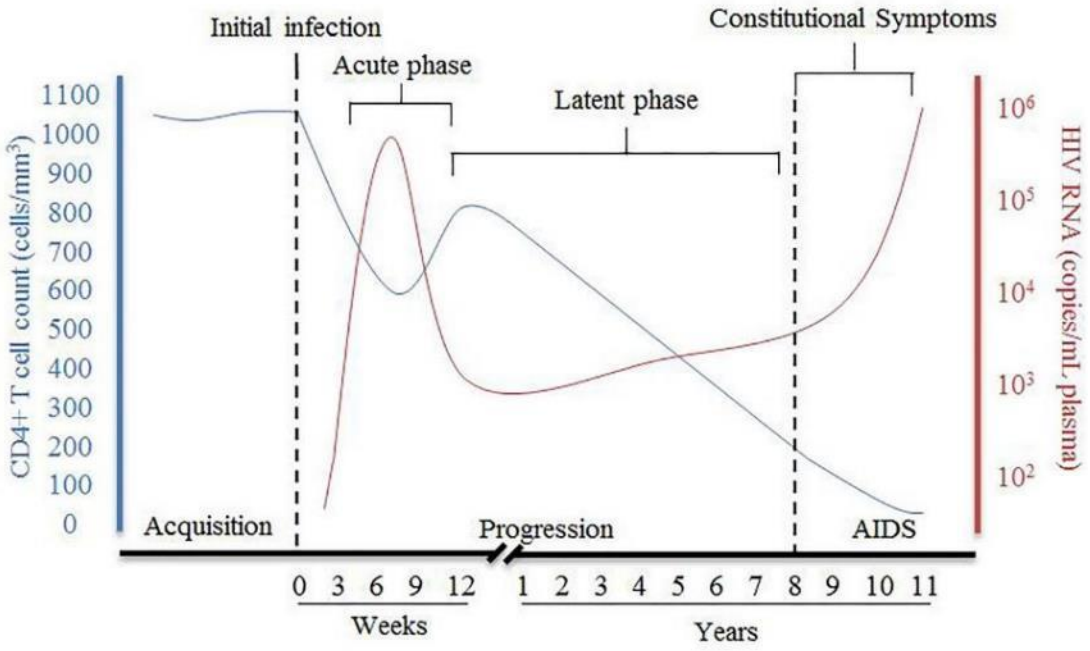

Figure 1.5. Figure from Tough et al (63). Natural course of HIV-1 infection without treatment.

Following the acute phase is a chronic infection stage, which can last from a few years to over a decade without treatment. In chronic infection, the virus continues to replicate, but at lower levels. Over time, this persistent viral replication leads to gradual immune system damage, characterized by a slow decline in CD4+ T cell counts (66). Most individuals experience no specific HIV-related symptoms during this stage, though mild lymph node swelling may occur. This stage is also called asymptomatic HIV infection (67). Antiretroviral therapy (ART) plays a pivotal role in managing this stage by

suppressing viral replication, thereby slowing disease progression, and preventing the transmission of the virus (68).

Without effective treatment, chronic HIV-1 infection can progress to AIDS, the most severe phase of HIV infection. AIDS is defined by a CD4+ T cell count below 200 cells per cubic millimeter of blood or the occurrence of specific opportunistic infections or that are indicative of a severely compromised immune system (69). In this late stage, PLWH are vulnerable to a range of life-threatening infections and illnesses such as tuberculosis, cryptococcal meningitis, severe bacterial infections, and cancers such as lymphomas and Kaposi sarcoma, among others (70).

Antiretroviral Therapy (ART)

Combination ART has been the most significant breakthrough in the management of HIV/AIDS, transforming it from a fatal disease into a manageable chronic condition. ART consists of various inhibitors targeting different stages of viral life cycle (71), and its overall goals are to reduce the viral load to undetectable levels, and to preserve and hopefully restore immunological function, thereby reducing HIV-associated morbidity and mortality, and preventing further virus transmission. The development and evolution of ART have involved several key milestones, from initial introductions of largely ineffective monotherapy antiretrovirals to the sophisticated multi-drug cocktails and slow-release injectable treatment regimens available today.

The first breakthrough in HIV treatment came with the approval of zidovudine (AZT) in 1987 by the United States Food and Drug Administration (FDA) (72). AZT, a nucleoside reverse transcriptase inhibitor (NRTI), was the first drug that showed efficacy in slowing down the progression of HIV disease. However, the initial optimism was

tempered by the drug's toxicity and the rapid development of viral resistance when used as monotherapy (73, 74).

The realization that HIV could rapidly develop resistance to single-drug therapy led to the strategy of combining drugs in the mid-1990s, known as highly active antiretroviral therapy (HAART) or cocktail therapy (75, 76). Introduced in the mid-1990s, HAART typically combines three or more antiretroviral drugs, often from different classes. Protease Inhibitors (PIs), such as Ritonavir (Norvir) and Indinavir (Crixivan), were among the first classes to be included in combination therapy, targeting the virus's ability to mature and replicate (77). This approach has dramatically improved the effectiveness of HIV treatment, reducing plasma viral loads (pVLs) to undetectable levels and significantly extending the lifespan of individuals with HIV.

Over the years, several classes of antiretroviral drugs have been developed, Besides NRTIs, PIs mentioned above, some non-nucleoside reverse transcriptase inhibitors (NNRTIs) were developed. For instance, Efavirenz (Sustiva) and Nevirapine (Viramune) also target the RT enzyme but do not require phosphorylation to be active, differing from NRTIs (78). Integrase strand transfer inhibitors (INSTIs), such as Dolutegravir (Tivicay) and Raltegravir (Isentress) can block viral integrase and hence prevent viral DNA from integrating into the host genome (79). Moreover, entry inhibitors, such as Enfuvirtide (Fuzeon) and Maraviroc (Selzentry), can prevent the virus from entering cells by targeting the gp41 subunit of the viral envelope or the CCR5 co-receptor on the host cell surface (80). However, earlier regimens, especially those involving first-generation PIs, were often associated with significant adverse effects, including lipodystrophy, gastrointestinal issues, and metabolic disturbances (81, 82).

Newer regimens, particularly those involving INSTIs, are generally associated with fewer side effects, better tolerability, and a lower pill burden, making adherence easier for patients (83).

However, drug resistance mutations (DRMs) in HIV-1 arise through the natural process of viral replication due to the high error rate of viral RT. HIV-1 drug resistance mutations pose a significant challenge to the long-term success of ART. By employing comprehensive management strategies, including resistance testing, regimen optimization, and adherence interventions, healthcare providers can mitigate the impact of drug resistance (84).

Comorbidities in PLWH in ART Era

As PLWH taking an effective ART regimen now have a more normal lifespan, comorbidities have become a significant health management concern. Comorbidities in PLWH are multifaceted and can arise from residual effects of the virus itself, the effects of long-term ART, lifestyle factors, or combinations thereof. These conditions can complicate the management of HIV-1 and significantly impact the quality of life and life expectancy of those affected.

PLWH has an elevated risk of several comorbid conditions, which collectively complicate HIV-1 management. Cardiovascular diseases (CVD), diabetes mellitus, and renal diseases are notably more prevalent among PLWH (85-87). Furthermore, PLWH now experience increased risks for non-AIDS-defining cancers, including malignancies like lung, liver, and anal cancers (88, 89). The elevated risk can be attributed to the prolonged inflammatory and immunosuppressive state induced by HIV infection, compounded by other risk factors such as smoking and viral coinfections (90).

Notably, PLWH also faces significant risks related to neurocognitive disorders. HIV-associated neurocognitive disorders (HAND) span a spectrum from asymptomatic neurocognitive impairment to more severe forms like HIV-associated dementia (HAD) and HIV encephalitis (HIVE) and affect up to 50% of PLWH (91). This is largely due to the capacity of HIV-1 to infect and impact the central nervous system (CNS) (91), highlighting the pervasive effects of HIV-1 infection beyond the immune system. Previous studies have reported that despite suppressive ART HIV-1 proviruses and viral production could be readily detected in the brain (92, 93), and severe HIV-associated brain pathologies and immune activation, accompanied by microgliosis and astrogliosis, would be detected in the brains of ART-naïve PLWH with late-stage infection (94, 95). Notably, most of those studies focused on subtype B HIV-1, the neuropathogenesis of other HIV-1 subtypes, including the most prevalent subtype C, is much less explored.

These comorbidities underscore the evolving landscape of health challenges faced by PLWH in the ART era, necessitating a broadened focus on comprehensive healthcare and preventive measures to address the full spectrum of comorbidities associated with HIV infection.

HIV-1 Reservoirs: The Major Obstacle for A Cure

The existence of numerous comorbidities has affected the life quality of PLWH during even under suppressive ART, but the more troubling issue is that ART cannot cure HIV- 1 infection. This is mainly because ART drugs can only prevent viral replication and block new rounds of infection but cannot eradicate integrated proviruses that hide within various reservoirs in PWLH. Additionally, ART penetration efficiencies are not consistent to different anatomical locations, which further limits their abilities to eliminate HIV-1

from the body. Moreover, transcriptionally active and intact proviruses in the reservoirs can harbor DRMs or adapt to develop DRMs as a result of suboptimal penetrance of the ART components. Interruption of ART or non-adherence leads to HIV rebound from such latent proviruses in long-living memory T cells in blood and tissues and from different tissue and cellular reservoirs. Therefore, lifelong ART is necessary.

Despite the fact that subtype B only accounts for 12% of all HIV-1 infections globally, most of our understanding about HIV-1 reservoirs derives from studies on this HIV-1 subtype. This is predominantly because of the requirement for highly sophisticated technologies to study reservoirs, and because subtype B prevalence is highest in high-resource regions, such as North America and Europe. HIV-1 reservoirs can be categorized into tissue reservoirs, cellular reservoirs, and molecular reservoirs (**Figure 1.6**) (96), each with their unique characteristics and challenges for HIV eradication efforts.

Tissue reservoirs refer to specific anatomical locations where HIV-infected cells can persist. The blood (97, 98), lymphoid tissues (99-101), gastrointestinal (GI) tract tissues including gut-associated lymphoid tissues (GALTs) (102-104), and central nervous system (CNS) (105-107) have been well-documented as subtype B HIV-1 tissue reservoirs where proviruses and viral production were readily detectable. Other peripheral tissues including genital tract tissues (108), liver (109), lung (110), kidney (111), pancreas (112), and prostate (113), have also been inconsistently reported as potential subtype B HIV-1 reservoirs. Despite extensive research, the complete landscape of subtype B HIV-1 reservoirs is still not fully understood, and recent studies suggest that HIV proviruses can also persist in other less characterized tissues, such as adipose tissue (114).

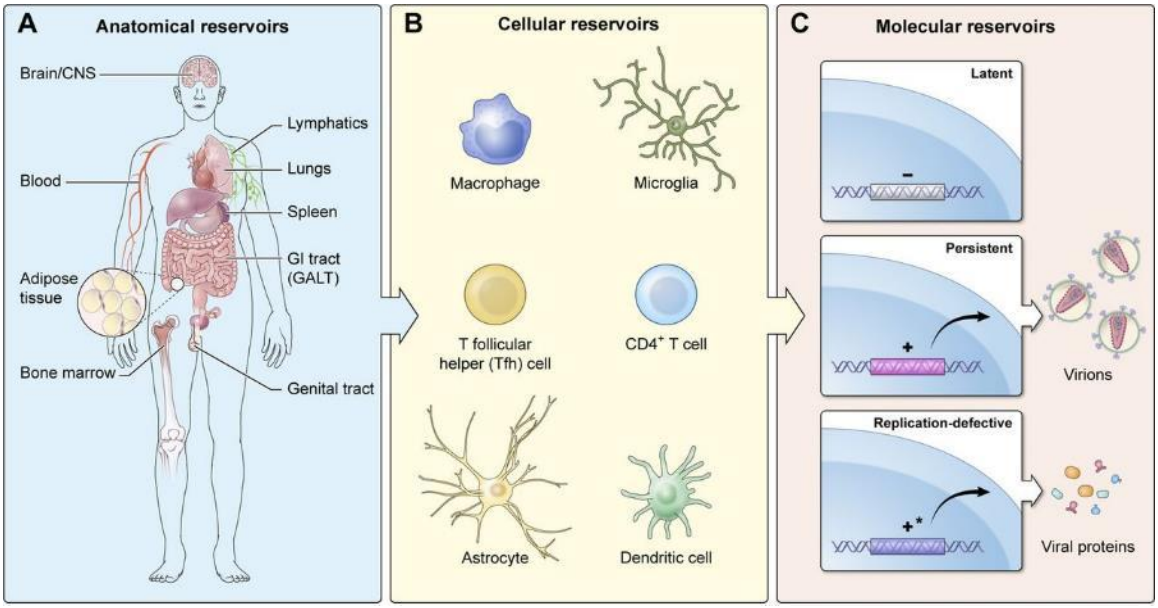

Figure 1.6. Figure from Henderson, et al. (96). Summary of types of HIV-1 reservoirs.

Cellular reservoirs consist of specific cell types that harbor latent, replication-competent HIV. HIV-1 infected cell types varied among different tissues. The most well-characterized cellular reservoirs are long-lived memory CD4+ T cells in different tissues (114-116). These cells can revert to a resting state and retain integrated HIV DNA for extended periods. Other cells, such as microglia in the CNS (117), macrophages and dendritic cells (DCs) in some peripheral tissues (108, 118-121) have also been implicated as cellular reservoirs. These cells can maintain latent HIV and, under certain conditions, produce viral particles, contributing to viral persistence and rebound if ART is interrupted.

At the molecular level, the integrated HIV DNA exists as either defective or intact proviruses. Due to the error prone nature of viral RT, approximately 95% of integrated proviruses contain mutations or deletions that render them incapable of producing infectious viruses (44). Fully intact proviruses, on the other hand, are capable of initiating

new rounds of replication if reactivated, although their production could be low to 1 copy per million cells in a virally suppressed subject (122). Moreover, while defective proviruses cannot contribute to viral replication, they are, in some cases capable of gene expression and even transcription of novel unspliced forms of HIV-RNA transcripts with translatable open reading frames (ORFs). Defective but transcriptionally active integrates can be found in the peripheral blood CD4+ T cells of patients at all stages of HIV-1 infection (55). The viral proteins encoded from defective proviruses may even form extracellular virus-like particles and certainly can trigger immune responses. Expression of HIV regulatory proteins such as Tat could indirectly affect cellular functions even without the production of infectious various. The persistent production of HIV-1 proteins in the absence of viral replication may, in part, explain persistent immune activation despite suppressive ART. The co-existence of intact and defective proviruses in the same reservoir complicates measurement and characterization of the HIV reservoir.

Tissue and cellular reservoirs provide a sanctuary where the virus can hide, while molecular reservoirs, particularly intact proviruses, represent a direct source of viral antigen and rebound. Understanding and targeting these reservoirs is central to the development of curative strategies, which may involve reactivating and eliminating latent virus ("shock and kill") (123), permanently silencing viral expression ("block and lock") (124), or a combination of approaches.

Host Factors that Affect HIV-1 Reservoirs

The majority of our understanding of these reservoirs derives from studies on subtype B HIV-1, predominantly because of its prevalence in regions where much of the early HIV research was conducted. The maintenance and dynamics of HIV-1 reservoirs

are complex and might be influenced by a complex interplay of the provirus, host, clinical, and lifestyle factors.

Host factors

The immune response of the host plays a critical role in controlling HIV replication and shaping the reservoir through a coordinated action of intrinsic, innate, and adaptive immune defenses. Intrinsic immunity involves immediate antiviral responses by host cells, including the production of restriction factors such as APOBEC3G, Tetherin, and SAMHD1. These proteins can inhibit HIV replication directly in infected cells by degrading viral RNA, preventing virus release, and blocking reverse transcription, respectively. Despite HIV's ability to counter some of these effects via Vif, Vpu, and Vpx accessory proteins, intrinsic responses provide an initial layer of defense that can reduce viral spread and influence the seeding of the reservoir.

Innate immunity also plays a crucial role, with natural killer (NK) cells, dendritic cells, and macrophages responding to HIV infection by producing antiviral cytokines and presenting antigens to activate adaptive immune responses. NK cells can kill infected cells directly, potentially limiting the establishment of reservoirs before adaptive immunity is fully activated. However, HIV has evolved mechanisms to evade some of these responses, such as downregulating HLA class I molecules to escape NK cell detection.

Adaptive immunity, particularly involving CD8+ T cells and CD4+ T cells, is vital for controlling HIV replication long term. CD8+ T cell responses can suppress viral replication effectively but may also contribute to the establishment of latency by selecting for cells where the virus remains dormant. The activation state of CD4+ T cells at the

time of infection significantly influences their likelihood of becoming part of the reservoir. Resting memory CD4+ T cells, which are less permissive to active replication, are a key component of the latent reservoir. Moreover, these cells can harbor HIV DNA for extended periods, eluding immune detection and ART.

Host genetic factors, such as HLA type and polymorphisms in genes involved in immune regulation, can further impact the effectiveness of both innate and adaptive responses in controlling HIV and the establishment of the reservoir. For example, certain HLA alleles are associated with better control of HIV due to more effective presentation of viral antigens to CD8+ T cells, leading to a more robust cytotoxic response that can lower the viral set point and influence the size and distribution of viral reservoirs.

The immune response of the host plays a critical role in controlling HIV replication and shaping the reservoir. CD8+ T cell responses, for example, can suppress viral replication but may also contribute to the establishment of latency by selecting for cells where the virus remains dormant (125). Moreover, the activation state of CD4+ T cells at the time of infection influences their likelihood of becoming part of the reservoir. Resting memory CD4+ T cells, which are less permissive to active replication, are a key component of the latent reservoir (126). Host genetic factors, such as HLA type and polymorphisms in genes involved in immune regulation (127), can also impact the immune control of HIV and the establishment of the reservoir.

Clinical factors

The timing of ART initiation and ART efficacy and adherence have been evaluated for their impacts on HIV-1 reservoirs. Early initiation of ART, particularly during the acute phase of infection, can limit the size of the reservoir by preventing the

widespread seeding of HIV (128, 129). While later initiation, after the establishment of chronic infection, may result in larger and more widely distributed reservoirs. Poor adherence or suboptimal ART regimens have been shown to lead to ongoing viral replication and replenishment of the reservoir (130).

Besides ART-related factors, co-infections in PLWH, such as hepatitis B virus (HBV), tuberculosis (TB), or human papillomavirus (HPV) (131-133), can drive immune activation and inflammation, potentially impacting the size and distribution of HIV reservoirs. For example, chronic HBV co-infection has been associated with increased levels of T-cell activation, a factor that could potentially enhance the establishment and maintenance of HIV-1 reservoirs (133). Additionally, TB-associated immune dysregulation may facilitate the establishment of latent HIV-1 infection in resting CD4+ T cells, contributing to reservoir persistence (131).

Lifestyle factors

Lifestyle factors, including alcohol use, smoking, and substance use have been reported to influence systemic inflammation and immune function (134, 135), potentially affecting reservoir dynamics indirectly. Substance use varies widely, from illicit drug use to the medicinal and recreational use of cannabis. Substances such as cocaine and opioids have been shown to modulate immune responses and may contribute to the persistence and dynamics of HIV-1 reservoirs through various mechanisms, such as suppressing immune responses, increasing anti-inflammatory cytokines, and enhancing HIV-1 replication (136, 137).

Potential Impacts of Cannabis Use on PLWH

Among the lifestyle co-factors that might affect HIV-1 reservoirs, cannabis use emerges as a significant, yet under-researched factor, due to its potential anti-inflammatory properties, and its increasing legalization. Moreover, some studies have reported its widely used among PLWH (138-140). Globally, cannabis is the most frequently used recreational psychoactive substances, with estimates suggesting that approximately 192 million people worldwide used cannabis in 2018 (141). Usage varies in prevalence across different regions largely as a function of legality. Among PLWH, cannabis use is reported to be accessed for managing symptoms such as chronic pain, anxiety, and nausea associated with ART (138).

Prevalence of regional cannabis use

In North American and European adults, the prevalences of cannabis use were reported to be around 18% (140) and 8% (139), respectively. However, Compared to that in general populations, the levels of lifetime cannabis use were reported to be approximately 3-fold higher among PLWH in North America (over 50%) (142, 143), and Europe (over 20%) (144).

Cannabis use in SSA adult populations, where subtype C HIV-1 is prevalent, appears to be approximately 12% (138). The level of cannabis use among sub-Saharan PLWH was reported to be similar to that in the general population. Notably, regional differences exist in the prevalence of cannabis use, with high prevalence cannabis use reported in South Africa [16.7% (9.1–26.0%)] and Zambia [36.5% (34.3–38.7%)](138, 145-147).

Impacts of cannabis use on HIV-1 infection

Of the more than 100 cannabinoids in *Cannabis sativa*, Δ9-tetrahydrocannabinol (THC) and cannabidiol (CBD) are the primary psychoactive and non-psychoactive ingredients (148). To date, the effects of cannabis on HIV-1 have only been evaluated for subtype B HIV-1 infections. Existing information on positive or negative effects is inconclusive and variable based experimental approach or model. Studies based on medical records report that cannabis either had no effect on HIV-1 infection (149, 150), or detrimental effects on the ART adherence of PLWH (139, 151). Other studies indicated that cannabinoid exposure is associated with lower HIV pVL (152). Several studies using SIV/SHIV-infected macaques showed reduced levels of inflammation under cannabinoid administration (153-155). Notably, most of these studies utilized subtype B and only surveyed blood samples to study impacts, including reservoirs. Thus, it remains unclear whether cannabis use impacts the size of HIV-1 tissue reservoirs. Moreover, the impact of cannabis use in non-B subtype reservoirs is unexplored. Given possible widespread use of cannabis in SSA, where over two-thirds of all PLWH HIV-1 reside, a closer examination of cannabis impacts on HIV-1 reservoirs, and those formed by subtypes other than B, is warranted.

Disparities in the HIV-1 Research Focus

The landscape of HIV-1 research has long been marked by significant disparities, particularly in the focus and depth of studies among the various HIV-1 subtypes. Historically, the majority of HIV-1 research, including clinical trials for antiretroviral drugs, vaccine development, and reservoir studies, has centered on subtype B. This focus is largely because subtype B is the most prevalent HIV-1 subtype in North America and

Europe, regions that have been at the forefront of HIV/AIDS research funding and infrastructure. As a result, the scientific community has amassed a wealth of knowledge on subtype B, from its molecular characteristics and progression patterns to its response to various ART. However, subtype B accounts for only about 12% of all HIV infections worldwide, raising concerns about the generalizability of these findings.

Subtype C HIV-1 accounts for approximately 50% of all HIV infections globally. Despite the high global prevalence, in stark contrast to subtype B, much less studies have focused on subtype C, none of the study was on subtype C HIV-1 reservoirs. This is due to the difficulties to conduct systematically molecular investigation in resource limiting setting such as sub-Saharan Africa (SSA) and India where subtype C HIV-1 is prevalent. The subtype C dominance in the global HIV epidemic while few studies on its reservoirs underscores a critical gap in our understanding of its reservoir dynamics and mechanisms of persistence.

More importantly, previous studies have highlighted significant differences between subtype B and subtype C HIV-1 regarding the transmission fitness, replication capacity, coreceptor usage, and disease progression (156-158). For example, subtype C exhibits higher transmission fitness (156) and slower disease progression (157) compared to subtype B. Subtype C also predominantly uses the CCR5 coreceptor throughout infection, rarely switching to CXCR4 (158), which may contribute to its unique pathogenesis and immunopathogenesis. Moreover, there are two NF-κB binding sites in subtype B HIV-1 LTR while subtype C HIV-1 LTR contains an additional NF-κB binding site (28), which might render a higher transcription activity for subtype C HIV-1

proviruses. All these may contribute to differences in the size and distributions of tissue reservoirs between the two HIV-1 subtypes, which need to be further investigated.

Additionally, the lack of subtype-specific research hinders the development of broadly effective vaccines that can provide immunity across different HIV-1 subtypes. More importantly, the subtype C research efforts overlooked the socio-economic and healthcare challenges faced by the regions most affected by this subtype, which are critical factors in the global HIV/AIDS response.

Research Aims

HIV-1 reservoir remains the main obstacle for HIV cure with little is known about co-factors that could affect HIV-1 reservoirs. Subtype C HIV-1 is the most widespread and accounts for nearly 50% of global HIV-1 infections, while few if any HIV-1 reservoir studies have focused on this subtype. That is, mostly, due to the difficulties of conducting systematic tissue sampling and molecular investigation in low-resource sub-Saharan Africa (SSA) and India, where subtype C HIV-1 is predominant. The overall objective of our project is to identify and characterize the HIV-1 reservoirs in virally suppressed (aviremic) subtype C HIV-1 infected African individuals, and then determine the impact of lifestyle habits such as cannabis use on those reservoirs. We hypothesize that subtype C infected ART treated individuals will have persistent viral infections with HIV reservoirs in the peripheral tissues and in the brain tissues, and cannabis which has anti-inflammatory effects can reduce persistent HIV-1 replication, in turn, leading to a reduction in the size and distribution of subtype C HIV-1 tissue reservoirs. To accomplish these goals, I will address four specific aims in my research.

Aim 1. To identify all potential subtype C HIV-1 tissue reservoirs in ART-treated aviremic individuals using autopsy cases and quantify the viral DNA and RNA in these tissue reservoirs.

Aim 2. To identify and characterize novel tissue reservoirs for subtype C HIV-1 infected ART treated aviremic individuals and determine the extent of infection and infected cell types in these tissue reservoirs.

Aim 3. To determine whether brain tissues can serve as HIV reservoir in subtype C infected individuals, and the extent of neuropathology, viral burden, CD8+ lymphocyte infiltration, and immune activation.

Aim 4. To determine whether cannabis use impacts the size, distribution as well as inflammatory cytokine expression in subtype C HIV-1 reservoirs.

Given that subtype C accounts for approximately half of the global HIV-1 pandemic and considering that HIV-1 reservoirs pose a significant challenge to achieving a cure in the era of ART, it is crucial to meticulously identify and characterize subtype C reservoirs. Furthermore, assessing the influence of co-factors on these reservoirs is vital. Through the comprehensive research conducted in this study, we aim not only to deepen our understanding of HIV pathogenesis but also to contribute valuable insights that will guide the development of guidelines for cannabis use among PLWH. Additionally, our findings will inform the creation of therapeutic strategies tailored to HIV-1 subtype C and adapted to specific regional contexts, enhancing the effectiveness of interventions, and supporting personalized medicine approaches in the fight against HIV.

Note:

With several paragraphs of this chapter, ChatGPT was employed to check for grammatical mistakes, for correctness of the word choices, and to enhance the flow of the paragraphs.

CHAPTER 2:

SUBTYPE C HIV-1 RESERVOIRS THROUHOUT THE BODY IN ART-SUPPRESSED INDIVIDUALS

Abstract

While the location, magnitude, dynamics, and reactivation responses of subtype B HIV-1 reservoirs have been intensively investigated, our understanding of reservoirs in other subtypes and how they respond to antiretroviral therapy (ART) is substantially less, including the most widespread subtype C HIV-1 genotype. To characterize subtype C HIV-1 reservoirs more thoroughly, we implemented postmortem frozen, and formalin fixed paraffin embedded (FFPE) tissue sampling of the central nervous system (CNS) and various peripheral tissues from African ART-suppressed subjects. HIV-1 *LTR*, *gag*, *envelope* (*env*) DNA and RNA detection and quantification were accomplished using genomic DNA and RNA extracted from frozen tissues, respectively. RNAscope *in situ* hybridization (ISH) was conducted to define the localization of subtype C HIV-1 DNA and RNA in FFPE tissue. Despite uniform viral load suppression of every subject in our cohort treated with the same ART regimen, PCR results showed that subtype C HIV-1 proviral DNA copies vary both in magnitude and tissue distribution. Proviral DNA was mainly detected in peripheral tissues, especially the lymph nodes (LNs), spleen, ileum, and interestingly, the appendix. In contrast to subtype B, subtype C HIV-1 proviral DNA was rarely detectable in the CNS. While HIV-1 RNA was detected in peripheral tissues of 6 out 8 ART-suppressed cases - mostly in lymphoid tissues, there was no detectable HIV-1 RNA in the CNS tissues harboring proviral DNA. In addition to active HIV-1 expression in lymphoid tissues, RNAscope revealed HIV RNA can also be detected in CD4-expressing

cells in the appendix, suggesting this tissue as a potential treatment resistant reservoir for subtype C HIV-1, which has not been reported previously.

Introduction

Human immunodeficiency virus (HIV) can infect CD4 expressing immune cells and eventually cause acquired immunodeficiency syndrome (AIDS). AIDS was universally fatal with opportunistic co-infections due to the loss of CD4 T cell mediated immunity and HIV-associated neurocognitive disorder (HAND) including severe HIV-associated dementia (HAD) (159, 160). Although the introduction of combined antiretroviral therapy (cART) has turned that once fatal disease into a managed care scenario, it is not a cure; it is accompanied with some side effects and life-long treatment is required (161). There are two HIV types, HIV-1 and HIV-2, with HIV-1 accounting for more than 95% of all worldwide HIV infections (23). Phylogenetics segregates HIV-1 into 4 groups: M (major group), O (outlier group), N (non-M, non-O), and P. Group M HIV-1 is responsible for more than 90% of all HIV infections and is subdivided in 10 separate subtypes: A, B, C, D, F, G, H, J, and K, as well as CRFs (circulating recombinant forms) that are essentially hybrid subtypes formed by recombination between at least two subtypes (26). These subtypes are unevenly distributed throughout the world, with subtype C being the most widespread. Subtype B HIV-1 is the predominant subtype in Europe, North Americas, Japan, and Australia, but accounts for only 12% of global HIV infections. In contrast, subtype C HIV-1 is prevalent in sub-Saharan Africa and India, and is responsible for more than 50% of all HIV infections (162). Investigations of HIV latency in non-subtype B lineages have been limited and is now important as effective treatment is increasingly available and utilized in areas where non-subtype B genotypes predominate.

Despite cART can suppress HIV-1 plasma viral load (pVL) to an undetectable level (<50 copies/ml) in a majority of treated people living with HIV (PLWH), it cannot eliminate HIV-1 from the body. This is because HIV reverse transcribes its RNA genome into a complimentary double-stranded DNA that then integrates into the host genome as a provirus, and it is the presence of this potentially replicable provirus that constitutes the latent HIV tissue reservoir. Establishment of HIV-1 reservoirs is thought to occur early after infection in different locations throughout the body (163). HIV-1 proviruses in different reservoirs might stay latent or persistently being expressed, which means a viral reservoir could be: 1) an active persistently expressing reservoir; 2) a silent but intact proviral reservoir, 3) a reservoir comprised of defective integrated provirus that may or may not have the capacity to express HIV-1 genes (96). However, it would seem likely that real tissues reservoirs could potentially contain all three 'states' of HIV-1 persistence. In some HIV-1 tissue reservoirs, it is difficult to achieve a high penetrance of ART due to drug chemistry, and physiological barriers. One example is the blood-brain barrier (BBB), which can limit some ART drugs access to the CNS (164). In addition, poor ART penetrance could result in localized persistent low-level replication in some tissues (persistent reservoir). Recent studies suggest that proviral DNA levels in PBMC decline with a half-life estimated around 12 years, and are not differentially affected by the specific antiretroviral regimen used to achieve and maintain viral suppression (165-167) (114). However, many studies have demonstrated that HIV will rebound after cessation of ART, and the rebounding virus originates from persistent reservoirs or reactivated latent reservoirs (100, 168). Therefore, lifelong ART is necessary, which carries both a

physiological and economic burden, especially in low-resource areas, such as sub-Saharan Africa.

Due to demonstration of a viral reservoir in PBMC and the difficulty in sampling other potential reservoir tissues, most HIV latency research has focused on large volume blood samples and lymphoid tissues obtained by biopsy from subtype B HIV-1 infected subjects (100, 169, 170), while some other studies alternatively utilized non-human primates (NHP) model or humanized mice model (171-175). Those studies have suggested that CNS tissues (171, 176-180), bone marrow (181-184), lung (110, 185), kidney (111), pancreas (186), prostate (187, 188), gastrointestinal (GI) tract tissue (189-191), reproductive tract tissue (108, 192, 193), and adipose tissue (194) serve as subtype B HIV-1 tissue reservoirs. However, as far as we know, only two studies had investigated HIV tissue reservoirs that utilized tissues from different anatomical locations of the same subject, including lymphoid, brain and GI tract tissues, and both were on subtype B HIV-1 (92, 186).

The challenges of collecting high quality systematic post-mortem human specimens from endemic areas to support molecular investigations had previously limited efforts to define subtype C HIV-1 reservoirs. It has been reported that subtype C HIV-1 can be detected at high levels in peripheral blood mononuclear cells (PBMCs) of ART naïve individuals (195). Our laboratory has also found that subtype C HIV-1 proviral DNA can be detected at low and variable levels in CNS tissues regardless of ART success or failure (196), but so far there has been little systematic characterization of the distribution of this subtype among major human organ systems, especially in those who are ART-experienced

with pVL suppression. Whether the magnitude, distribution, or state of activation of subtype C HIV-1 reservoirs is similar or dissimilar to that in HIV subtype B is unknown.

In this study, various flash-frozen and formalin fixed paraffin embedded (FFPE) brain and peripheral tissues were collected postmortem to support quantification of HIV reservoirs in eight subtype C HIV-1 infected aviremic Zambian subjects. Our results reveal that there are very few tissues harboring subtype C HIV-1 proviral DNA and potential intact viral genome in the brain, and all are at low copy number. Moreover, there is no detectable viral RNA in the brain. These indicate that, in contrast to subtype B, the brain is not a robust reservoir for HIV-1 subtype C. In the periphery, the HIV-1 subtype C proviral reservoir distribution and magnitude varied among different tissues and individuals with lymphoid tissues harboring consistent viral burden in most subjects, as anticipated. Notably, we detected a robust HIV-1 tissue reservoir in the appendix of 100% of subject which is, to our knowledge, the first report of this tissue as a site of HIV persistence in treated subjects. Lymph nodes (LNs) were the major compartments where persistent viral RNA expression was detected suggesting that ART fails to eliminate HIV-1 production from these tissues despite pVL suppression. Furthermore, using RNAscope, viral DNA and RNA can be detected in parenchymal appendix tissue where it is colocalized with CD4 expressing cells. Evaluation of subtype C HIV-1 reservoirs in this study addresses crucial gaps in our understanding of the magnitude and unique distribution of subtype C HIV-1 tissue reservoirs in the context of viral suppression. Such understanding may contribute to a greater capacity to understand HIV-1 infection and better future strategies for HIV cure.

Materials and methods

Study setting, ethics statement and sample collection

Zambia is a sub-Saharan African country where HIV-1 prevalence remains high and infection with subtype C HIV-1 is predominant (197, 198). UTH is the largest hospital in Zambia and its pathology department performs approximately 1300 forensic autopsies annually, 17% of which are on HIV-1 positive subjects. When a potential autopsy case arrived at the UTH morgue, a clinical officer or study nurse counselor approached the family members of the deceased to determine whether the deceased met study inclusion criteria with regard to time of death, and to seek informed consent for the post-mortem collection of tissue specimens. Because sociodemographic and lifestyle behaviors could not be directly assessed from the deceased, the nurse counselor, working with the clinical officer, surveyed the next-of-kin, the individual who provided consent for tissue collection, for demographic information about the deceased. The nurse counselor utilized a validated WHO-ASSIST survey instrument designed to collect social demographic and behavioral data. At the same time, we also accessed clinical records to extract portions of the patient's medical history, including ART regimen and duration. Only study personnel will have access to the study database and only de-identified data will be made available for data analysis. Post-mortem samples were obtained using standardized procedures. Within 48 hours of the subject's death, multiple CNS and collateral tissues were collected and stored by two methods: 1) half of the sample was stored at -80°C; 2) the other half was fixed at 4% paraformaldehyde then further processed for FFPE tissue blocks. In addition, plasma samples from all subjects were also obtained and stored at -80°C until use.

HIV-1 serology and real-time quantitative reverse transcription PCR (qRT-PCR) for plasma HIV-1 viral load quantification

HIV-1 serological test was conducted using HIV Rapid Test or Alere Determine HIV-1/2 Ag/Ab Combo test in Zambia (199), and those serological results were further verified in the laboratory in the U.S. with HIV-1-2.0 First Response kit (Premier Medical Corporation Limited, Daman, India). To quantify the plasma HIV-1 viral loads, total RNA in plasma sample was extracted in one batch with standard AcroMetrix HIV-1 setting (5E2, 5E3, 5E4, 5E5, 5E6/ml, respectively) (Thermo Fisher Scientific, Fremont, CA) via QIAamp Viral RNA Kit (Qiagen, Hilden, Germany) with DNase I treatment to remove any DNA. Same volume (5 μl) plasma samples and AcroMetrix HIV-1 setting were subjected to qRT-PCR as triplicates using the RNA UltraSense One-Step qRT-PCR System (Invitrogen, Waltham, MA) to detect the plasma viral loads. Primers and a probe against HIV-1 *LTR* were used. The procedure for qRT-PCR is 50°C for 15 minutes, 95°C for 2 minutes to synthesize cDNA, then 40 cycles by 95°C for 15 seconds for DNA denaturation and 60°C for 1 minute for annealing and elongation. The cutoff of plasma HIV-1 *LTR* RNA detection is 70 copies/ml.

Extraction of genomic DNA and RNA from postmortem tissues

Small pieces of snap-frozen tissues were collected in two sets of 1.5 ml centrifuge tubes by 1 mm biopsy punch tool (Robbins Instruments, Chatham, NJ) on dry ice for DNA and RNA extraction, respectively. For genomic DNA extraction, 600 μl cell lysis buffer and 10 μl proteinase K solution (Qiagen, Hilden, Germany) were added in tubes containing the tissues, then the samples were incubated overnight in 55°C water bath. Each sample was then incubated at 37°C with 10ul RNase-A solution (Qiagen, Hilden,

Germany) for 1 hour to remove any RNA. After RNA removal, the samples were chilled on ice for 3 minutes before adding 200 µl protein precipitation solution into each tube, the samples were then vigorously vortexed and spun down at 16,000 x g for 10 minutes at 4°C to precipitate protein. During centrifugation, 400 µl isopropanol and 0.5 µl glycogen were added into a new tube. The supernatant was transferred to the new tube containing isopropanol and glycogen for genomic DNA precipitation by inverting tube 50 times followed by 16,000 x g for 1 minute. The supernatant was then discarded, the DNA pellet at the bottom of the tube was washed once with 70% ethanol and air dried for 5-10 minutes. Then 30-100 µl hydration solution (Qiagen, Hilden, Germany) was added in the tube to resuspend the DNA pellet. After a brief vortex, the tubes were incubated at 65°C for at least 1 hour to completely dissolve the DNA pellet. The genomic DNA samples were further purified by phenol chloroform, and the DNA concentrations were measured via Qubit™ dsDNA BR assay kit (Invitrogen, Waltham, MA). The DNA samples were stored at -20°C until use.

For total RNA extraction from tissues, 700 µl QIAzol lysis reagent (Qiagen, Hilden, Germany) was added to each tube containing the fresh tissue. After 5 minutes incubation of the homogenate, 140 µl chloroform followed by 12,000 x g at 4°C for 15 minutes to separate phases. Total RNA from the top aqueous phase was then extracted with QIAgen miRNeasy mini kit (Qiagen, Hilden, Germany) according to manufacturer's protocol. On-column DNase I treatment was also applied during the RNA extraction. The RNA concentrations were measured via Qubit™ RNA BR assay kit (Invitrogen, Waltham, MA), the RNA samples were then stored at -80°C for the subsequent viral RNA analyses.

HIV-1 subtyping

To confirm HIV-1 clade C infection in the aviremic cases studied, nested PCR with primers against gp120 V3 loop was performed with the following procedure for both rounds: polymerase activation at 95°C for 10 minutes, then 35 cycles of denaturation at 95°C for 30 seconds, annealing at 55°C for 30 seconds and elongation at 72°C for 2 minutes, then one cycle of 72°C for 7 minutes. In first round, 100 ng genomic DNA was used as template with *envelope* primers (Forward: CCTGCTGGTTATGCGATTCTAAA; Reverse 1: ACCTCCTGCCACATGTTTATAATTTG) were applied. Then 2 μl of the first round PCR product was utilized as template for the second round with another pair of *envelope* primers (Forward: CCTGCTGGTTATGCGATTCTAAA; Reserve 2: CAATAGAAAAATTCTCCTCTACAATTAAA). Products from the second round nested PCR were checked for size and purified via gel extraction, then sequenced with the forward primer. A recombinant identification program (RIP) and BLAST-based HIV-1 genotyping tool were used for subtyping sequence alignments.

Real time qPCR for HIV-1 DNA quantification

100 ng extracted genomic DNA from each tissue was used as template for both quality control GAPDH and HIV-1 *LTR*, *gag*, and *env* DNA detection. TaqMan® Universal PCR Master Mix (Thermo Fisher Scientific, Fremont, CA) was used with 300 nM each of HIV-1 *LTR* U5 forward and reserve primers (GCCTCAATAAAGCTTGCCTTGA; GGGCGCCACTGCTAGAGA) and Fam-labeled HIV-1 *LTR* probe (/56-FAM/CCAGAGTCACACAACAGACGGGCACA/3BHQ_1). For HIV-1 *gag*, each HIV-1 *gag* forward and reserve primers (CAAGCAGCCATGCAAATGTT; ATGTCACTTCCCCTTGGTTCTC) and Fam-labeled

HIV-1 *gag* probe (/56-FAM/CCTGGTGCAATAGGCCCTGC/3BHQ_1/) were used. For HIV-1 *env*, each HIV-1 *env* forward and reserve primers (TGTTCCTTGGGTTCTTGGGAG; TGCTGCTGCACTATACCAGAC) and HEX-labeled HIV-1 *env* probe (HEX-TCTGGCCTGTACCGTCAGCG-IFBQ) were used. Genomic 8E5 cellular DNA containing a single proviral HIV-1 genome in each cell was mixed with uninfected peripheral blood mononuclear cells (PBMCs) genomic DNA to generate standards that contain 5, 10, 100, 1000 8E5 HIV-1 copies in 100 ng total genomic DNA, respectively. DNA sample from an uninfected individual was used as negative control. Standards and tissue DNA samples were applied in QuantStudio™ 3 Real-Time PCR System (Thermo Fisher Scientific, Fremont, CA) in triplicates with a reaction volume of 20 µl for each. The thermal cycling conditions utilized in real time qPCR were: 95°C for 15 seconds for polymerase activation, then 40 cycles of 95°C for 15 seconds for DNA denaturation and 60°C for 1 minute for annealing and elongation.

Digital PCR (dPCP) for HIV-1 DNA quantification

HIV-1 DNA copies in the genomic DNA from LN, appendix, testis, and occipital lobes of cases 2, 3 and 4 were also determined by dPCR performed on QIAcuity One instrument with QIAcuity probe PCR kit (Qiagen, Hilden, Germany). Briefly, genomic DNA samples were first digested with restriction enzyme SalI whose recognition site does not exist in the target HIV-1 LTR sequences to reduce sample viscosity and increase template accessibility. Human beta-globin internal control and HIV-1 *LTR* DNA in triplicates with 10 ng digested DNA beta-globin detection and 700 ng digested DNA as templates were used. Each dPCR reaction mixture in total volume of 40 µl consisted of 1X QIAcuity probe master mix, 800 nM each of HIV-1 LTR primers, 400 nM FAM-

labeled HIV-1 LTR probe, template DNA and molecular grade water. The reaction mixtures were then transferred to a 26K 24-well nanoplate (Qiagen, Hilden, Germany) and, sealed with a plate seal, then amplified in the QIAcuity One thermocycler. The thermal cycling conditions used for dPCR were: 95°C for 2 minutes, 40 cycles of 95°C for 15 seconds for DNA denaturation and 60°C for 30 seconds for annealing and elongation. The threshold for dPCR positivity was determined using signals for viral DNA detection in digested genomic DNA from the corresponding tissues of an HIV-1 negative individual, and DNA from the mesenteric LN of a HIV-1 viremic case was used as positive control (supplementary table 5). By dividing the mixture into partitions, the instrument measured and calculated the target sequence copies after end-point PCR cycling based on the presence or absence of a fluorescent signal for human beta-globin or HIV-1 *LTR* DNA in every individual partition. Analysis was performed using the software suite, providing the concentration in copies per ml of LTR sequence as well as for human beta-globin.

RT-qPCR for HIV-1 tissue RNA load quantification

To quantify HIV-1 RNA copies in tissues that harbor viral DNA, total RNA in the tissues was extracted as described above. 500 ng total RNA and 2.5 ul AcroMetrix HIV-1 standards (5, 50, 500, 5000, 50000 copies of cell free HIV-1, respectively) were subjected into RT-qPCR in triplicates by RNA UltraSense One-Step RT-qPCR System (Invitrogen, Waltham, MA) to detect the tissue viral RNA loads. Using primers and probes against HIV-1 *LTR*, *gag*, and *env* region used for DNA copy determination. The thermocycle procedure for RT-qPCR was the same as that for plasma viral load determination.

RNAscope *in situ* hybridization (ISH) and immunohistochemistry (IHC)

To identify the tissue parenchymal location of HIV-1 nucleic acids and infected cell type, 6 μm of adjacent sections was cut from FFPE appendix tissues of subject case 3 and then subjected for RNAscope ISH and IHC staining. For viral DNA and RNA detection, one section of each appendix tissue was stained with DNAscope antisense probe using RNAscope® 2.5 HD red reagent kit (Advanced Cell Diagnostics, CA) based on the RNAscope® 2.5 HD red reagent kit instruction and a previously reported protocol (200). Other adjacent sections were stained with *Homo sapiens* ubiquitin C (UBC) probe as positive control and dihydrodipicolinate reductase (dapB) probe as negative control by RNAscope, respectively. One of adjacent slides was stained for CD4 cell marker by IHC with mouse anti-human CD4 monoclonal antibody (M7310, 1:100, Dako), and the staining signal was developed with substrate diaminobenzidine (DAB) by Dako Envision and Peroxidase kit. Matched IgG 1 isotype controls were applied in IHC staining to confirm signal specificity. For viral p24 protein detection, IHC was performed on FFPE inguinal LN from case 3, monoclonal mouse anti-HIV p24 antibody was utilized (M0857, 1:20, Dako). The stained slides were then digital scanned by MoticEasyScan Pro instrument (Motic, Xiamen, China) according to the instruction manual provided by the manufacturer.

Statistical analysis

To examine the differences in HIV-1 LTR DNA copies between brain and periphery of the ART-suppressed individuals, and the differences in HIV-1 LTR DNA copies between group 1 (LNs, spleen, and appendix) and group 2 (other peripheral tissues) of the ART-suppressed individuals, both Wilcoxon matched-pairs signed rank test

and nonparametric Mann-Whitney test were used to assess the differences between comparison groups. GraphPad Prism 9 (Graphpad Software, San Diego, CA) was utilized for statistical analyses. All tests were 2-tailed and P-values < 0.05 were considered as significant.

Results

Tissue sampled and subtype determination in ART-suppressed aviremic individuals

The experimental design highlighting the collected postmortem sampling in this study is shown in **Figure 2.1A**. Serologic testing for HIV was conducted for screening HIV-1 infected individuals using femoral or cardiac plasma samples. Plasma RNA preparations from HIV-1 positive cases were subjected to standard qRT-PCR to quantify plasma viral loads. Eight male subjects were identified as seropositive but lacking detectable plasma viral loads (< 70 copies/ml) and were defined as 'aviremic' (**Table 2.1**).

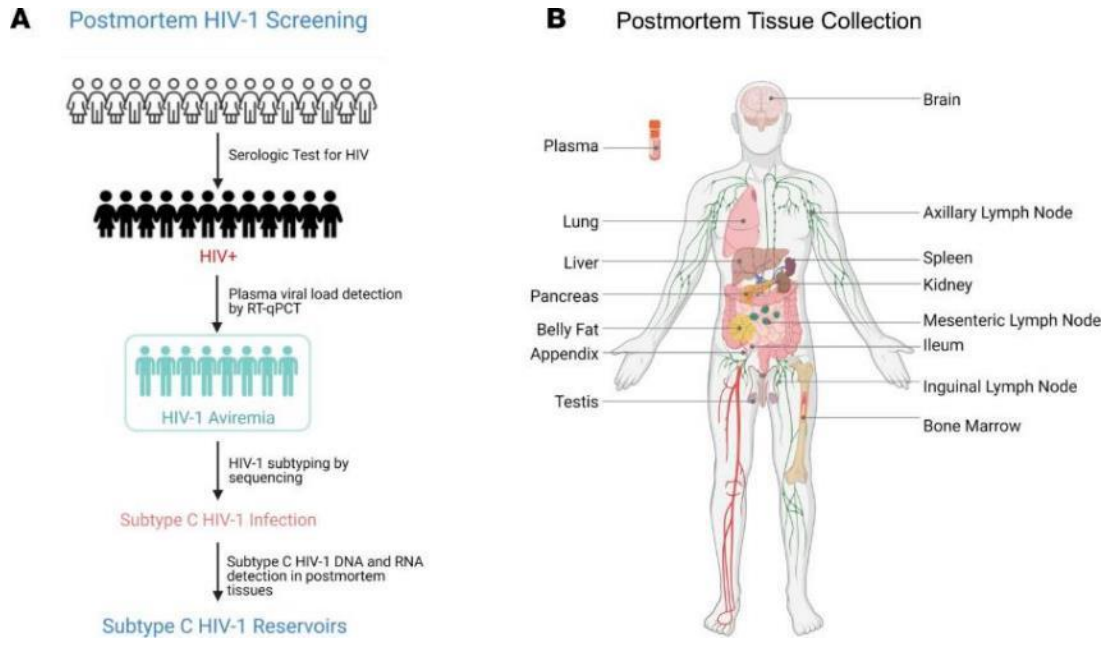

Figure 2.1. HIV-1 aviremic cohort and postmortem sample collection. (**A**) The flow diagram showed postmortem HIV-1 screening. HIV serologic tests were conducted on plasma samples of all postmortem cases to identify HIV-1–infected individuals. qPCR was utilized for plasma viral load detection, and those cases with undetectable plasma viral load were then subjected for HIV-1 subtyping to confirm clade C HIV-1 infection in those aviremic

individuals. Eventually, an 8-case cohort was identified to be infected with subtype C HIV-1. Viral DNA and RNA copies were determined by different PCR-based methods from frozen tissue genomic DNA and total RNA. To characterize more detail for subtype C HIV-1 reservoirs, RNAscope was performed on representative FFPE tissues. (**B**) Postmortem samples were collected within 48 hours of a subject's death. Half of each brain and peripheral tissue was collected and processed into a frozen sample, while the other half was processed into a FFPE sample. Frozen plasma samples were also collected.

The samples listed in **Figure 2.1B**, including 8 CNS tissues, [frontal lobe, parietal lobe, temporal lobe, occipital lobe, hippocampus, cerebellum, basal ganglia, and choroid plexus (CPx)], and 13 peripheral tissues (mesenteric LN, axillary LN, inguinal LN, spleen, bone marrow, Ileum, appendix, liver, kidney, lung, pancreas, belly fat, testis), and plasma were collected within 48 hours of the aviremic subject's death. The median age of the 8 patients at death was 46 (range from 39 to 60). Among the 8 aviremic individuals, information about ART duration was obtained for 6 (information missing for case 3 and 7) whose median duration of ART was 6.5 years (range from 4 to 10 years). Self-reported data indicated that, after commencing on ART, those 6 subjects received ART until their deaths (**Table 2.1**).

Table 2.1. HIV-1 aviremic subjects analyzed

ID	Age	Gender	Plasma VL	Age of ART Initiation	ARV Duration	ART Regimen[a]	Post-mortem Interval	HIV-1 Subtype
Case 1	40	M		32	8 years	Atripla	30 hours	C
Case 2	60	M		52	8 years	Atripla	7 hours	C
Case 3	45	M		Unknown	Unknown	Atripla	3 hours	C
Case 4	50	M	<70	40	10 years	Atripla	4 hours	C
Case 5	53	M	copies/ml	48	5 years	Atripla	< 48 hours	C
Case 6	40	M		36	4 years	Atripla	26 hours	C
Case 7	47	M		Unknown	Unknown	Atripla	18 hours	C
Case 8	39	M		34	5 years	Atripla	33 hours	C

Note: a, Atripla is a combination of 3 different ART medications (efavirenz, emtricitabine, and tenofovir disoproxil fumarate) in 1 tablet form.

In Zambia, Atripla, which is a combination of efavirenz, emtricitabine, and tenofovir disoproxil fumarate in 1 tablet form, is the only ART regimen offered by government clinics serving as the first line of treatment sites where all the decedents received treatment. Tissues from all 8 aviremic, presumably ART-suppressed, subjects were evaluated for HIV reservoirs.

To first determine the HIV-1 subtype and to validate HIV serologic testing on the 8 aviremic cases, we subjected equivalent genomic DNA extracts from frozen postmortem tissues to nested PCR for the HIV-1 *env* gene. The HIV-1 *env* gene sequences were amplified from at least one peripheral tissue for all individuals, and those amplification products were gel-purified and then sequenced using primers against the HIV-1 gp120 V3 loop. Application of Recombinant Identification Program (RIP) and a BLAST-based HIV-1 genotyping tool to *env* sequence alignments revealed highest alignment with HIV-1 subtype C (**Table 2.1**).

Brain is not a good reservoir for subtype C HIV-1 in aviremic individuals

After subtyping, we proceeded to identify tissues harboring subtype C HIV-1 provirus. Genomic DNA samples from frozen postmortem tissues were tested for quality through cellular gene GAPDH amplification, and then subjected to qPCR with primers against the HIV-1 *LTR*, *gag*, and *env* DNA, respectively. Similar amplification efficiencies of those three pairs of primers had been validated through qPCR utilizing 8E5 genomic DNA, which carries a single copy of integrated HIV genome.

The brain has been documented as a reservoir for subtype B HIV-1, but it is unclear whether it is a robust reservoir for other subtypes, including subtype C. Our qPCR results show that, among 64 tested brain tissues (8 tissues for each subject),

subtype C HIV-1 LTR DNA was only detected in 12 (18.8%) brain tissues. The frontal lobe and basal ganglia are the two CNS sites with highest frequency in harboring HIV-1 proviruses. However, the HIV-1 viral DNA copies in brain vary in different individuals and different brain regions (**Figure 2.2**). Particularly, subtype C HIV-1 *LTR* DNA was detected in the frontal lobe of cases 5, 6, and 8 with 57, 20, 37 viral DNA copies/10^6 cells, respectively: in the basal ganglia of cases 1, 5, and 6 with 37, 30, 18 viral DNA copies/10^6 cells, respectively. Furthermore, subtype C HIV-1 *LTR* DNA were also detected in the occipital lobe of cases 4 and 7, the hippocampus of cases 1 and 6, and the CPx of cases 2 and 7, whereas there was no detectable viral *LTR* DNA in the parietal lobe, temporal lobe, and cerebellum. Among those 12 HIV-1 *LTR* DNA harboring brain tissues, case 8 frontal lobe, cases 1 and 5 basal ganglia tissues, case 4 occipital lobe, and case 7 CPx were identified to contain HIV-1 *gag* DNA with 46, 44, 14, 22, 89 viral DNA copies/10^6 cells, respectively. Eventually, besides harboring HIV-1 *LTR* and *gag* DNA, cases 1 and 5 basal ganglia tissues, and case 7 CPx were found to harbor HIV-1 *env* DNA with 30, 54, 28 viral DNA copies/10^6 cells, respectively (**Figure 2.2B**). The presence of all three subtype C HIV-1 genes implied the potential full-length or nearly full-length subtype C HIV-1 proviruses in those 3 brain tissues, while the presence of viral *LTR* DNA but lack of *gag* or *env* DNA indicated probable existence of defective HIV-1 reservoirs in the other 9 of 12 viral DNA harboring brain tissues (75%).

Besides showing a variation among different CNS tissues, the frequencies, and the copies of subtype C HIV-1 proviruses in the CNS also varied among different individuals. In general, subtype C HIV-1 *LTR* DNA was detected in at least one brain tissue in 7 of 8 cases (87.5%), while viral provirus was not detectable in any brain tissue

from case 3. Three brain regions from case 6, the frontal lobe, hippocampus and basal ganglia were identified as tissues harboring subtype C HIV-1 provirus. Moreover, each case 2, 4 and 8 has only one brain tissue containing HIV-1 provirus, which is the CPx, occipital lobe, and frontal lobe, respectively. However, cases 1, 5, and 7 have two different brain tissues with detectable HIV-1 proviruses (**Figure 2.2A**). Among those 7 subjects harboring viral *LTR* DNA in brain, 5 cases (1, 4, 5, 7 and 8) harboring viral gag DNA were identified, and 3 cases (1, 5 and 7) were further determined to contain viral *env* DNA in brain. Notably, the viral DNA copies in brain tissues were all lower than 100 copies/10^6 cells after normalizing to one million cells (**Figure 2.2B**). The medians of detectable viral DNA copies were all 0, no matter in the same brain region of different subjects or in different brain regions of same subject. Moreover, we did not observe a specific pattern regarding the distribution of subtype C HIV-1 reservoirs in the brain.

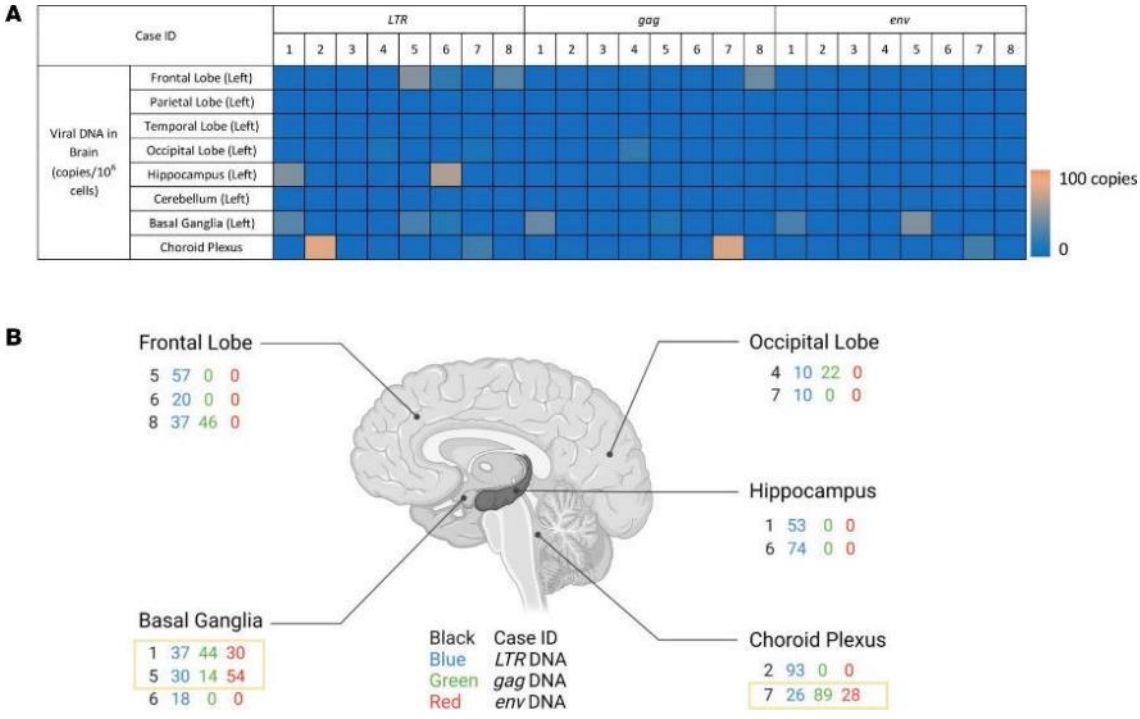

Figure 2.2. Subtype C HIV-1 DNA in aviremic brain tissues. (A) Heatmap of subtype C HIV-1 DNA in aviremic brain tissues. A heatmap displaying the abundance of 3 subtype C HIV-1 DNA (LTR, gag, and env) in different brain regions of 8 aviremic subjects was generated by qPCR analysis. Blocks with colors indicate undetectable (0) DNA copy (blue) to increase DNA copies (brown, up to 93 copies/1 × 106 cells). CNS tissues from the same hemisphere were analyzed (left). (B) Copy numbers of subtype C HIV-1 DNA detected in aviremic brain. The different regions harboring viral DNA and the viral DNA copy numbers in the brain of the 8 aviremic subjects were shown. There was no detectable viral DNA in the parietal lobe, temporal lobe, and cerebellum of 8 aviremic cases. HIV-1 DNA copies were identified by qPCR with 100 ng genomic DNA as a template. HIV-1 LTR (blue), gag (green), and env (red) DNA copy numbers were calculated as the mean of triplicate qPCR reactions and normalized to 1 million cells. The rectangles mark 3 tissues that have all 3 viral genes, indicating potential intact viral genome in those tissues.

Despite the rare and low subtype C HIV-1 viral DNA detected in aviremic brain, we wanted to know whether those proviruses express any viral RNA. However, according to the results of one-step RT-qPCR utilizing total RNA that extracted from brain tissues harboring viral DNA and RNA sample quality confirmed by cellular RNA PPIB amplification, there was no detectable viral RNA (*LTR,* or *gag,* or *env* RNA) in any aviremic brain region.

Detection of subtype C HIV-1 peripheral tissue reservoirs

In contrast to the rare presence in brain, subtype C HIV-1 proviruses were extensively detected in different peripheral tissues throughout the body, and the overall viral DNA copies detected in periphery was remarkably higher than that in the brain ($P<0.001$) (**Figures 2.2A** and **2.3**). Moreover, 82 out of 103 peripheral tissues (79.6%) were identified harboring HIV-1 DNA, and this frequency is also significantly higher than that in the brain (18.8%) ($P<0.0001$) (**Figure 2.3**).

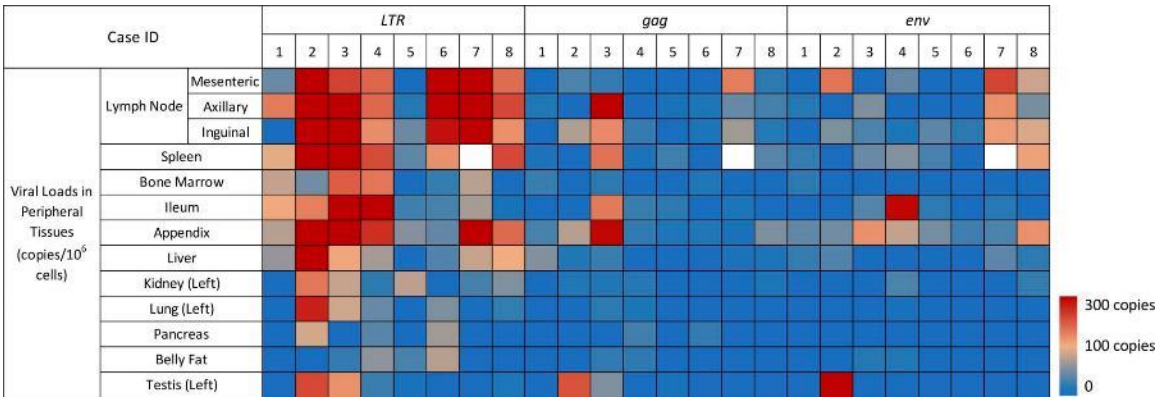

Figure 2.3. Heatmap of subtype C HIV-1 DNA in aviremic periphery. A heatmap displays the abundance of 3 subtype C HIV-1 DNA (LTR, gag, and env) in peripheral anatomical locations of the 8 aviremic subjects based on qPCR analysis. Blocks with colors indicate undetectable (0) DNA copy (blue) to increased DNA copies (up to 1538 copies/1 × 10^6 cells). Spleen of case 7 failed to be sampled (blank cell). HIV-1 DNA copies were identified by qPCR with 100 ng genomic DNA as a template. All samples were analyzed in triplicate qPCR reactions, and viral DNA copy numbers were calculated as the mean of triplicate and normalized to 1 million cells.

Unlike the brain, no specific peripheral tissue was found to be completely free of viral DNA. Furthermore, there is no correlation between the viral burden in the brain and periphery. Subtype C HIV-1 proviral DNA copies varied in different peripheral tissues, which indicated different proviral reservoir sizes. Notably, of the 13 types of peripheral tissues analyzed, only two types of lymphoid tissue, the LNs and spleen, and two types of GI tract tissue, the ileum and appendix, were found to contain viral *LTR* DNA in all aviremic subjects (**Figure 2.3**). Furthermore, compared to other peripheral tissues, LNs, spleen, Ileum, and appendix showed higher viral *LTR* DNA burdens, with the median of *LTR* DNA copies at 308, 213, 88, 211 copies/10^6 cells, respectively (**Table 2.2**). Another lymphoid tissue, bone marrow, was found to have viral *LTR* DNA in 6 aviremic subjects with the median *LTR* DNA copies of 62 copies/10^6 cells. Other tissues involved in different human organ systems were also found to harbor HIV-1 *LTR* DNA. They include the liver, kidney, lung, pancreas, adipose tissue, and testis, which have the median of HIV-1 *LTR*

DNA copies at 75, 41, 33, 0, 11, 8 copies/10^6 cells, respectively. The highest viral *LTR* DNA copy is 1538 copies/10^6 cells in the mesenteric LN of case 7 (**Table 2.2**).

Among the 82 HIV-1 *LTR* DNA harboring peripheral tissues, 56 tissues were found to also contain HIV-1 *gag* DNA, and 43 tissues were further identified to harbor HIV-1 *env* DNA, indicating that intact HIV-1 provirus might be integrated into the host genome of those 43 tissues. Interestingly, only the LNs and appendix were determined to harbor all three proviral genes in all aviremic cases (**Table 2.2**). Proviruses that harbor HIV-1 *LTR*, *gag* and *env* DNA were also found in the spleen of cases 1, 3, 4, 5 and 8. In addition, potential intact proviruses were also detected in the bone marrow, ileum, liver, kidney, lung, adipose tissue, and testis of some cases, whereas there was no detectable viral *env* DNA in any pancreas tissue (**Table 2.2**).

Table 2.2. Subtype C HIV-1 viral DNA copies in the aviremic case periphery

Viral DNA in Peripheral Tissues (copies/10^6 cells)																																
Case ID		1			2			3			4			5			6			7			8									
LN	Mesenteric	44	*0*	**0**	1102	*32*	**166**	223	*22*	**0**	183	*4*	**42**	0			541	*0*	**0**	1538	*156*	**220**	174	*20*	**84**							
	Axillary	159	*15*	**18**	342	*0*	**0**	983	*645*	**53**	180	*0*	**0**	18	*7*	**0**	338	*12*	**0**	570	*43*	**134**	215	*29*	**50**							
	Inguinal	0			412	*74*	**52**	868	*141*	**32**	139	*22*	**12**	45	*3*	**39**	278	*10*	**20**	455	*67*	**121**	134	*18*	**90**							
Spleen		94	*8*	**23**	601	*0*	**0**	398	*170*	**44**	213	*8*	**55**	40	*27*	**30**	134	*0*	**0**	NA			215	*37*	**117**							
Bone Marrow		81	*25*	**20**	47	*0*	**0**	192	*20*	**0**	165	*0*	**0**	0			23	*14*	**0**	77	*0*	**0**	0									
Ileum		108	*0*	**0**	153	*0*	**0**	348	*160*	**36**	537	*25*	**291**	28	*20*	**19**	31	*0*	**0**	69	*10*	**18**	7	*0*	**0**							
Appendix		76	*31*	**41**	358	*75*	**47**	1169	*291*	**132**	244	*21*	**81**	56	*11*	**49**	41	*14*	**26**	430	*7*	**32**	179	*53*	**133**							
Liver		62	*54*	**23**	338	*14*	**34**	112	*25*	**0**	68	*0*	**0**	0			35	*0*	**0**	82	*8*	**38**	104	*9*	**20**							
Kidney (Left)		0			164	*13*	**0**	82	*13*	**0**	20	*17*	**32**	78	*0*	**0**	0			29	*0*	**0**	54	*12*	**23**							
Lung (Left)		0			261	*0*	**0**	85	*20*	**0**	43	*12*	**5**	0			52	*0*	**0**	4	*0*	**0**	23	*0*	**0**							
Pancreas		0			88	*0*	**0**	0			37	*28*	**0**	0			67	*22*	**0**	0			0									
Belly Fat		0			0			22	*21*	**17**	60	*20*	**15**	31	*0*	**0**	75	*0*	**0**	0			0									
Testis (Left)		0			215	*205*	**650**	134	*53*	**0**	25	*0*	**0**	6	*5*	**0**	0			0			11	*0*	**0**							

Note: Regular (*LTR* DNA); Italic (*gag* DNA); Bold (*env* DNA); 0 (HIV DNA negative)

The comparison of the variations in the proviral DNA copy number among different tissues from different cases are shown in **Figure 2.4**. In scatter plots, quantified

viral DNA copy numbers from tissues of case 1 to 8 were indicated as red, orange, yellow, green, blue, purple, pink, and gray dots, respectively. In general, three cases with relative shorter postmortem interval (PMI), cases 2 (7 hours), 3 (3 hours) and 4 (4 hours) had relatively higher overall viral *LTR* DNA burden than that in other three cases with longer PMI, cases 1 (30 hours), 6 (26 hours), and 8 (33 hours) (**Figure 2.4A**).

Moreover, although the PCR detection may have limited our ability to capture extremely low levels of viral DNA in some tissues, we have detected more tissues harboring HIV-1 *LTR* DNA for cases 2, 3, and 4 than cases 1, 6, and 8 (**Figure 2.4A**). Particularly, viral *LTR* DNA was detected in nearly every peripheral tissue of cases 2, 3 and 4, except the belly fat of case 2 and pancreas of case 3 (**Figure 2.4A, Table 2.2**). In contrast, case 1 had the least peripheral tissues with detectable HIV-1 DNA. However, except for displaying a negative correlation in ileum (correlation coefficient = -0.8015, R^2 = 0.6424), we did not observe the correlation of PMI with levels of viral DNA detected in other peripheral tissues.

With regard to potential intact proviruses, cases 4 and 8 have most peripheral tissues, 8 and 7 tissues, respectively, harboring HIV-1 *LTR*, *gag*, and *env* DNA, whereas case 6 only had two peripheral tissues (inguinal LN and appendix) containing all three viral genes. Additionally, case 5 displayed lowest overall subtype C HIV-1 reservoir magnitude possessing <100 copies/10^6 cells of proviral DNA in every HIV-1 provirus containing peripheral tissues (**Figure 2.4, Table 2.2**). For most cases, those with higher viral DNA copies in the LNs appeared to have higher viral DNA copies in other peripheral tissues, except for cases 6 and 7 whose viral DNA copies in LN were high but low in other peripheral tissues relatively to other cases.

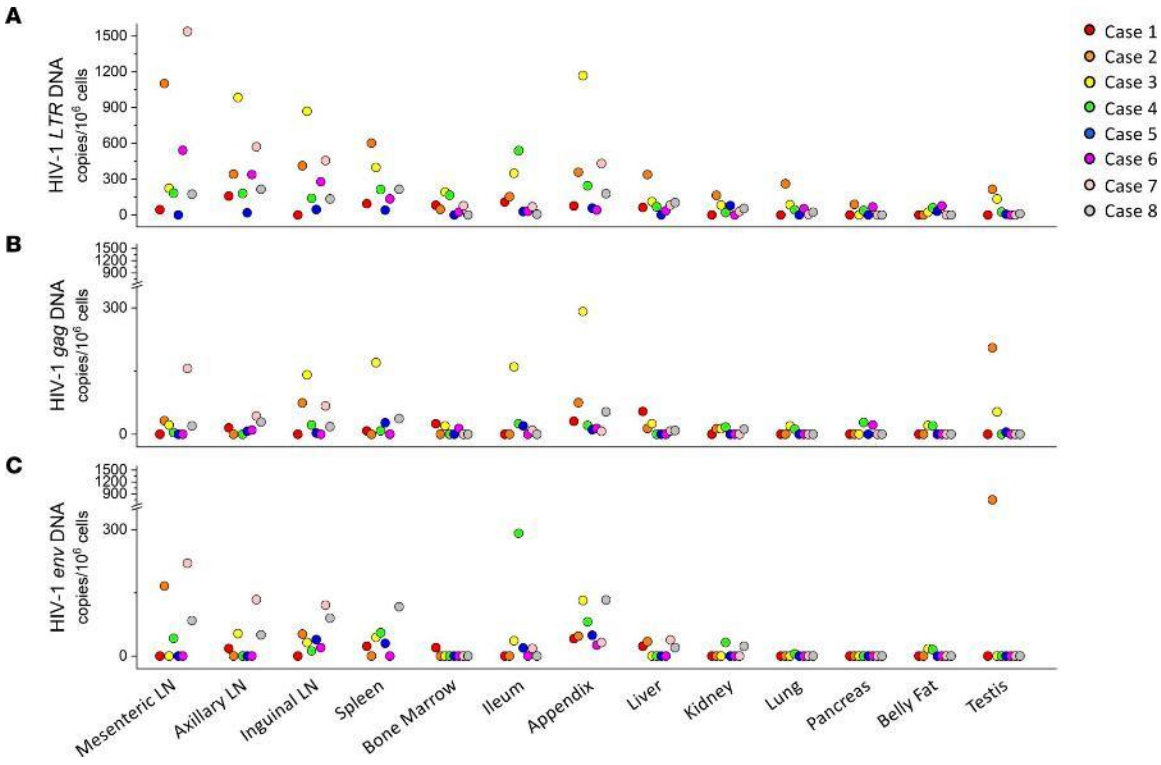

Figure 2.4. Subtype C HIV-1 DNA quantification in peripheral anatomical locations. Scatter plots sorted by different peripheral tissues and colored for different subjects. The y axis showed HIV-1 DNA copies/1 × 10^6 cells. (A) HIV-1 LTR DNA in the periphery. (B) HIV-1 gag DNA in the periphery. (C) HIV-1 env DNA in the periphery. In total, 100 ng genomic DNA was used in each qPCR reaction as template. The dots represent the means of triplicate qPCR reactions for the HIV-1 DNA copies.

To confirm our real time qPCR results, we also performed ultra-sensitive digital PCR (dPCR) to obtain absolute HIV-1 DNA copies. Considering the similar amplification efficiencies of *LTR*, *gag*, and *env* primers and the higher overall viral *LTR* DNA copies in cases 2, 3 and 4, we have utilized the same *LTR* primers and same batch of genomic DNA used in qPCR from occipital lobe, mesenteric LN, appendix, and testis of cases 2, 3 and 4, to perform dPCR. The dPCR results showed good correlation with qPCR results for both CNS tissue occipital lobe and three other peripheral tissues (**Figure 2.5**). Overall, it showed a positive qPCR/dPCR efficiency correlation with a 0.7054 R^2 value (**Figure 2.5B**). The dPCR results further confirmed and strengthened our findings by qPCR.

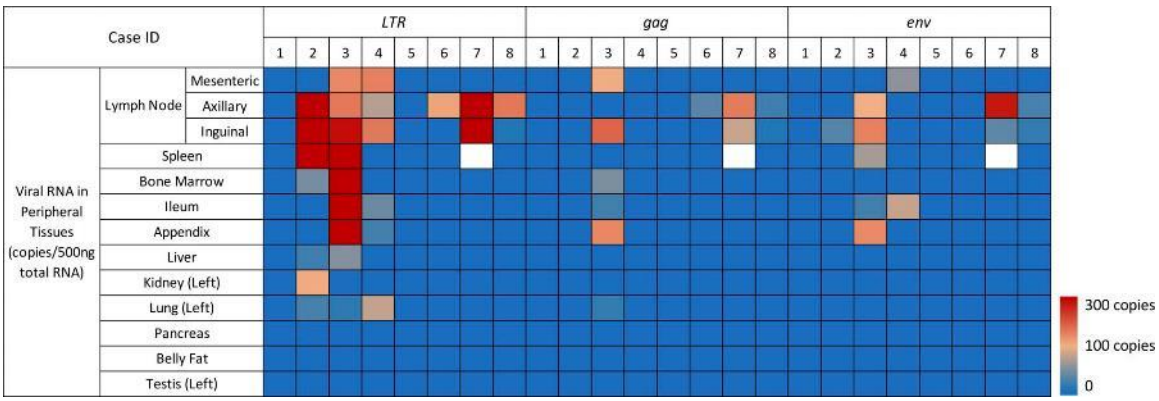

Figure 2.5. Heatmap of subtype C HIV-1 RNA in aviremic periphery. A heatmap displaying viral RNA transcript (LTR, gag, and env) abundance in the periphery of 8 aviremic subjects was produced by qPCR analysis. Blocks with colors indicate undetectable (0) DNA copy (blue) to increased RNA copies (up to 1,566 copies/500 ng total RNA). HIV-1 RNA copies were identified by qPCR with 500 ng input RNA as template. All samples were analyzed in duplicate qPCR reactions.

Persistent expressing of subtype C HIV-1 proviruses in periphery

It is well documented that defective integration is common in retroviruses (55, 201-203), the presence of viral *LTR* DNA but lack of *gag* or *env* DNA in some tissues of our cohort suggests the existence of defective subtype C HIV-1 reservoirs in those tissues, while the higher *LTR* DNA copies than *gag* or *env* DNA copies in most tissues suggests that intact and defective subtype C HIV-1 proviruses might co-exist in those tissues. However, proviral DNA detection in tissues is not necessarily indicative of a functional latent reservoir. Therefore, total RNA was extracted from frozen tissues that harbored viral DNA and subjected to one-step qRT-PCR with HIV-1 *LTR*, *gag*, and *env* primers after DNase I treatment.

As seen in **Figure 2.5** and **Table 2.3**, HIV-1 *LTR*, or *gag*, or *env* RNA was detected in 6 of 8 aviremic cases (undetectable in cases 1 and 5). Subtype C HIV-1 RNA was mainly detected in lymphoid tissues (LNs, spleen, bone marrow), and the predominant site of concordant viral gene expression was the LNs. Among those 6 cases

harboring viral RNA in the lymph nodes, three cases (cases 6, 7 and 8) did not have any detectable viral RNA besides the lymph nodes.

Table 2.3. Copy numbers of subtype C HIV-1 RNA in peripheral tissues harboring viral DNA

Viral RNA in Peripheral Tissues (copies/500 ng input RNA)																							
Case ID		1	2			3			4			5	6			7			8		
LN	Mesenteric	0	0			143	*105*	-	153	*0*	**59**	-	0			0			0		
	Axillary	0	1609	-	**0**	164	*0*	**102**	75	-	-	0	115	*37*	-	1566	*157*	**272**	141	*26*	**30**
	Inguinal	-	466	*0*	**36**	283	*184*	**152**	162	*0*	**0**	0	0			794	*83*	**40**	13	*14*	**22**
Spleen		0	423	-	**0**	326	*0*	**69**	0			0	0			NA			0		
Bone Marrow		0	49	-	**0**	444	*51*	-	0			-	0			0			-		
Ileum		0	0			497	*27*	**28**	45	*0*	**82**	0	0			0			0		
Appendix		0	0			481	*144*	**141**	28	*0*	**0**	0	0			0			0		
Liver		0	26	*0*	**0**	56	*0*	-	0			-	0			0			0		
Kidney (Left)		-	106	*0*	**0**	0			0			0	-			0			0		
Lung (Left)		-	29	-	**0**	20	*22*	-	81	*0*	**0**	-	0			0			0		
Pancreas		-	0			-			0			-	0			-			-		
Belly Fat		-	-			0			0			0	0			-			-		
Testis (Left)		-	0			0			0			0	-			-			0		

Note: Regular (*LTR* RNA); Italic (*gag* RNA); Bold (*env* RNA); 0 (HIV RNA negative); - (HIV DNA negative)

As shown in **Figure 2.6** for case 2 (orange), case 3 (yellow) and case 4 (green) which had higher overall viral *LTR* DNA burden, viral *LTR*, and/or *gag*, and/or *env* RNA were also sporadically detected in spleen, bone marrow, ileum, appendix, liver, kidney, and lung at variable RNA copies in addition to lymph nodes. The presence of viral RNA indicated potential persistent expression of proviruses in those tissue reservoirs. Pancreas, testis, and belly fat tissues in all aviremic individuals were found to be devoid of detectable subtype C HIV-1 RNA. Additionally, all tissues that expressed viral *gag* or *env* RNA were found to contain viral *LTR* RNA (**Figure 2.6**).

In the peripheral tissues harboring HIV-1 DNA, more viral *LTR* RNA (ranging 0 to 1609 copies/500 ng total RNA) was detected, compared to viral *gag* RNA (ranging 0 to

184 copies/500 ng total RNA) (p=0.0045) or *env* RNA (ranging 0 to 272 copies/500 ng total RNA) (p=0.0049), respectively. The main reason is that our *LTR* primers target proviral sequence region encoding leader exon 1 which exists in all HIV-1 transcripts variants. It is also possible that there are undefined promoters outside the provirus allowing the 3' end *LTR* gene to transcribe, or some subtype C HIV-1 defective proviruses with deletions in *gag* or *env* region were transcribed, hence leading to more *LTR* transcripts than *gag* or *env*.

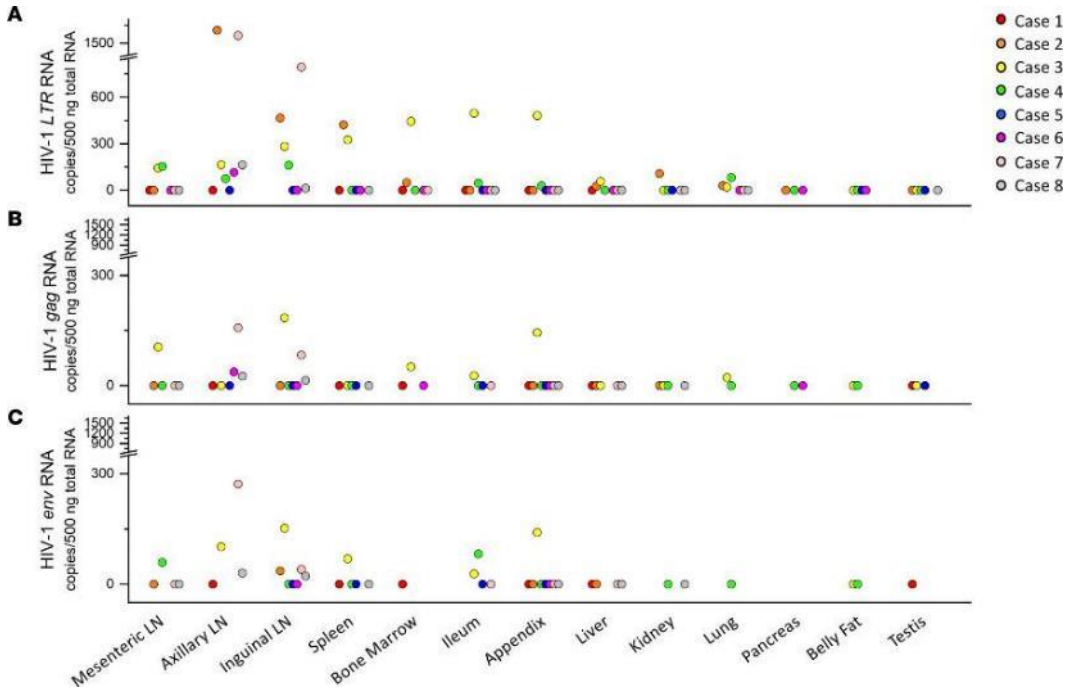

Figure 2.6. Subtype C HIV-1 RNA quantification in peripheral tissues harboring viral DNA. Scatter plots sorted by different peripheral tissues and colored for different subjects. The y axis showed HIV-1 RNA copies/500 ng input RNA. (A) HIV-1 LTR RNA in the periphery. (B) HIV-1 gag RNA in the periphery. (C) HIV-1 env RNA in the periphery. In total, 500 ng input RNA was applied in each qPCR reaction as a template. Viral RNA copy numbers were calculated as the mean of duplicate qPCR reactions.

The appendix as a novel subtype C HIV-1 reservoir

To our knowledge, the appendix tissue has not previously been investigated or reported as an HIV-1 reservoir. The systematic nature of our sample collection has

allowed this first investigation of the appendix as a potential reservoir in fully suppressed subtype C HIV-1 infection. Interestingly, subtype C HIV-1 *LTR*, *gag* and *env* DNA were detected in the appendix from all aviremic individuals, indicating the very likely presence of full-length subtype C HIV-1 proviral integrants. HIV-1 *LTR*, *gag* and *env* RNA were also detected in appendix tissue from case 3, suggesting a possible persistent reservoir in this unique tissue. Blood contamination was unlikely to confuse our results from tissue samples because all our cases have undetectable pVL. To identify whether proviral DNA resulted from lymphocyte infiltration into appendix under inflammation, we first perform histology on appendix FFPE of all aviremic subjects. Classical appendicitis histology would display scattered clusters of dark blue dots (hematoxylin-stained lymphocyte nuclear) in the muscle layer, which we did not observe in any appendix FFPE slide of the 8 aviremic cases, indicating proviral DNA was not from infiltrated lymphocyte (**Figure 2.7**).

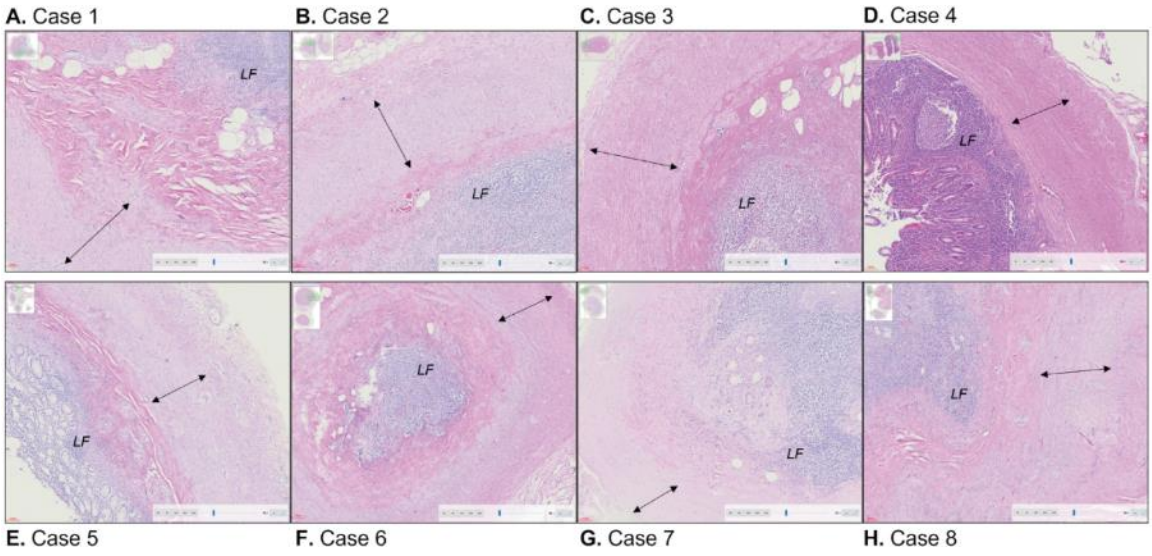

Figure 2.7. No detectable inflammation in the appendix of the aviremic subjects. The inflammatory statuses, as a pathological indicator of appendicitis of the 8 aviremic appendix tissues were analyzed by histology. Classical appendicitis histology would display scattered clusters of dark blue dots (hematoxylin-stained lymphocyte nuclear) in the muscularis propria,

which was not observed in the appendix FFPE slides of 8 aviremic cases (panel A-H). Black arrows mark the muscularis propria and LF means lymphoid follicle. Thumbnails and magnification of representative areas (10X) are also shown.

To further determine whether proviral signal quantified in frozen tissues corresponded to parenchymal cell infection and the potential cell types involved, we performed RNAscope with subtype C HIV-1-specific probes on case 3 appendix tissue FFPE. Adjacent 6 µm sections were cut from case 3 appendix tissue FFPE, and then processed for subtype C HIV-1 DNA and RNA detection by RNAscope and CD4 staining by immunohistochemistry (IHC). Using adjacent sections, we stained different cells in the same area of consecutive slides with CD4 cell markers and subtype C HIV-1 specific RNAscope probe for HIV-1 nucleic acids. The unique structure of the appendix allowed us to focus precisely on a small area of adjacent slides where the HIV nucleic acid is concentrated. In agreement with our qPCR results, both viral DNA (horizontal arrows) and RNA (vertical arrows) were detected in case 3 appendix (**Figure 2.8**).

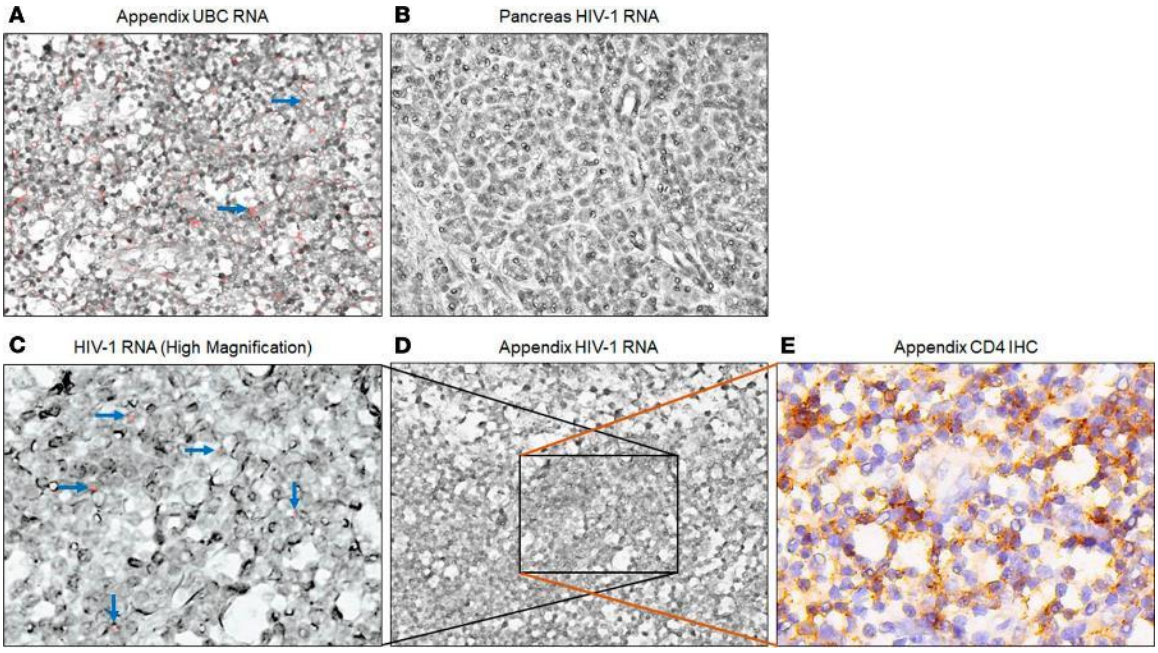

Figure 2.8. Adjacent 6 µm FFPE sections of the appendix of case 3 were stained by RNAscope or IHC. (A) Homo sapiens ubiquitin C^{+} (UBC^{+}) control in the appendix of case 3. (B) No HIV-1 DNA or RNA detected in the pancreas (HIV-1 DNA negative by qPCR) of case

3. (D) RNAscope for HIV-1 nucleic acid in case 3 appendix. (C) Higher magnification of D to show HIV-1 DNA and RNA in the appendix of case 3. (E) CD4 staining by IHC on the adjacent section of D, shown as the same region of C. Representative UBC^{+} signals are pointed by blue arrows in A, while signals positive for HIV-1 DNA are indicated by horizontal arrows in C, shown as pink foci in the nucleus, and HIV-1 RNA signals are pointed by vertical arrows, shown as pink foci outside of the nucleus. CD4 staining is shown brown in E. Black rectangles highlight representative regions containing cells positive for HIV-1 RNA and/or DNA and CD4 expression.

Viral RNA (pink foci) was localized outside the counterstained nuclei while viral DNA staining colocalized with the nucleus. The co-localization of viral DNA signal (pink foci) and CD4 staining (brown) in appendix tissue suggested appendix-associated lymphoid tissues (CD4 expressing cells) can persist as a potentially transcriptionally active and treatment resistant cellular reservoir for subtype C HIV-1 (**Figure 2.8C&E**). Collectively, the results showed that appendix is a subtype C HIV-1 tissue reservoir in our aviremic subjects analyzed.

Discussion

Characterizing the distribution and magnitude of HIV-1 reservoirs in tissues other than lymphoid cells, as well as their capacities for reactivation is a crucial step toward developing optimal strategies to eliminate or permanently silence HIV-1 proviruses in PLWH under ART suppression. The majority of HIV-1 tissue reservoir studies have focused on subtype B HIV-1, which is prevalent in high-resource European and North American countries. Yet even in those settings, technical limitations and the difficulty in obtaining appropriate tissues have resulted in only a few HIV-1 studies that encompassed diverse human tissues systems, such as CNS tissues, lymphoid tissues, GI tract tissues, etc., to investigate HIV-1 subtype-B tissue reservoirs (92, 186). Instead, blood samples or those collected through routine biopsy methods, such as colonoscopy or surgically obtained colon tissue, have been the focus (190, 204). Alternatively, macaques or

humanized mice have been systematically sampled (171, 174, 205). These approaches have indeed provided a substantial body of about subtype B HIV-1 reservoirs. Despite the global prevalence of subtype C HIV- 1 and its detection in PBMCs of ART naïve individuals (195), the localization, magnitude and expression activity of those reservoirs after ART suppression is relatively unknown. In part this is because pathology resources and individuals with appropriate skills and access to instrumentation for systematic post-mortem invetigations are uncommon in the sub-Saharan which is the epicenter of subtype C HIV-1 infection. This study focused on sensitive recruitment of defined postmortem tissue collection, systematic sampling, and careful fixation and processing focused toward unambiguous downstream molecular applications on subtype C HIV-1 infected postmortem tissues, through our long-term collaborative pathology laboratory resource at the University of Zambia Teaching hospital in Lusaka, Zambia. This unique postmortem collection of frozen and FFPE specimens allowed us to accurately identify potential anatomical locations of subtype C HIV-1 reservoirs.

In previous studies, the brain has been reported as a reservoir of subtype B HIV-1 even under ART suppression, despite being somewhat immunologically privileged and separated from the circulating immune system by the blood brain barrier (BBB) (206-208). It is generally believed that the relatively poor penetration of ART drugs into the brain due to the protection of the BBB, and therefore the limited capacity of ART to eliminate infiltrated HIV-1 infected cells or cell-free HIV-1 virions is the main reason that brain serves as subtype B HIV-1 reservoir.

Currently, little is known about the extent to which the brain serves as a reservoir for subtype C HIV-1, and likewise, long-term neurocognitive impacts of subtype C HIV-1

are unclear in the ART treated and virally suppressed. A previous study showed that subtype B HIV-1 DNA was detected in 48/87 (55.2%) of brain tissues from HIV-1 infected ART-suppressed patients at levels >200 HIV-1 DNA copies/10^6 cell equivalents (92). In contrast, our laboratory had detected subtype C HIV-1 proviral DNA at low and variable levels in CNS tissues regardless of ART success or failure (196). However, the small size of ART-suppressed cohort (n=4) and lack of systematic collection of other major organ tissues had limited the exploration of subtype C HIV-1 reservoirs throughout the bodies. In this study, we demonstrated that HIV-1 DNA was only detected in 12/64 (18.8%) of Zambian brain tissues from subtype C infected but aviremic individuals. And when detectable, the brain tissue proviral levels were quite low (< 100 HIV-1 DNA copies/10^6 cell equivalents). Our findings are consistent with previous studies that have suggested lower neurotropism of subtype C in comparison to subtype B HIV-1. First, clinically, subtype C HIV-1 infected patients showed a reduced incidence of HAND (209). In addition, severe combined immunodeficiency (SCID) mice injected with subtype C HIV-1-infected macrophages exhibited less cognitive deficits and brain pathology than that infected with subtype B HIV-1 (210). Furthermore, subtype C HIV-1 was found to have slower replication kinetics in monocyte-derived macrophages, resulting in lower levels of macrophage-mediated neurotoxicity *in vitro* (211). Together these investigations suggest subtype C HIV-1 differentially accesses the CNS parenchyma in comparison to subtype B, indicating that brain is an unfavorable or inaccessible reservoir site for subtype C HIV-1. However, despite our sampling of eight distinct brain regions it is still possible that subtype C proviral DNA preferentially integrates and establishes reservoirs in very specific tissue locations in the CNS that we

failed to sample. In addition, the presence of detectable proviral sequences despite the absence of viral RNA in the brain suggests the possibility that some latent subtype C HIV-1 reservoirs in the CNS may be intact in some PLWH. Studies on subtype B HIV-1 have shown that microglia, astrocyte, and macrophage can be infected by HIV-1 (212-214). Unfortunately, these approaches cannot be readily applied to the brain sections from aviremic cases to determine the subtype C HIV-1 infected cell types in the brain, because the subtype C HIV-1 DNA copy was so low in the brain that the total number of cells needed to detect infected cells with detectable viral DNA is beyond what can be observed in a single brain section.

Infection and reservoir formation in peripheral tissues has been adequately investigated for subtype B HIV-1. Lymphoid and GI tract tissues had been identified as primary sites of subtype B HIV-1 infection and persistence (186). In agreement with these observations, we also detected subtype C HIV-1 reservoirs in lymphoid and GI tract tissues. These sites (LNs, spleen, ileum, and appendix) showed significantly higher levels of subtype C HIV-1 DNA than other peripheral tissues. Consistent with subtype B studies (215, 216), we likewise found subtype C HIV-1 RNA primarily in lymphoid and GI tract tissues. We detected subtype C HIV-1 DNA in diverse peripheral tissues, including testis and adipose tissues, which remain the subject of some debate as subtype B HIV-1 reservoirs. Nevertheless, subtype C HIV-1 proviruses were also detected in all other peripheral tissues analyzed but with variable levels, and differ among individuals. Our results suggest that, even under ART suppression, subtype C HIV-1 tissue reservoirs are unevenly distributed and occur at various magnitudes throughout the body, posing a huge challenge for a functional or sterile cure of subtype C HIV-1.

The co-existence of three viral genes indicated the potential for full-length or nearly full-length HIV-1 proviruses in those tissues. Single genome amplification and sequencing (SGA/S) would increase the sensitivity of integrity analysis of proviral genome, but these methods require high cellular input, which may limit the ability to explore subtype C HIV-1 reservoirs. In tissues with relatively low infected cell numbers, for instance, the CNS, adipose tissue, and testis, these analyses would be prohibited. In such cases our 3-gene amplification method provides a viable approach to assess the potential intactness of subtype C reservoirs. However, recent studies utilizing intact proviral DNA analysis (IPDA) have shown that both intact and defective subtype B HIV-1 proviruses exist in tissue reservoirs, with the majority being defective (217-219). In agreement with those findings, we also detected lack of stoichiometric equality of *LTR*, *gag* and *env* DNA detection in the same tissue, suggesting that intact and defective subtype C HIV-1 proviruses might also co-exist. Notably, among 94 tissues of our cohort harboring subtype C HIV-1 DNA, 48 tissues (51.1%) have detectable *LTR* but lack *gag* or *env* DNA, indicating the majority of proviruses are defective in subtype C HIV-1 reservoirs.

It would be important to determine whether proviruses in the reservoirs are replication-competent, whether they are intact and express viral RNA and protein to better determine whether they may stay latent or persistent expressing, particularly in those infected individuals under ART suppression. Although quantitative viral outgrowth assay (QVOA) is considered as gold standard assay for detecting and measuring potential for reactivation of replication-competent HIV-1 virus (220-223). Our limitation is that QVOA has not yet been successfully conducted from postmortem tissues. From tissues

harboring viral DNA, we tested for expression of viral *LTR*, *gag*, and *env* and found that subtype C HIV-1 RNA can only be detected in peripheral (non-CNS) tissues, suggesting that proviruses in those tissue reservoirs might be replication-competent and persistently expressing viral RNA. We attempted IHC for HIV-1 p24 CA on the FFPE tissue the inguinal LN from case 3 which had the highest *gag* RNA copies (184 copies per 500 ng RNA input) in the corresponding frozen tissue, but there was no detectable viral p24 in the FFPE sections. It is possible there was a very low level p24 protein expressed in FFPE tissues but below the detection sensitivity of IHC or the efficiency of p24 antibody we used.

Notably, the appendix, a GI tract tissue rich in lymphoid cells and recently described as having important immune functions (224), has not previously been reported as an HIV-1 tissue reservoir. In our analysis, we detected viral *LTR*, *gag*, and *env* DNA in all 8 appendix tissues, implying the presence of at least some intact subtype C genomes in the appendix. Moreover, viral RNA has also been detected in two appendix tissues (cases 3 and 4). Interestingly, previous studies had revealed that the prevalence of appendicitis in PLWH is 4-fold higher than that in uninfected individuals (225-227), and opportunistic infections and immune reconstitution inflammatory syndrome (IRIS) at initiation stage of ART were thought to be the reasons. Given our findings, there may also be active HIV-1 proviruses existing in the appendix of those other cases studied, and persistent HIV-1 expression could be another reason for the higher occurrence of appendicitis in HIV infected people. However, the co-localization of CD4 staining with proviral DNA signal is not sufficient to identify the infected cell type in appendix because CD4 is expressed by multiple immune cell types, such as T cell, macrophage, and dendritic cell. Defining

the specific cell type of the appendix HIV-1 reservoir needs to be further studied via multiple immunostainings with different cell markers. Additionally, whether appendix can harbor ART resistant HIV-1 also needs to be determined.

The study had some clear limitations. First, we only had eight aviremic cases for full body post-mortem evaluation. A bigger cohort size could potentially provide more information on subtype C HIV-1 reservoirs. Second, as a result of deaths in the community as opposed to be under clinical care, our study subjects lacked detailed clinical information, including: HIV diagnosis date, ART initiation date, ART adherence, HIV load data, additional health status, and CD4 cell counts prior to death, etc. This information is often difficult to obtain even in studies with subtype B under different settings, thus it has been very challenging to gather such information in Zambia where clinical records are not typically computerized or linked. Furthermore, subtype C HIV-1 is responsible for approximately 99% of HIV infections in Zambia, and we hence failed to sample a single subtype B HIV-1 infected Zambian subject in the past 4 years of our study. It is also not possible to obtain autopsy samples from HIV/AIDS diseased cases in North America or Europe or from countries with subtype B infection to establish tissue matched controls for subtype C HIV-1, especially of the need to systematically collect 8 brain and 13 peripheral subtype B HIV-1 infected biopsy or autopsy tissues from a single individual. Additionally, although dPCR results from several tissues supported our qPCR results, the sensitivity of qPCR may limit our ability to capture extremely low level of subtype C HIV-1 proviruses in some tissues. Besides case 3 appendix FFPE tissues, RNAscope was also performed on case 2 mesenteric LN, case 3 axillary LN, and case 4 appendix tissues, estimated to have lower copies of proviral DNA by PCR. Nevertheless,

no proviruses were detectable in those three FFPE tissues by RNAscope. It is possible that low copy number of the HIV-1 proviruses may not be evenly distributed and were not in the embedded section of the tissues we investigated, or RNAscope may still be not sensitive enough to identify very low level of proviruses in subtype C HIV-1 infected aviremic FFPE tissues. Finally, since all the subjects were deceased, the generalizability of our findings to healthy PLWH cannot be ascertained.

In summary, this study demonstrates that subtype C HIV-1 DNA copies varied among viral suppressed individuals and anatomical compartments, and the CNS is poorly accessed or not a robust reservoir. To our knowledge, this is the first study which systematically quantify the magnitude and distribution of subtype C HIV-1 reservoirs in human tissues from different compartments throughout the body of subtype C HIV-1 infected individuals under ART suppression. Our findings that the appendix is a potentially important persistent reservoir, but CNS is not for subtype C HIV-1 is significant. Whether subtype B or other HIV-1 subtypes can establish a persistent reservoir in the appendix needs to be examined. Whether other non-subtype B HIV-1 is similar to subtype C HIV-1 that do not efficiently establish persistent infection in the CNS also needs to be determined. Considering that over 50% prevalence of subtype C HIV-1 among all HIV-1 infections and the relative high economic burden caused by lifelong ART, especially in low-source regions, our findings that only few and very low level subtype C HIV-1 DNA with no detectable viral RNA in the brain but can be readily detectable in the appendix could provide useful information for the cure effort against subtype C HIV-1, including optimization and administration of ART towards the various tissue reservoirs involved.

CHAPTER 3:

CELLULAR TROPISM AND VIRAL GENETICS IN APPENDIX TISSUE RESERVOIRS OF SUBTYPE C HIV-1 INFECTED AVIREMIC INDIVIDUALS

Abstract

Antiretroviral therapy (ART) can suppress plasma viral loads in people living with HIV-1 (PLWH) and enable them to have a normal lifespan. However, the infection cannot be readily cured because HIV-1 persists in various tissue reservoirs, and lifelong ART is required since HIV-1 will rebound after ART cessation. There are a number of well characterized tissue reservoirs such as lymph nodes and gut-associated lymphoid tissues that can harbor latent viruses. We have recently identified the human appendix as a novel tissue reservoir in subtype C HIV-1 infected individuals. Here we utilize single genome analysis (SGA) of the amplified HIV-1 *env* DNA and compared the viral sequences obtained from appendix tissues and lymph nodes of the same subtype C infected individuals. We found that the viral populations from the appendix were less heterogeneous when compared to the lymph nodes, suggesting that there could be reduced selective pressures by ART or there may be a unique compartmentalization of HIV-1 in the appendix. Furthermore, we demonstrated that the follicular dendritic cells (FDCs) within the appendix are the main cell types harboring proviral DNA, representing a key cell population for viral persistence in this tissue reservoir. These results highlight the importance of analyzing all potential tissue reservoirs, including the less characterized tissues across different HIV-1 subtypes, to improve our understanding of HIV-1 persistence and inform tailored therapeutic strategies that include considerations for the diverse tissues reservoirs that may differ across HIV-1 subtypes.

Introduction

With approximately 39.0 million individuals living with HIV-1 worldwide, the proposed ending of the AIDS epidemic by 2030 will continue to pose a challenge (12). This is mainly due to persistent viral infection in different tissue reservoirs established soon after acute HIV infection during the viremic phase, with viruses spreading to, and populating various tissues throughout the body (228-232). Long-term antiretroviral therapy (ART) can suppress plasma viral loads (pVLs) to undetectable levels (aviremia) in people living with HIV (PLWH), yet it is not curative because of its inability to eliminate integrated proviruses that are persistence in tissue reservoirs (233-235). HIV-1 could rebound from different tissue reservoirs after the interruption of ART (235, 236).

HIV-1 is characterized by its high genetic diversity, with multiple subtypes and circulating recombinant forms (CRFs) (26, 237). Most of the research to date has focused on subtype B HIV-1 predominant in resource-rich Western countries (237). Previously studies have shown that, in ART-treated aviremic individuals, subtype B proviruses and viral production were readily detectable in the blood (97, 98), lymphoid tissues (99-101), gastrointestinal (GI) tract tissues including gut-associated lymphoid tissues (GALTs) (102-104), and central nervous system (CNS) (105-107). Other peripheral tissues including genital tract tissues (108), liver (109), lung (238), kidney (111), pancreas (112), and prostate (113), were also reported as potential subtype B HIV-1 tissue reservoirs. Despite extensive research, the complete landscape of subtype B HIV-1 reservoirs is still not fully understood, and recent studies suggest that HIV proviruses can also persist in other less characterized tissues, such as the adipose tissue (114). Additionally, HIV-1 infected cell types varied among different tissues, such as CD4+ T cells in different

tissues (114-116), microglia in the CNS (117), and macrophages and dendritic cells (DCs) in some peripheral tissues (108, 118-121).

Despite the fact that subtype C accounts for nearly 50% of all HIV-1 infections, few HIV studies have focused on this subtype. This is because subtype C HIV-1 is prevalent mostly in resource limiting setting such as sub-Saharan Africa (SSA), India, and parts of South America, where it has been difficult to conduct systematical molecular investigation. Notably, utilizing postmortem tissues from virally suppressed individuals enrolled in SSA, our laboratory had identified subtype C tissue reservoirs throughout the body (239). Although subtype C HIV-1 proviruses were also mainly detected in lymphoid and GI tract tissues, unlike subtype B, it poorly accesses the CNS (239). These findings suggest that subtype-specific variations of HIV-1 tissue reservoirs might exist. Furthermore, our lab had also recently identified that human appendix, which was never reported previously as a HIV-1 tissue reservoir, harbored relatively high copies of subtype C HIV-1 proviral DNA in most HIV+ individuals despite viral suppression, suggesting the potential role of appendix serving as a novel HIV-1 tissue reservoir (239, 240). Although almost every GI tract organ, including esophagus (112, 241) , stomach (241), duodenum (112, 241-243), jejunum (112), ileum (112, 242, 244), colon (112, 241, 242), and rectum (245, 246), has been identified as HIV-1 tissue reservoir in subtype B HIV-1 studies, the appendix has not been investigated since it has been historically considered as vestigial.

The human vermiform appendix has recently gained interest for its potential immunological functions, acting as a site for immune cell priming and potentially contributing to regional immunity within the intestine (247-249). It possesses a similar

structure and immune cell composition as the small intestine Peyer's patches (PP) (250). The appendix has also been proposed to act as a "sanctuary" for intestinal bacteria by offering protection from diarrheal clearing and intestinal peristalsis, which could be attributed to the location of the appendix and its tubular, cul de sac morphology (251). Its histological structure includes muscularis (MS), submucosa (SM), and lamina propria with multiple lymphocyte follicles (LFs) (248). The appendix contains dense concentrations of immune cells, including B cells, T cells, dendritic cells, macrophages, and follicular dendritic cells (FDCs), which could provide a favorable setting for HIV-1 replication and persistence (248, 252).

Building on our previous findings that human appendix could be a novel HIV-1 tissue reservoir under suppressive ART (239, 240), we sought to delve deeper into the unique characteristics of this organ to serve as a subtype C HIV-1 reservoir, including potential viral compartmentalization and cellular tropism in this tissue. We conducted single genome analysis (SGA) of the v1-v5 region of subtype C HIV-1 *env* DNA from both appendix and intestine-draining mesenteric lymph node (LN) tissues. Interestingly, bootstrapping phylogenetics indicates that subtype C HIV-1 genotypes in the aviremic appendixes were less heterogeneous compared to those in LNs, suggesting unique selective pressures or viral compartmentalization in the infected appendix. Follicular dendritic cells (FDCs) appeared to harbor the majority of subtype C HIV-1 in the appendix tissue reservoir. Our findings not only contribute to the growing body of knowledge on HIV-1 reservoirs but also underscore the need to account for HIV-1 subtype-specific variations in potential tissues as therapeutic targets and a better understanding of HIV-1 pathogenesis.

Materials and methods

Study setting and sample collection

With our long-term collaboration with University Teaching Hospital (UTH) in Lusaka, Zambia, we are able to collect postmortem appendix and LN tissues via forensic autopsies. When a potential autopsy case arrived at the UTH mortuary, a clinical officer or study nurse counselor approached the family members of the deceased to determine whether the deceased met study inclusion criteria with regard to time of death. Deceased persons were consented by the next-of-kin for the postmortem tissue collection at the UTH mortuary. Sociodemographic information as well as available medical history were collected whenever possible. Eventually, appendix and mesenteric LN of the 14 deceased Zambians analyzed in this study were collected within 48 hours of these individuals' deaths. These tissues were cryopreserved at -80°C or processed to formalin-fixed, paraffin-embedded (FFPE) blocks.

HIV-1 *env* v1-v5 amplification using nested PCR

To amplify HIV-1 *env* v1-v5 DNA, nested PCR with high-fidelity (HF) Q5 DNA polymerase (New England Biolabs, MA, USA) and primers against env was performed with the following procedure for both rounds: polymerase activation at 95°C for 10 minutes, then 35 cycles of denaturation at 95°C for 30 seconds, annealing at 55°C for 30 seconds and elongation at 72°C for 2 minutes, then one cycle of 72°C for 7 minutes. In the first round, 100 ng genomic DNA was used as template with env primers (Forward 1: 5'-GATGCTTGAGGATATAATCAGTTTATGGGA-3'; Reverse 1: 5'-ATTGATGCTGCGCCCATAGTGCT-3') were applied. Then 2 μl of the first round PCR product was utilized as template for the second round with another pair of env primers

(Forward 2: 5'- AGTTTATGGGACCAAAGCCTAAAGCCATGT-3'; Reserve 2: 5'-ACTGCTCTTTTTTCTCTCTCCACCACTCT-3'). The second round of env PCR products were gel-purified and then subjected to bulk sequencing.

Single genome analysis (SGA)

To perform SGA, nested PCR against HIV-1 env v1-v5 using serial diluted genomic DNA samples was utilized. Serial dilution of genomic DNA samples from both appendixes and LNs of aviremic and viremic individuals was conducted to make sure the positivity of the 2nd round of nested PCR to be around 22~30%. Gel-purification of those positive *env* products were then conducted. Sequencing results of those *env* products confirmed that each of those products was amplified from a single copy of HIV-1 provirus.

Phylogenetic analysis

Appendix *env* sequences in aviremic individuals from bulk sequencing, and SGA *env* sequences from appendixes and LNs of aviremic and viremic individuals were analyzed by phylogenetics. Initially, multiple sequence alignment (MSA) of bulk and SGA data was performed using CLUSTAL Omega (v1.2.4). The alignment data were then converted into phylogeny objects using the *as.phyDat()* function from phangorn package in R. The unweighted pair group method with arithmetic Mean (UPGMA) was employed as a hierarchical clustering method to construct the phylogenetic trees. For the estimation of evolutionary distances, different models were applied based on the type of sequence data using the *dist.ml()* function in R. The Dayhoff model was used to generate distance matrices for amino acid sequences, leveraging its ability to account for the observed rates of amino acid substitution. In contrast, for DNA sequences, the Felsenstein

1981 (F81) model was selected over the simpler Jukes-Cantor model (JC69). This choice allowed for a more accurate representation of nucleotide substitutions. To assess the robustness of the inferred phylogenetic relationships, bootstrapping was performed using the *bootstrap.phyDat()* function in R, which provides a measure of support for each clade in the tree. Finally, the generated trees with branch lengths and bootstrap values were imported into iTOL (Interactive Tree of Life) tool for further customization and visualization of the constructed phylogenetic trees.

Histological H&E staining

For H&E staining, sections of 6 μm thickness were cut from FFPE appendix tissues from both HIV- and HIV+ individuals. Slides were first deparaffinized using xylene (American MasterTech Scientific, Lodi, California) washes and then rehydrated by serial washes with 100% ethanol (twice) (Thermo Fisher Scientific, Pittsburgh, USA), 85% ethanol, 70% ethanol. Slides were then stained with hematoxylin (American Mastertech Scientific, Lodi, California), followed by 1% acid alcohol (American Mastertech Scientific, Lodi, California), and then 0.05% ammonia water. After washing in distilled water, slides were placed in 95% ethanol, followed by staining with eosin (American MasterTech Scientific, Lodi, California). Slides were then dehydrated through two 100% ethanol washes and two xylene washes, mounted with Cytoseal-60 (Thermo Fisher Scientific, Pittsburgh, USA) and left to dry overnight at room temperature.

Immunohistochemistry (IHC)

For IHC, sections of 6 μm thickness were also cut from all FFPE appendix tissues. Briefly, sections on slides were deparaffinized and rehydrated as described above. Endogenous peroxidase was quenched using 3% H202 (Thermo Fisher Scientific,

Pittsburgh, USA) in methanol (Thermo Fisher Scientific, Pittsburgh, USA) for 30 minutes at room temperature. After washing in distilled water, antigen retrieval was performed using sodium citrate (pH = 6.0) at 98 ℃ water bath for 15 minutes. Slides were then washed in phosphate buffered saline (PBS). Tissue sections were blocked with 10% normal goat serum (NGS, Vector, Burlingame, CA) for 30 minutes at room temperature. After blocking, primary antibody solution was put onto the slides and the slides were incubated overnight at 4℃. The following primary antibodies were then used: mouse-anti HIV-1 p24 (Invitrogen, 1:50 dilution), goat-anti CD4 (Biotechne, 1:50 dilution), rabbit-anti CD3 (Abcam, 1:200 dilution), rabbit-anti CD21 (Abcam, 1:5000 dilution), and rabbit-anti CD68 (Abcam, 1:5000 dilution). After that, slides were washed in PBS and HRP secondary antibody (Dako) was added to each slide. Slides were incubated with anti-mouse or anti-rabbit HRP at room temperature for 30 minutes, and then washed with PBS. Diaminobenzidine (DAB, Dako) was prepared according to manufacturer's instructions. Similar DAB developing time was applied to all slides. After DAB development, slides were stained with hematoxylin (American MasterTech Scientific, Lodi, California). Slides were dehydrated using serial ethanol and xylene washes. Matched IgG 1 isotype controls were applied in IHC staining to confirm signal specificity. Eventually, the slides were cover-slipped with Cytoseal-60 for subsequent scanning. The stained slides were then digital scanned by MoticEasyScan Pro instrument (Motic, Xiamen, China) according to the instruction manual provided by the manufacturer.

Immunofluorescence triple staining on FFPE tissue

IF triple staining was used to visualize protein co-localization. As described in the IHC protocol, adjacent slides were deparaffinized, followed by antigen retrieval in sodium citrate solution for 15 min at 98 °C, and then blocked for 30 min using Bloxall (Vector Labs). Primary antibodies were added, and the slides were incubated at 4°C overnight. The same primary antibodies and dilutions used IHC were also utilized in IF, including antibodies against viral p24 and cellular CD4, CD3, CD21, and CD68. After washing, the slides were incubated with their corresponding secondary antibody (donkey anti-mouse AF647 (Invitrogen, 1:100), donkey anti-rabbit AF405 (Invitrogen, 1:100), donkey anti-goat AF488 (Invitrogen, 1:100)) for 2 h at RT. The slides were then counterstained with 300 nM DAPI for 30 min at RT and mounted using Fluoro-gel (Electron Microscopy Sciences, Hatfield, PA, USA). The representative IF images were taken with an image analysis software (Keyence, Itasca, IL).

Results

Study cohort

We have previously shown that subtype C HIV-1 *LTR* DNA could be detected in the appendix of most aviremic individuals (pVL < 70 copies/ml) analyzed (253), indicating the potential role of human appendix serving as a novel HIV-1 tissue reservoir. To have a better understanding of the unique characteristics of this subtype C HIV-1 tissue reservoir, 14 aviremic individuals with detectable viral *LTR* DNA in their appendixes were enrolled in this study (**Table 3.1**). In addition, two viremic individuals (P088 and P049), whose pVLs were 1.74 x 10^6 copies/ml and 2.90 x 10^6 respectively, and an uninfected individual (P070) were also enrolled and utilized as positive and negative

controls in this study (**Table 3.1**). More information of our studied cohort including age, gender, ART duration, and post-mortem interval, was also shown in **Table 3.1**.

Table 3.1. Information of the cohort analyzed

Case ID	Gender	Age	HIV Status	Plasma VL (copies/mL)	ART Duration	Post-mortem Interval	*LTR* DNA in Appendix (copies/10^6 cells)	*env* v1-v5 in Appendix	HIV-1 Subtype
P003	M	53	Aviremia	< 70	5 years	< 48 hours	56	Detectable	C
P086	M	60	Aviremia	< 70	8 years	7 hours	358	Detectable	C
P092	M	47	Aviremia	< 70	Unknown	18 hours	430	Detectable	C
P113	M	45	Aviremia	< 70	Unknown	3 hours	1169	Detectable	C
P176	M	36	Aviremia	< 70	Unknown	18 hours	66	Detectable	C
P227	M	39	Aviremia	< 70	5 years	33 hours	179	Detectable	C
P280	M	28	Aviremia	< 70	Unknown	5 hours	19	Detectable	C
P031	M	40	Aviremia	< 70	4 years	26 hours	41	Not detectable	C
P040	M	40	Aviremia	< 70	8 years	30 hours	76	Not detectable	C
P124	M	50	Aviremia	< 70	10 years	4 hours	244	Not detectable	C
P191	M	25	Aviremia	< 70	Unknown	6 hours	251	Not detectable	C
P293	M	60	Aviremia	< 70	Unknown	27 hours	12	Not detectable	C
P308	M	59	Aviremia	< 70	Unknown	40 hours	12	Not detectable	C
P360	M	28	Aviremia	< 70	Unknown	14 hours	6	Not detectable	C
P049	M	45	Viremia	2.90×10^6	Unknown	33 hours	3099	Detectable	C
P088	M	35	Viremia	1.74×10^6	Unknown	18 hours	6072	Detectable	C
P070	M	25	HIV-	N/A	N/A	12 hours	N/A	N/A	N/A

Homogeneous HIV-1 genotypes in the appendix of virally suppressed individuals

The appendix tissues from the 14 aviremic individuals were further characterized to determine the heterogeneity of the proviral sequences by analyzing HIV-1 *env* sequences. Genomic DNA was extracted from the 14 postmortem cryopreserved appendix tissues and subjected to nested PCR against HIV-1 *env* v1-v5. However, HIV-1 *env* DNA was only detected in the appendixes of 7 of the 14 aviremic individuals (P003, P086, P092, P113, P176, P227 and P280) (**Table 3.1**), indicating that at least 50% of the

appendix tissues harbored defective proviral viruses lacking the *env* gene. HIV-1 *env* DNA was detected in the LNs of those 7 aviremic individuals. Additionally, genomic DNA was also extracted from the appendixes and mesenteric LNs of viremic individuals P088 and P049, and the uninfected individual P070. As expected, HIV-1 *env* DNA was readily detectable in the appendix tissues from both P088 and P049, and none was detectable in the P070 uninfected control.

We first conducted bulk sequencing of the amplified *env* DNA from appendix tissues of the 7 aviremic individuals and compared them to the viral *env* sequences from the mesenteric LNs of the same aviremic individuals. The viral *env* sequences from the mesenteric LNs of all aviremic individuals analyzed displayed high genetic diversity and no predominant viral sequence was detectable (data not shown). Interestingly, bulk sequencing of amplified *env* DNA from all 7 aviremic appendixes displayed high homologies. Bootstrapping phylogenetics of these appendix *env* DNA sequences revealed that these *env* sequences are clustered with reference subtype C HIV-1 sequences, but not with other subtypes. This is consistent with our previously subtyping results showing that all the 7 aviremic individuals characterized were infected with subtype C HIV-1 (**Figure 3.1A**, (240)). These phylogenetical results also suggest the potential presence of appendix-tropic viruses. Alternatively, it could be due to the persistence of the latent founder virus which spreads to the appendix tissue early in infection where there is a lack of selective pressure on the virus for it to replicate and diversify.

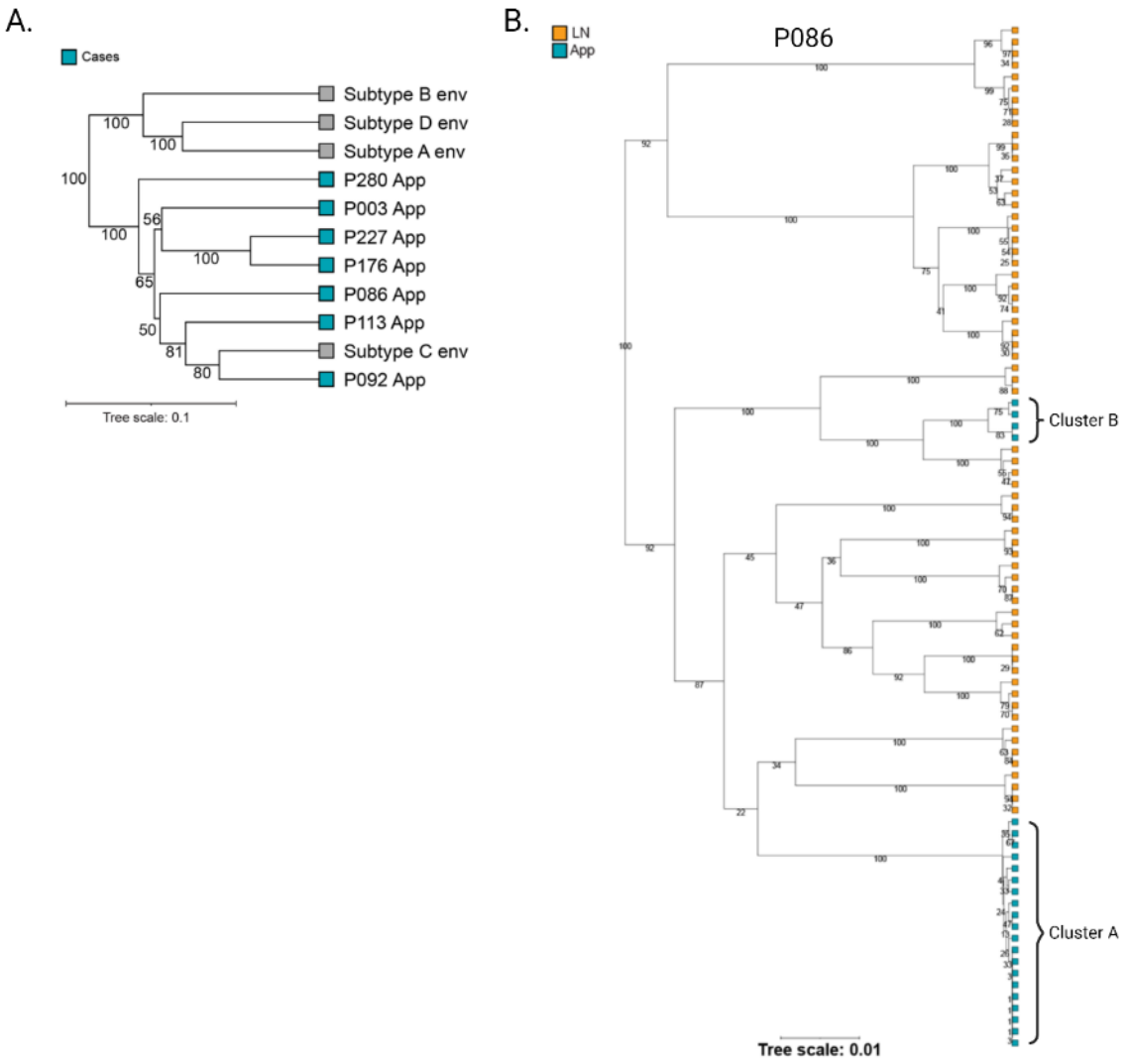

Figure 3.1. Subtype C HIV-1 proviral DNA sequences are less heterogeneous in the appendix than LN from aviremic individuals. HIV-1 *env* DNA v1-v5 regions were amplified from the appendix and LN and then subjected to both bulk sequencing and single genome analysis (SGA). (A) Bulk sequencing results showed homogeneous HIV-1 *env* sequences from appendixes of 7 aviremic individuals. Phylogenetics analyses showed the *env* sequences clustered with subtype C clade reference sequence, consistent with previous subtyping results. (B) Bootstrapping phylogenetics with SGA *env* sequences from the appendix and mesenteric LN of one aviremic individual (P086). The presence of distinct cluster of P086 appendix *env* sequences (Cluster A) confirmed less heterogeneity of subtype C HIV-1 genotypes compared to those from mesenteric LN.

To confirm that the viral *env* DNA sequences from the appendix are homogeneous whereas those from the LNs are heterogeneous from the aviremic cases, we further conducted single genome analysis (SGA) of HIV-1 env v1-v5 sequences from the

appendix and mesenteric LN of one aviremic individual (P086) which we have enough appendix tissue DNA for analysis to evaluate the potential in viral diversity between the two viral reservoirs. Consistent with bulk sequencing results bootstrapping phylogenetics with SGA *env* sequences revealed that the majority of P086 appendix HIV-1 genotypes (Cluster A) are likely to be derived from clonal expansion and largely distinct from the peripheral circulating (LN) genotypes (**Figure 3.1B**). This implies the possibility of the maintenance of a potential appendix specific viral variant. However, a second minor cluster of the appendix *env* sequences (Cluster B) intermixed and shared homology with the *env* sequences obtained from the LN (**Figure 3.1B**).

Less homogeneity of SGA *env* sequences from the appendix of viremic individuals

To characterize the HIV-1 genotypes in the appendix of viremic individuals we also conducted SGA of the amplified HIV-1 *env* DNA from appendix tissues and LNs in viremic individuals (P088 and P049) since the sequences were too heterogeneous to be analyzed using bulk sequencing. As expected, the HIV-1 *env* sequences from both viremic appendixes and LNs displayed high heterogeneity and intermixed with each other with the phylogenetic analyses. This was likely due to the circulating infected cells throughout the body of these individuals, hence leading to shared appendix viral genotypes with peripherally circulated genotypes (**Figure 3.2**). However, in viremic individual P088, there is a presence of two clusters of the appendix *env* sequences (Clusters 1&2), possibly representing a clonal expansion of a subpopulation of proviruses in P088 appendix and sharing most of the genotypes with peripheral circulating viral genotypes since it is a viremic case (**Figure 3.2A**). However, for P049 there was little evidence of appendix tropism or compartmentalized HIV-1 proviruses in the appendix

since the derived *env* sequences were found to be intermixed with its LN *env* sequences (**Figure 3.2B**).

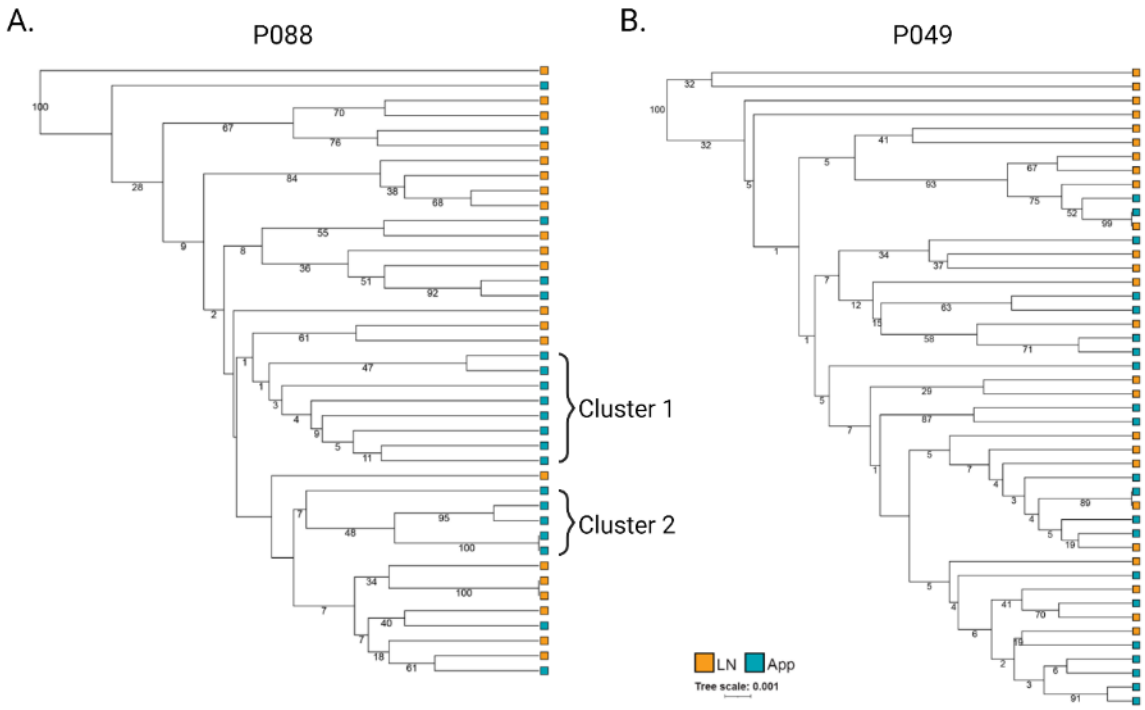

Figure 3.2. SGA *env* sequences from the appendix tissues and LNs of viremic individuals. HIV-1 *env* sequences from both appendixes and LNs of viremic individuals P088 and P049 displayed high heterogeneities. (A) Bootstrapping phylogenetics for HIV-1 *env* sequences from P088 appendix and LN showed intermixed *env* sequences between these two tissues, although the presence of clusters 1 and 2 *env* sequences in P088 appendix suggested potential less extensive heterogeneity than LN. (B) Phylogenetic analysis of HIV-1 *env* sequences from P049 indicated similar levels of heterogeneity in the *env* sequences between the appendix and LN.

In addition to conducting phylogenetic analysis using HIV-1 *env* DNA sequences, we also evaluated HIV-1 *env* amino acid (aa) sequences from both appendix tissues and LNs from both aviremic and viremic individuals to identify non-synonymous changes and whether they affect potential glycosylation. We conducted an analysis comparing the potential N-linked glycosylation patterns of HIV-1 envelope proteins between the appendixes and lymph nodes (LNs). We focused on the gp120 subunit encoded by env c1-v5, known for its extensive glycosylation at approximately 25 sites. The analysis

utilized predictions based on the N-X-S/T amino acid motifs and did not reveal any discernible differences in the glycosylation patterns of HIV-1 viruses between appendixes and LNs of both aviremic and viremic individuals (data not shown). Moreover, there was no consensus sequence observed when aligning appendix *env* aa sequences from 9 HIV+ individuals (data not shown), suggesting there is no common appendix-tropic viruses across individuals.

Histological changes in appendix tissues of subtype C HIV-1 infected individuals

To characterize the potential histological changes of the appendix tissues in HIV-1 infected individuals, Hematoxylin and Eosin (H&E) staining was conducted on formalin-fixed, paraffin-embedded (FFPE) appendix tissues of HIV negative (P070), HIV+/viremic (P088 and P049), and HIV+/aviremic (P092 and P086) individuals. In HIV- P070 appendix, normal structures of muscularis (MC) layer, submucosa (SM), and the lamina propria with lymphatic follicles (LFs) were observed (**Figure 3.3A**). Compared to HIV-1 negative appendix, there are reduced lymphocytes and fewer numbers of lymphatic follicles in HIV+ appendix tissues (**Figure 3.3B-E**). Moreover, severe degradation of LFs was observed in the appendix tissues of viremic individuals (P088 and P049), accompanied by CD4 depletion (**Figure 3.3B&C**). In addition, in all analyzed appendix tissues (HIV+ and HIV-), there was no obvious inflammation observed, which is usually characterized as infiltrating lymphocytes into the MC layer (254).

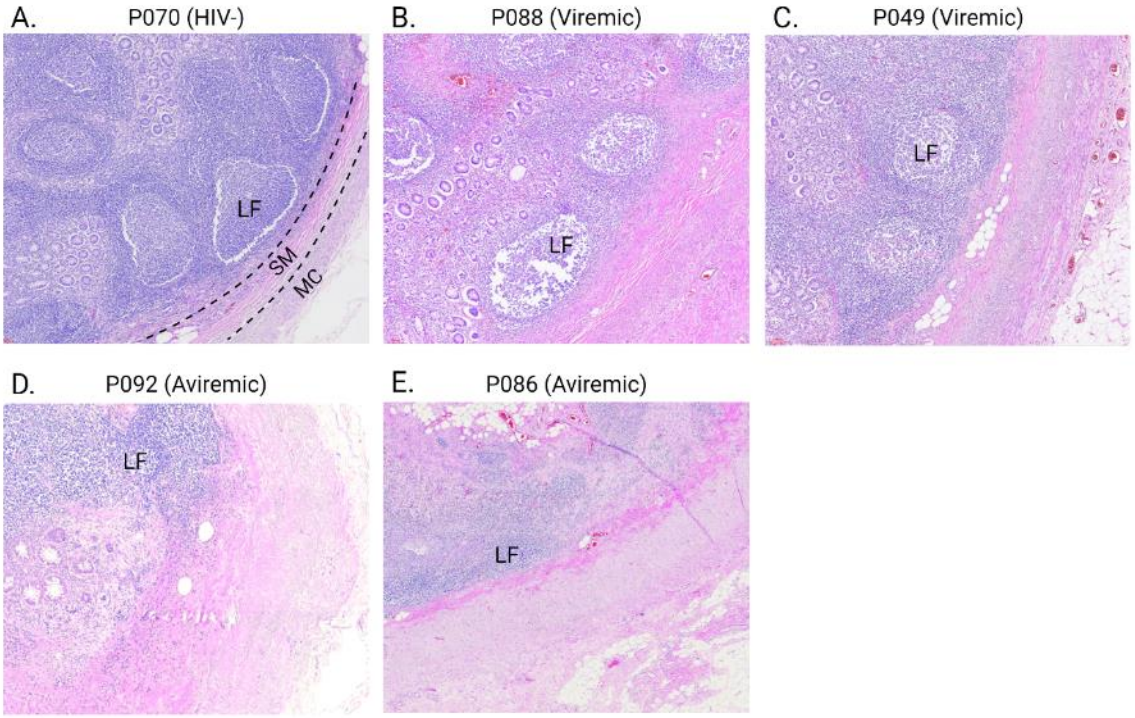

Figure 3.3. Histological changes observed in the appendix from HIV-1 infected individuals. Hematoxylin and Eosin (H&E) staining was conducted on HIV negative, HIV+/Viremic, and HIV+/Aviremic individuals. Overall, there was no inflammation observed in both HIV- and HIV+ appendixes, which usually displayed infiltrating lymphocytes into the muscularis (MC) layer. (A) The normal structures of MC layer, submucosa (SM), and the lamina propria with lymphatic follicles (LFs) were observed in the HIV negative individual (P070). (B-C) There were reduced number of LFs and varying degrees of LF degradation, likely accompanied by CD4 depletion, in viremic as compared to HIV-1 infected appendix tissues. (D-E) There was no overt LF degradation in aviremic appendixes in contrast to viremic appendix tissues.

HIV antigen detection and potential cellular reservoirs in HIV+ appendix tissues

To determine the cell types that harbor subtype C HIV-1 in the appendix, we performed IHC to detect HIV-1 antigen (p24 capsid protein) in the infected individuals. Among the 7 aviremic individuals, HIV-1 p24 was only detected in P092 appendix but remained undetectable in the other 6 aviremic appendix tissues even though proviral DNA was detected. For the 2 viremic individuals, HIV-1 p24 was readily detected in their appendix tissues. To determine the infected cell types, we conducted IHC with antibodies against different cellular surface markers (CD4, CD3, CD21, CD68). While CD3+

identified all T cells but CD4+ cells would represent all potential HIV-1 target cells in the appendix since CD4 is the required major HIV-1 receptor needed for HIV-1 binding and entry. Anti-CD21 antibodies would detect both B cells and follicular dendritic cells (FDCs), and anti-CD68 antibodies would detect macrophages in the appendix.

IHC was performed on adjacent FFPE sections of the appendix tissues from aviremic (P092) and one viremic (P049) individual serving as positive control, and with HIV negative P070 as negative control. The representative IHC images are shown in Figure 4. For the aviremic P092 appendix, the majority of HIV-1 p24 was detected in the LFs. On the adjacent FFPE tissues, positive signals were detected with cellular CD4 and CD21 in the same regions where viral p24 was detected but not with CD3 or CD68 (**Figure 3.4**). Although CD21 could also detect B cells, they cannot be infected by HIV-1, therefore, the potential co-localization between viral p24 and cellular CD21 indicated that FDCs are the potential cellular reservoirs in the appendix. In addition, HIV-1 antigen in viremic appendix (P049) was also mainly detected in the LFs, with much stronger p24 signals as compared to the aviremic appendix. Similarly, IHC on adjacent appendix tissue sections of the viremic P049 also indicated overall co-localization between the viral p24 and cellular CD21. Nevertheless, due to the intense HIV-1 p24 antigen signals, some CD3+ T cells and CD68+ macrophages could also be co-localized within the viral p24 stained region in this viremic appendix tissue (**Figure 3.4**). Taken together, these results indicated that FDCs could be the major cell type that harbored subtype C HIV-1 in human appendix.

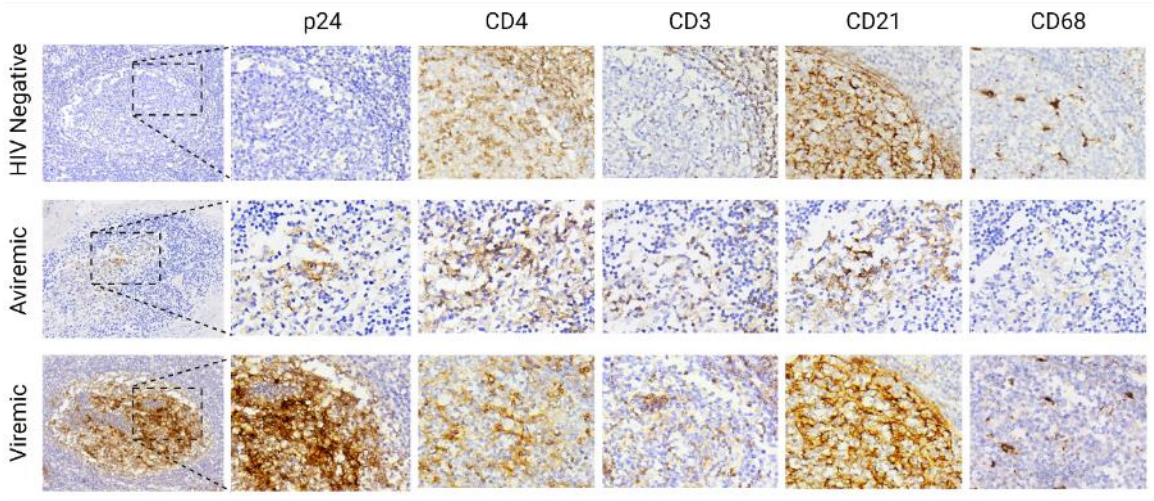

Figure 3.4. IHC for potential HIV-1cellular targets in the human appendix. IHC with antibodies against viral p24 and different cellular markers (CD4, CD3, CD21, CD68) were conducted on the adjacent FFPE sections of the appendix tissues of an HIV negative (P070), HIV+/Aviremic (P092) and an HIV+/Viremic (P049) individuals. Viral p24 protein was detected in both aviremic and viremic individuals, with the majority of p24 signals in the follicular regions of the appendix tissues. CD4 cellular maker, the major receptor for HIV-1 entry, indicated all potential susceptible cell targets. Among those CD4+ cell targets, CD3 cellular marker indicated T cells, while CD21 represented follicular dendritic cells (FDCs), and CD68 for macrophage in the appendix. IHC results showed that the majority of viral p24 signal was colocalized with CD21 cellular marker, suggesting the potential of FDCs as major cellular reservoir for subtype C HIV01 in the appendix.

Follicular dendritic cells harboring and expressing majority of subtype C HIV-1 in appendix

To confirm the IHC data we further conducted immunofluorescence (IF) triple labeling with antibodies against viral p24 and with different cellular markers, including CD4/CD21, CD4/CD3, and CD4/CD68 on the same appendix FFPE tissue section for co-localization. The different antibody panels were utilized to determine if FDCs (CD4+/CD21+), or CD4+ T cells (CD4+/CD3+), or macrophages (CD4+/CD68+) in the appendix can serve as cellular reservoirs for subtype C HIV-1.

For the aviremic P092 appendix, the IF signals for viral p24 (red) co-localized with both cellular CD4 (green) and CD21 (blue) (**Figure 3.5A-D**), which is consistent

with the IHC results. Although the IF CD4 labeling on P092 appendix appeared to be atypical of p24 staining and seemed to be more punctated, nevertheless this result indicated that FDCs in the appendix of aviremic individuals harbored subtype C HIV-1. Whereas, on the adjacent sections, there was no detectable CD68 (blue) co-colocalizing with viral p24 (red) (**Figure 3.5I-L**). Our results suggested there were no detectable macrophage reservoirs, and with very rarely detectable cellular CD3 (blue) and CD4 (green) cells co-localized with p24 (red) in the aviremic appendix tissue analyzed (**Figure 3.5E-L**).

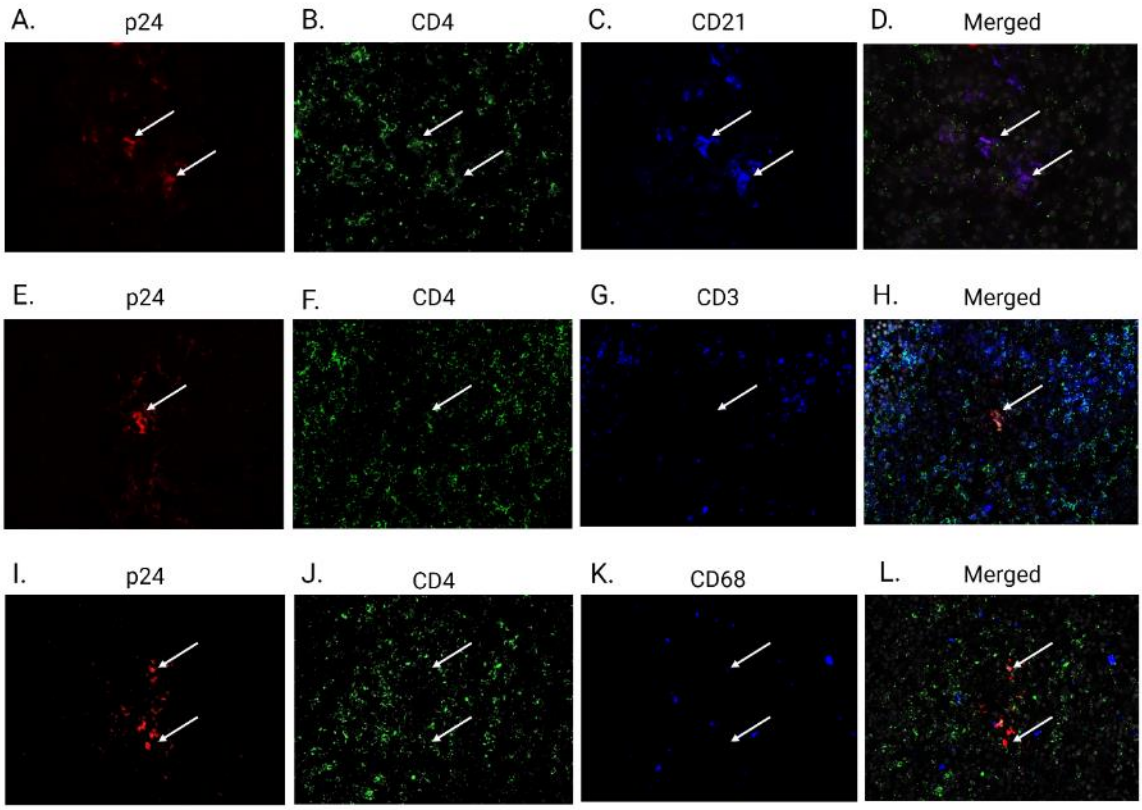

Figure 3.5. Follicular dendritic cells (FDCs) as major cellular reservoir for subtype C HIV-1 in aviremic appendix. Triple immunofluorescence (IF) staining with antibodies against viral p24/CD4/CD21, or p24/CD4/CD3, or p24/CD4/CD68 were conducted on the same FFPE section of aviremic P092 appendix. (A-D) Colocalization of CD4, and CD21 with majority of p24 was observed in the P092 appendix, indicating the major infected cell type in aviremic appendix is FDC. (E-H) There was no identifiable CD3+ T cell colocalizing with p24

signals in the aviremic P092 appendix. (I-L) There was also a lack of D68+ macrophage co-localizing with p24 signals in the aviremic P092 appendix. Arrows are representative IF signals.

For the viremic appendix (P049), the majority of viral p24 was also detected in the lymphoid follicles. The p24 signals (red) were also co-localized with FDCs (CD4+/CD21+) (**Figure 3.6A-D**), although the CD4 signals in the appendix lymphoid follicles were weaker than the region outside probably due to reduction or depletion CD4 T-cells because of active HIV-1 infection.

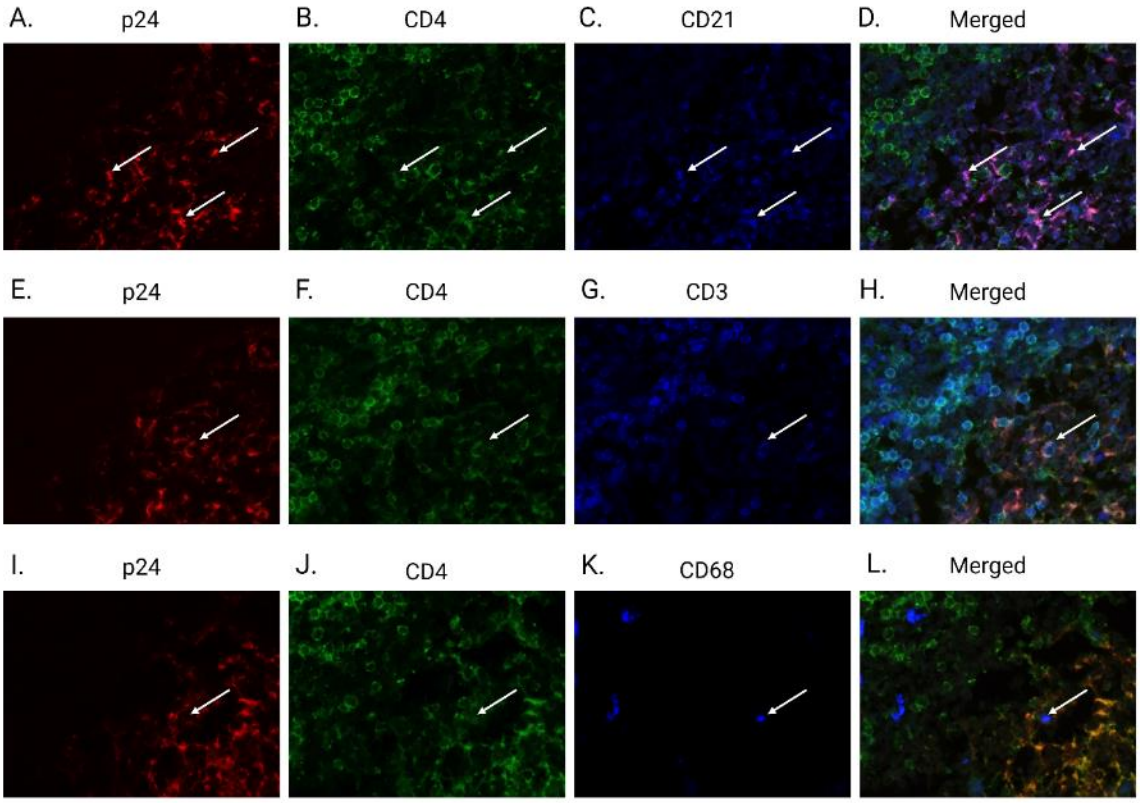

Figure 3.6. Cellular reservoirs of subtype C HIV-1 in viremic appendix. Triple IF staining was conducted on the same FFPE section of viremic P049 appendix. (A-D) There is a clear colocalization of CD4, and CD21 with majority of the p24 in viremic appendix, demonstrating FDC as a major cellular reservoir in the appendix. (E-H) Some p24 signals colocalized with CD4/CD3 cells in the viremic appendix, indicating THC are also targets of HIV-1 in the appendix. (I-L) Some p24 signals co-localized with CD4/CD68 in viremic appendix were detected, demonstrating the potential role of macrophage as additional HIV-1 cellular reservoir in the human appendix. Arrows are representative IF signals.

Additionally, some CD3+ T cells (blue) and CD68+ macrophages (blue) were found to be also co-localized with viral p24 (red) in the viremic appendix (**Figure 3.6E-L**), as shown by the representative IF signals indicated by arrows. Our IF triple labeling results further confirmed that FDCs are the main cell type that harbored majority of the subtype C HIV-1 in the appendix tissues of infected individuals.

Discussion

Despite the successes of ART in controlling HIV replication and disease progress in PLWH, the presence of various tissue and cellular HIV-1 reservoirs has hampered ART's ability to cure HIV-1 infection (255). Although various tissue and cellular HIV-1 reservoirs were identified, they were mostly limited to cellular reservoirs in the peripheral blood and biopsies tissues. In addition, most information generated on the HIV-1 tissue reservoirs were mainly from subtype B HIV-1 (99, 108, 112, 115), and very little is known about other subtypes. Whether there are any tissue and cellular differences between HIV-1 subtypes is not known. We have recently reported through autopsies analyses of various bodily tissues of subtype C infected individuals, and showed that in addition to the known tissue reservoirs, the appendix could be a potential reservoir for the most widespread HIV-1 subtype C. In this study we have further confirmed the appendix as a potential reservoir tissue for this subtype and demonstrated that FDCs are the most common infected cell lineage. Our study has not only contributed to the growing literature on the heterogeneity of HIV-1 reservoirs, and more importantly, suggest a rationale for further evaluation to determine if human appendix could also serve as a tissue reservoir in PLWH infected with subtype B and other non-C HIV-1 subtypes. Insights from this study also informed the need of region-specific strategies for

combating HIV-1 in areas where subtype C is prevalent, such as sub-Saharan Africa and India.

Since the appendix is mainly composed of lymphoid tissues, it was anticipated that the proviral sequences will reflect what can be found in other gut associated lymph nodes, even in aviremic individuals. Interestingly, our finding that the subtype C HIV-1 genotypes in the appendix tissues are less heterogeneous compared to those in mesenteric LNs based on bulk sequencing of the DNA from all the aviremic cases. Moreover, from the one aviremic case (P086) hat we have enough appendix tissues DNA to conduct single genome analyses, we found that in general the viral sequences in the appendix were much more homogeneous and appeared to be more compartmentalized than those observed in the mesenteric lymph node from the same individual, most likely through clonal expansion within the appendix. However, the presence of a minor cluster of the appendix *env* sequence which intermixed and shared homology with the *env* sequences obtained from the LN suggested that may be some circulating infected cells in the blood between these two anatomical locations even under viral suppression, or the appendix reservoir was established early during primary infection by founder viruses but have undergone only limited clonal expansion in the appendix due to less selective pressures, including ART, which differs from those from the lymph nodes that have undergone substantial clonal expansion and diversifications, but still share some viral sequence homologies to those presence in the appendix. It is also possible that the proviral sequences we found in the appendix are footprints of defective viruses established in this reservoir since we were not able to detect p24 expression in this appendix tissue. However, even though we were able to detect both HIV-1 *env* DNA and p24 capsid

protein in the appendix from another case (P092), currently we do not know if the proviruses in this tissue were defective or replication competent, which will require detection of full-length HIV-1 genomes and infectious viral particles that cannot be carried out due to tissue limitations. Our findings nevertheless suggest that the subtype C HIV-1 genotypes in the appendix tissue are less heterogeneous compared to that in mesenteric LNs, and that the appendix may present a distinct tissue environment for viral persistence or potential compartmentalization of proviruses.

The identification of FDCs as most plausible cell lineage harboring subtype C HIV-1 proviral DNA in the appendix is of significance. Previous studies showed that FDCs in the LNs can retain antigens and virions for a prolonged duration and can serve as HIV-1 cellular reservoirs (256-258). In this study, IF triple staining results confirmed that the FDCs in the appendix have the capacity to harbor and express subtype C HIV-1. Like the other HIV reservoirs, appendix FDCs that harbor HIV-1 might also contribute to both low-level viremia and viral resurgence upon cessation or failure of ART. In addition, previous *in vitro* studies reported that FDC could up-regulate the expression of CXCR4 but not CCR5 on the CD4+ T cell surface, therefore render surrounding follicle T cells highly susceptible to infection with X4 tropic HIV-1 (259, 260). There may be a similar scenario in the appendix on the interaction between CD4 T follicular helper (CD4 T_{fh}) cells and FDCs under HIV-1 infection, which warrants further investigation.

Our histological staining results showed that the appendix tissues from our infected individuals compared to those from uninfected have reduced cell density and different levels of follicle lysis in infected tissues. This may be due to microbial translocation from intestinal tissues, including the appendix, since chronic HIV-1

infection has been shown to lead to inflammation and cell death (261-263), Moreover, the inflammatory status of the appendix may influence the establishment and maintenance of HIV-1 reservoirs since chronic inflammation can impact viral replication and persistence. Although there were no overt inflammatory pathologies observed in the appendix tissues analyzed in this study, we have previously reported that the mRNA levels of pro-inflammatory cytokines IL-1β and IL-6 were significantly higher in aviremic appendix compared to uninfected cases (240). In addition, previous epidemiological studies have also reported a 3 to 4-fold increase of the incidence of appendicitis in HIV-1 infected individuals compared to healthy individuals (225, 264). As reported in previous findings, our results showing that HIV-1 infection and replication in human appendix infected by subtype C HIV-1 could lead to increase changes in the tissue histological structure and could be associated with the level of microbial translocation. This could also lead to a possible increase in the incidence of appendicitis in subtype C infected individuals that warrant further investigations. Future studies will also be needed to elucidate the possibility of productive viral infection of FDCs in the appendix, and the mechanisms by which the appendix and FDCs contribute to HIV-1 persistence, the potential impact of the appendix's unique microenvironment on viral latency and reactivation, as well as their role in gut microbiome perturbations and microbial translocation.

There are also some limitations in this study. First, the study was only able to investigate a limited number of postmortem appendix samples from subtype C HIV-1 infected individuals due to the difficulties in obtaining a larger number of aviremic subtype C infected individuals to conduct complete autopsies in our study setting. Expanding the study to include a larger and more diverse cohort, including individuals

with different HIV-1 subtypes and those with varying histories of ART use would further confirm that the appendix is a unique and important viral reservoir that warrants attention in the era of HIV cure. Moreover, the current study was not able to distinguish between replication-competent and defective viruses within the follicular dendritic cells due to the limitations with autopsies tissues in isolating viable cells for isolation of infectious viruses. In addition, due to lack of computerized clinical documentation in Zambia and linkage to HIV/ART use databases, information such as time since diagnosis of HIV infection, treatment histories and adherence to ART treatment, were not available.

In summary, our study has contributed to the knowledge on the diversity of HIV-1 in tissue reservoirs, emphasizing the need to investigate the role of various tissue types to further understand the complexities of viral persistence. The identification of the appendix as a reservoir raises intriguing questions about the cellular and molecular mechanisms that allow the virus to persist in this tissue. Moreover, considering the global prevalence of subtype C HIV-1, establishing the human appendix as an additional tissue reservoir has implications for the need to develop region-specific therapeutic strategies. Tailoring interventions based on the specific characteristics of subtype C reservoirs, such as the now identified human appendix, could enhance the effectiveness of antiretroviral therapies, and contribute to the global effort to cure HIV-1.

CHAPTER 4:

LIMITED HIV-ASSOCIATED NEUROPATHOLOGIES AND LACK OF IMMUNE ACTIVATION IN SUB-SAHARAN AFRICAN INDIVIDUALS WITH LATE-STAGE SUBTYPE C HIV-1 INFECTION

Abstract

Although studies with subtype B HIV-1 have suggested that proviruses in the brain are associated with physiological changes and immune activation accompanied with microgliosis and astrogliosis, the natural course of neuropathogenesis of the most widespread subtype C HIV-1 has not been adequately investigated, especially for people living with HIV (PLWH) in sub-Saharan Africa. To characterize the natural neuropathology of subtype C HIV-1, postmortem frontal lobe and basal ganglia tissues were collected from nine ART-naïve individuals who died of late-stage AIDS with subtype C HIV-1 infection, and eight uninfected deceased individuals as controls. Histological staining was performed on all brain tissues to assess brain pathologies. Immunohistochemistry (IHC) against CD4, p24, Iba-1, GFAP, and CD8 in all brain tissues was conducted to evaluate potential viral production and immune activation. Histological results showed mild perivascular cuffs of lymphocytes only in a minority of the infected individuals. Viral capsid p24 protein was only detected in circulating immune cells of one infected individual, suggesting a lack of productive HIV-1 infection of the brain even at the late-stage of AIDS. Notably, similar levels of Iba-1 or GFAP between HIV+ and HIV- brain tissues indicated a lack of microgliosis and astrogliosis, respectively. Similar levels of CD8+ cytotoxic T lymphocyte (CTL) infiltration between HIV+ and HIV- brain tissues indicated CTL was not likely to be involved in subtype C

HIV-1 neuropathogenesis. Our study suggests that there is a lack of productive infection and limited neuropathogenesis by subtype C HIV-1 even at late-stage disease, which is in contrast to what was reported for subtype B HIV-1.

Introduction

There are approximately 39.0 million people living with HIV (PLWH) globally, 69% of whom are in sub-Saharan Africa (SSA) (12). HIV-1 can be subdivided into nine genetically distinct subtypes that are unevenly distributed geographically (26). Subtype C HIV-1 is predominant in SSA and India, and accounts for nearly 50% of new global HIV-1 infections, whereas subtype B is prevalent in North America and Europe, and is responsible for about 12% of all HIV-1 infections (26). The natural course of HIV infection includes an acute stage of intense viral replication and dissemination within several weeks following infection. The acute phase is followed by several years of chronic (asymptomatic) infection characterized by sustained immune activation, CD4 depletion and low-level viremia. Subsequently, the late stage is characterized by marked depletion of CD4+ T cells, elevated plasma viral load (pVL), and susceptibility to opportunistic infections that define the acquired immune deficiency syndrome (AIDS) (65, 265). Antiretroviral therapy (ART) has turned once fatal HIV-1 infection to a manageable scenario by suppressing pVL to undetectable levels (aviremia) (266, 267), ART does not eliminate HIV-1 from latently infected cells in tissue reservoirs throughout the body, including the central nervous system (CNS) (186, 253, 255). If ART is interrupted, HIV-1 will rebound from these tissue reservoirs and lead to disease (268-271).

The CNS as a sanctuary for subtype B HIV-1 has been well documented (93, 105, 107, 272). Reports show that subtype B proviral DNA was detected in between 86% - 100% of brain tissues from ART naïve (viremic) individuals (93, 105, 273), and HIV $p24_{CA}$, a marker for active viral replication (productive infection), was readily detectable in late disease stage viremic AIDS patients' brains and associated with HIV encephalitis (HIVE) (274, 275). Despite ART suppression, subtype B HIV-1 DNA can still readily be detected in the parenchymal brain tissues (> 50% brain tissues) (93, 276), and $p24_{CA}$ can also be detected in some aviremic brain tissues (93). Moreover, CNS-derived subtype B HIV-1 proviruses were reported to have the ability to reseed peripheral tissues (186). HIV-1 has been shown to reside in diverse brain cell types (214), including infiltrating CD4+ T cells (277-279), macrophages (171, 280), microglia (117, 281), and potentially astrocytes and pericytes (206, 282, 283). Subtype B HIV-1 studies have also shown that HIV-1 in the CNS can cause brain pathophysiological changes and immune activation, accompanied with microgliosis and astrogliosis (94, 95, 284-286). In addition, enhanced infiltration of CD8+ cytotoxic T lymphocytes (CTLs) into the human brain in response to HIV-1 infection is well documented (287-289). HIV-1 associated immune activation and neuroinflammation are the basis of neurological injury and neurocognitive impairment syndromes, such as HIV-1 associated neurocognitive disorders (HAND) (290, 291). The neuropathology of this condition is characterized by perivascular cuffs of lymphocytes, mixed with prominent giant multinucleated cells as well as parenchymal microglial nodules. In severe cases, when the perivascular lymphocytic infiltration is severe, it can lead to micro-infarcts, and in chronic states, a prominent astrocytic gliosis develops (292).

Neuropathogenesis for other HIV subtypes, including the much more abundant subtype C, is less well studied (196, 253). Subtype C HIV-1 viral DNA has been reported to be rarely detectable brain tissues from the aviremic (< 20% brain tissues) and in such cases, $p24_{CA}$ is undetectable (196, 253). To our knowledge, only a single case-report, derived from our group, has systematically sampled and assessed the various brain tissues from an entire brain hemisphere from an ART-treated, but viremic, subtype C infected subject (293). We showed lack of productive viral infection, and limited viral DNA distribution in the CNS. Given that subtype C HIV-1 infection is responsible for the majority of HIV infections, and concentrates in SSA, investigation of the neuropathogenesis of subtype C HIV-1 in more than one subject from the region is warranted.

The current study made use of postmortem brain tissue collections from ART-naïve individuals with late-stage subtype C HIV-1 infection to characterize the associated neuropathology. Frontal lobe and basal ganglia FFPE tissues from nine ART naïve individuals with late-stage subtype C HIV-1 infection, and from eight uninfected normal controls were analyzed. Histological results revealed brain pathologies in only a minority of infected individuals and the grading of those pathologies were mild when it existed at all. Immunohistochemistry (IHC) for CD4, p24, Iba-1, GFAP, and CD8 was conducted in all brain tissues. HIV $p24_{CA}$ was detected in the brain of one individual (11%), suggesting lack of productive subtype C infection in the brain tissues even at late stage/AIDS categorization. No significant differences in microgliosis and astrogliosis, based on detection of IBA-1 and GFAP, respectively, were detected between tissues from HIV+ and HIV- subjects. Likewise, we did not observe significant differences in CTL

infiltration into brain between HIV+ and HIV- individuals. Our study suggests that there is very limited neuropathogenesis by subtype C HIV-1 among SSA patients even at late-stage of infection. The lack of neuropathogenesis coupled to apparent lack CNS reservoirs (253, 294) is important to consider in strategies for curing subtype C infection and improving clinical management for PLWH in SSA.

Materials and methods

Study cohort and tissue collection

When a potential autopsy case arrived at the morgue of the University of Zambia Teaching Hospital (UTH) in Lusaka, Zambia, a clinical officer or study nurse counselor approached family members of the deceased to determine whether the deceased met study inclusion criteria with regard to time of death, and to seek informed consent for the postmortem collection of tissue specimens. Because sociodemographic and lifestyle behaviors could not be directly assessed from the deceased, the nurse counselor, working with the clinical officer, surveyed the next of kin for demographic information about the deceased. At the same time, we accessed clinical records to extract portions of the patient's medical history, including ART history and CD4 count. Only the local study personnel had access to the study database, and only de-identified data were made available for data analysis. Postmortem samples were obtained using standardized procedures. Within 48 hours of death, multiple CNS and lymph nodes were collected, fixed at 4% paraformaldehyde, and then further processed for FFPE tissue blocks.

HIV-1 subtype determination

To confirm subtype C HIV-1 infection in the HIV+ individuals studied, genomic DNA was extracted from lymph nodes from all HIV+ individuals. Nested PCR using

primers against gp120 V3 loop was performed with the following procedure for both rounds: polymerase activation at 95°C for 10 minutes, 35 cycles of denaturation at 95°C for 30 seconds, annealing at 55°C for 30 seconds and elongation at 72°C for 2 minutes, then 1 cycle of 72°C for 7 minutes. In first round, 100 ng genomic DNA was used as template with envelope primers (Forward: 5'-CCTGCTGGTTATGCGATTCTAAA-3'; Reverse 1: 5'-ACCTCCTGCCACATGTTTATAATTTG-3') were applied. Then, 2 μL of the first-round PCR product was utilized as a template for the second round with another pair of envelope primers (Forward: 5'-CCTGCTGGTTATGCGATTCTAAA-3'; Reserve 2: 5'-CAATAGAAAAATTCTCCTCTACAATTAAA-3'). Products from the second round–nested PCR were checked for size and purified via gel extraction; they were then sequenced with the forward primer. BLAST-based HIV-1 genotyping tools were used for subtyping sequence alignments.

Histological analysis with H&E staining

For H&E staining, sections of 6 μm thickness were cut from FFPE brain tissues from all individuals. Slides were first deparaffinized using xylene (American MasterTech Scientific, Lodi, California) washes and then rehydrated by serial washes with 100% ethanol (twice) (Thermo Fisher Scientific, Pittsburgh, USA), 85% ethanol, 70% ethanol. Slides were then stained with hematoxylin (American Mastertech Scientific, Lodi, California), followed by 1% acid alcohol (American Mastertech Scientific, Lodi, California), and then 0.05% ammonia water. After washing in distilled water, slides were placed in 95% ethanol, followed by staining with eosin (American MasterTech Scientific, Lodi, California). Slides were then dehydrated through two 100% ethanol washes and

two xylene washes, mounted with Cytoseal-60 (Thermo Fisher Scientific, Pittsburgh, USA) and left to dry overnight at room temperature.

Immunolabeling for CD4, p24, Iba-1, GFAP, CD8

For immunohistochemistry, sections of 6 μm thickness were also cut from all brain tissues. Briefly, sections on slides were deparaffinized and rehydrated as described above. Endogenous peroxidase was quenched using 3% H_2O_2 (Thermo Fisher Scientific, Pittsburgh, USA) in methanol (Thermo Fisher Scientific, Pittsburgh, USA) for 30 minutes at room temperature. After washing in distilled water, antigen retrieval was performed using sodium citrate (pH = 6.0) at 98 ℃ water bath for 15 minutes. Slides were then washed in phosphate buffered saline (PBS). Tissue sections were blocked with 10% normal goat serum (NGS, Vector, Burlingame, CA) for 30 minutes at room temperature. After blocking, primary antibody solution was put on the slides and the slides were incubated overnight at 4 ℃. The following primary antibodies were then used: anti-human HIV-1 p24 clone Kal-1 (Dako, 1:5 dilution), anti-human Iba-1 (1:750, Wako, Richmond, VA), anti-human glial fibrillary acidic protein (GFAP, Dako, 1:500 dilution), anti-human CD4 (Dako, 1:100 dilution), and anti-human CD8 clone C8/144B (Dako, 1:25 dilution). After that, slides were washed in PBS and HRP secondary antibody (Dako) was added to each slide. Slides were incubated with HRP at room temperature for 30 minutes, and then washed with PBS. Diaminobenzidine (DAB, Dako) was prepared according to manufacturer's instructions. Similar DAB developing time was applied to all slides. After DAB development, slides were stained with hematoxylin (American MasterTech Scientific, Lodi, California). Slides were dehydrated using serial ethanol and

xylene washes. Eventually, slides were cover-slipped with Cytoseal-60 for subsequent scanning.

Image analysis and cell quantification

After H&E and IHC staining, the stained slides were then digitally scanned by MoticEasyScan Pro instrument (Motic, San Antonio, TX) according to the instruction manual provided by the manufacturer. Scanned images were analyzed for Iba-1+, GFAP+, and CD8+ cell quantification. To quantify the percentage of Iba-1+/GFAP+/CD8+ cells in the brain tissues, a region of similar size was defined on all scanned images, which covered both white matter and gray matter. The defined region in each scanned image was then gridded into 360 partitions of the same size. Twelve random partitions were then selected to quantify the total cell number, as well as the number of Iba-1+ or GFAP+ cell numbers. The positive signal was identified using an image analysis software (Keyence, Itasca, IL). The proportions of Iba-1+, GFAP+, and CD8+ cells in the frontal lobe and basal ganglia were compared between HIV+ and HIV- individuals.

Statistical analysis

The statistical analyses conducted included Student's t-test and ANOVA. To examine the differences in the percentage of Iba-1+/GFAP+/CD8+ cells in the brain tissues between HIV+ and HIV- individuals, the Wilcoxon matched-pairs signed-rank test and the nonparametric Mann-Whitney U test were used to assess the differences between comparison groups. GraphPad Prism 9 (GraphPad Software) was utilized for statistical analyses. All tests were two-tailed, and P values < 0.05 were considered as significant.

Results

Brain tissue sampling and subtype determination

Since our previous case report study showed that frontal lobe and basal ganglia in the viremic brain are two sites having relatively higher frequencies of detectable subtype C HIV-1 viral DNA, we focused on these two brain regions to further investigate the neuropathology of subtype C HIV-1 infection in cases from Zambia. After HIV serological test using postmortem plasma samples, nine HIV+ with late-stage infection were selected. Their CD4 counts were < 200 cells/microliter, and causes of death were AIDS-defining opportunistic infections. Based on our previous report, postmortem frontal lobe and basal ganglia tissues were sampled and processed into FFPE blocks from the nine HIV+ individuals. Lymph nodes from those HIV+ individuals were also sampled for HIV-1 subtype determination. Corresponding brain tissues from eight age- and gender-matched, HIV-1 uninfected individuals were also sampled and used as controls. Information on age, gender, and cause of death of our cohort is shown in **Table 4.1**. Specifically, for the HIV+ individuals, their CD4 counts were < 200 cells/microliter (ranging from 7 to 141), and they all died from opportunistic infections including meningoencephalitis and tuberculosis. The median age of HIV+ individuals was 34 years (ranging from 22 to 60), and of HIV- individuals was 40.5 years (ranging from 25 to 54).

To determine the HIV-1 subtype in the HIV+ individuals, genomic DNA was extracted from lymph nodes of those individuals and subjected to nested PCR of the C2-V4 region of HIV-1 *envelope* DNA. PCR products were then sequenced and analyzed for subtype determination. Utilizing the REGA HIV subtyping tool and MEGA 5.10 software with maximum likelihood phylogenetic analysis, as well as group M reference

consensus sequences from the Los Alamos HIV Sequence Database, all HIV+ individuals in this study were confirmed to be infected by subtype C HIV-1 (**Table 4.1**).

Table 4.1. Clinical information of the cohort analyzed

ID	HIV Status	Gender	Age	CD4 count	Cause of Death	HIV-1 Subtype
PLWH 1	HIV+	M	39	109	Bacteria meningoencephalitis	C
PLWH 2	HIV+	M	32	68	Tuberculosis	C
PLWH 3	HIV+	M	60	35	Retroviral disease, Tuberculosis	C
PLWH 4	HIV+	M	22	115	Bacteria meningoencephalitis	C
PLWH 5	HIV+	F	35	59	Disseminated tuberculosis	C
PLWH 6	HIV+	F	36	7	Pulmonary tuberculosis	C
PLWH 7	HIV+	F	34	60	Retroviral disease, Tuberculosis, Meningitis	C
PLWH 8	HIV+	M	34	30	Toxic epidermal necrolysis	C
PLWH 9	HIV+	M	30	141	Toxoplasmosis	C
NC 1	HIV-	M	25	no data	Disseminated tuberculosis	NA
NC 2	HIV-	M	37	no data	Pulmonary tuberculosis relapse	NA
NC 3	HIV-	F	34	no data	Ischemic heart disease	NA
NC 4	HIV-	M	34	no data	Disseminated tuberculosis	NA
NC 5	HIV-	F	48	no data	Meningitis	NA
NC 6	HIV-	M	44	no data	Organophosphate Poisoning	NA
NC 7	HIV-	M	54	no data	Septicemia, Hypertensive encephalopathy	NA
NC 8	HIV-	M	45	no data	Pellagra	NA

Mild HIV-related brain pathologies in a minority of individuals with late-stage HIV-1 infection

To characterize the levels of HIV-related brain pathology in the individuals with subtype C HIV-1 late-stage infection, hematoxylin and eosin (H&E) staining was conducted on frontal lobe and basal ganglia from all HIV+ and HIV- individuals. Histological results revealed that most brain tissues showed no evident pathology. Brain pathologies that are not HIV-related, such as hypertensive and hypoxic changes, were

observed in tissues from some HIV+ and HIV- individuals (PLWHs 1 and 3; NCs 1, 4, 5, and 6) (**Table 4.2**).

Table 4.2. Neuropathological findings in this cohort

ID	Frontal Lobe	Basal Ganglia
PLWH 1	Moderate hypoxic changes	No pathology
PLWH 2	Mild perivascular cuffs of lymphocytes	Mild focal microglial nodule (1 nodule)
PLWH 3	Hypertensive changes/Lacunar infarct	Hypertensive changes/Lacunar infarct
PLWH 4	Mild perivascular cuffs of lymphocytes	Mild perivascular cuffs of lymphocytes
PLWH 5	No pathology	No pathology
PLWH 6	No pathology	No pathology
PLWH 7	Moderate perivascular cuffs of lymphocytes	Perivascular cuffs of lymphocytes/Infarct
PLWH 8	Sickle cell anemia	Sickle cell anemia
PLWH 9	No pathology	No pathology
NC 1	No pathology	Hypertensive changes
NC 2	No pathology	No pathology
NC 3	No pathology	No pathology
NC 4	Moderate hypoxic changes	No pathology
NC 5	Extensive subacute ischemic infarct	Extensive subacute ischemic infarct
NC 6	Mild hypoxic changes/diffuse cerebral edema	Severe hypertensive changes
NC 7	No pathology	No pathology
NC 8	No pathology	No pathology

However, among 9 PLWH with late-stage subtype C infection, PLWHs 2, 4, and 7 displayed overall mild levels of HIV-related brain pathology (**Figure 4.1**). Specifically, in PLWH 2, there were 5 perivascular cuffs of lymphocytes and 1 focal microglial nodule in the analyzed FFPE frontal lobe (**Figure 4.1A**) and basal ganglia (**Figure 4.1D**), respectively. In PLWH 4, mild perivascular cuffs of lymphocytes were observed in the frontal lobe (**Figure 4.1B**), and moderate perivascular cuffs of lymphocytes and small

recent microinfarct were observed in the basal ganglia (**Figure 4.1E**). For PLWH 7, moderate meningeal vascular inflammation was observed in the frontal lobe (**Figure 4.1C**), while the basal ganglia displayed severe pathologies, including multiple perivascular cuffs of lymphocytes and a large HIV-related subacute infarct (**Figure 4.1F**). Taken together, these histological results suggested that there are only mild levels of HIV-associated neuropathology in a minority of the individuals with late-stage subtype C HIV-1 infection.

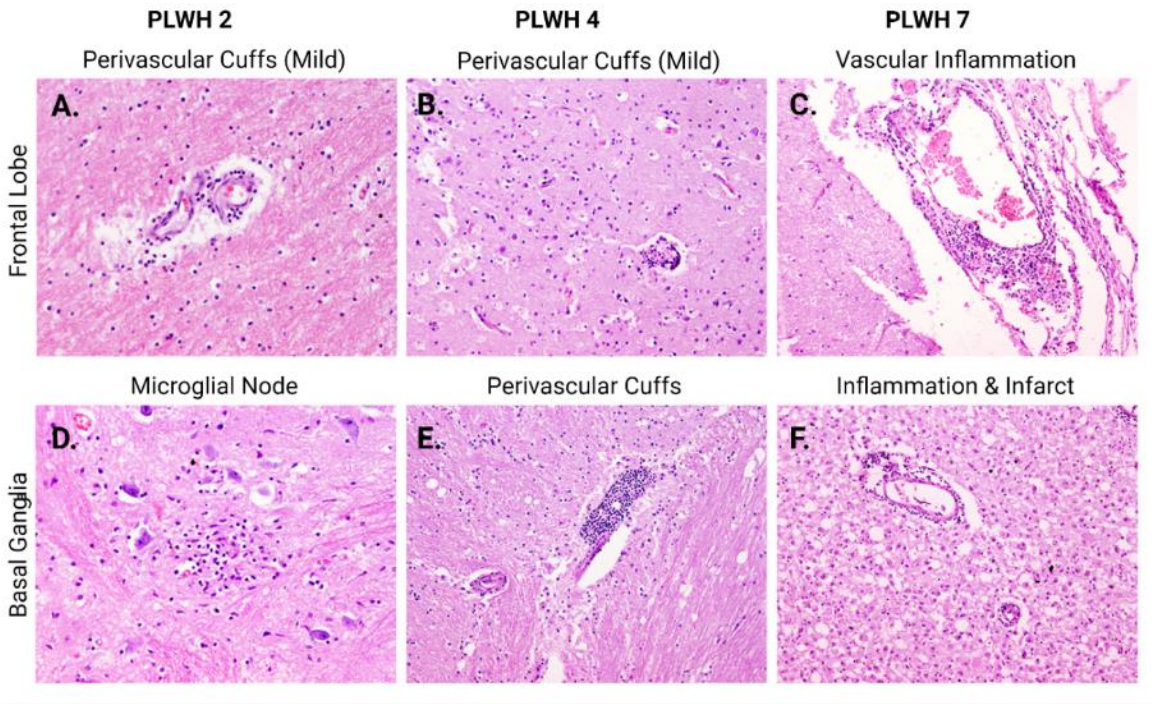

Figure 4.1. Overall mild brain pathology in individuals with late-stage subtype C HIV-1 infection. The minimal changes observed in cases PLWHs 2, 4, and 7 are presented. (A) A minimal accumulation of perivascular cuffs of lymphocytes was observed in the frontal lobe of PLWH 2. (B) A minimal accumulation of perivascular cuffs of lymphocytes was also observed in the frontal lobe of PLWH 4. (C) Meningeal vascular inflammation was observed in the frontal lobe of PLWH 7. (D) A single microglial node was observed in the basal ganglia of PLWH 2. (E) A moderate level of perivascular cuffs of lymphocytes was observed in the basal ganglia of PLWH 4. (F) in the basal ganglia of case PLWH 7, a subacute infarct characterized by abundant foamy macrophages was found in an area of perivascular inflammation.

Lack of infected cells expressing viral protein in the brain with late-stage subtype C infection

Subtype B HIV-1 studies indicated that HIV-1 established brain reservoir early during the acute infection stage (295, 296), probably via infected CD4+ T cells or monocytes that migrate across the blood brain barrier (BBB) as a "Trojan horse" (297), or via cell-free viruses (298, 299). To determine the extent of CD4+ cells infiltration into the brain at the late-stage of subtype C HIV-1 infection, we conducted IHC labeling using anti-CD4 antibody. However, among the 9 ART-naïve individuals, CD4+ cells were detected in the perivascular regions in the brain of one individual, but not in the others (data not shown). This is likely due to the low CD4 count in the peripheries of all HIV+ individuals with late-stage infection.

In ART naïve individuals with late-stage subtype B infection, it has been reported that there was active viral production in the infected brain cells, we then examined the brain tissues for subtype C viral p24 protein. Interestingly, subtype C viral p24 was only detected in the circulating inflammatory cells of PLWH 8 (**Figure 4.2A**), but not in any glial or parenchymal cells, and not in the frontal lobes of the other eight infected individuals (**Figure 4.2B-I**). Moreover, there was no detected p24 protein in the basal ganglia of any infected individuals (data not shown). Taken together, those results suggested a lack of infected cells expressing p24 viral protein in the brain even at late-stage of subtype C HIV-1 infection.

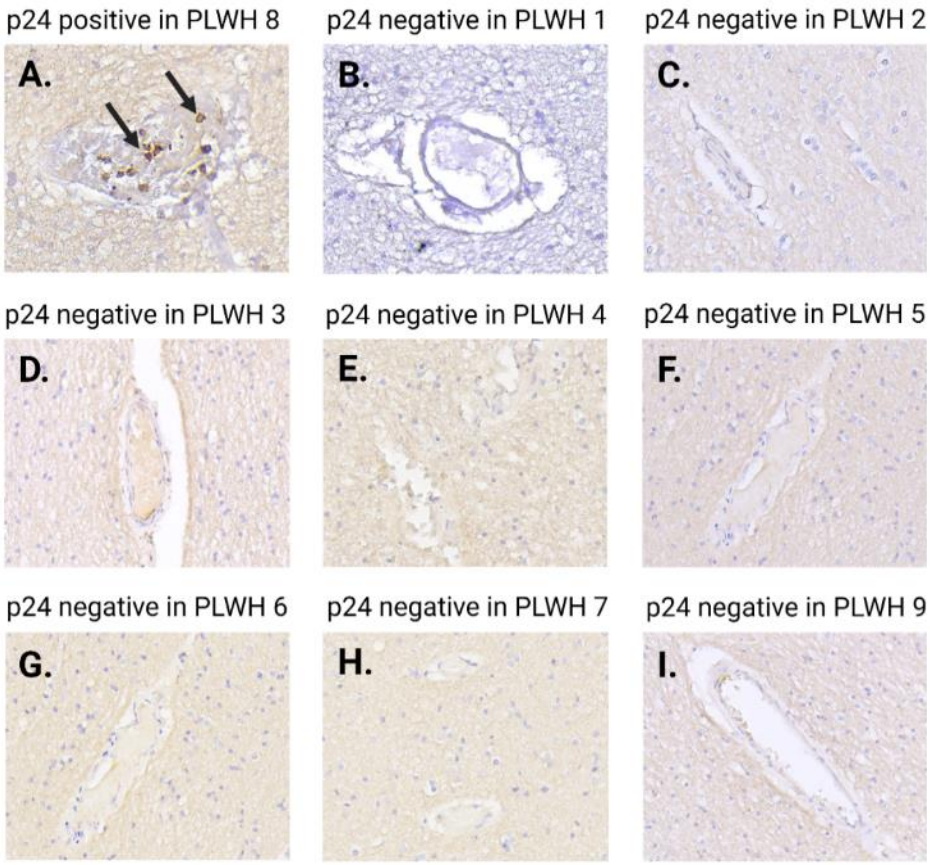

Figure 4.2. Lack of HIV+ cells in brains of individuals with late-stage subtype C HIV-1 infection. Immunohistochemistry with p24 antibodies was conducted on frontal lobe tissues of all 9 infected individuals. (A) p24 was robustly expressed in circulating immune cells within a blood vessel of PLWH 8, while no expression was detected in neural glial cells. (B) Viral p24 was not detectable in the frontal lobe of PLWH 1. (C) Viral p24 was not detectable in the frontal lobe of PLWH 2. (D) Viral p24 was not detectable in the frontal lobe of PLWH 3. (E) Viral p24 was not detectable in the frontal lobe of PLWH 4. (F) Viral p24 was not detectable in the frontal lobe of PLWH 5. (G) Viral p24 was not detectable in the frontal lobe of PLWH 6. (H) Viral p24 was not detectable in the frontal lobe of PLWH 7. (I) Viral p24 was not detectable in the frontal lobe of PLWH 9.

Similar activation levels of microglia and astrocytes between HIV+ and HIV- individuals' frontal lobes

We then investigated the impact of late-stage subtype C HIV-1 infection on immune activation in the brain tissues. Given that elevated microgliosis and astrogliosis have been well documented in subtype B HIV-1 infected individuals, we immunolabeled the brain tissues from HIV+ and HIV- individuals with Iba-1 and GFAP antibodies to

evaluate if late-stage subtype C HIV-1 infection will lead to the expected elevated levels of microgliosis (Iba-1+) and astrogliosis (GFAP+). After immunohistochemistry, the proportions of Iba-1+ or GFAP+ cells were quantified and compared between HIV+ and HIV- frontal lobes.

For the frontal lobe tissues, the mean (SD) of percentage of Iba-1+ cells in HIV+ individuals were 10.49% (1.36%), and it did not differ significantly from the HIV- individuals [9.96% (1.57%)] (**Figure 4.3A-C**). In addition, there were no significant differences in the mean (SD) of percentages of GFAP+ cells between HIV+ frontal lobes [22.20% (3.28%)] and HIV- frontal lobes [22.13% (3.59%)] (**Figure 4.3D-F**).

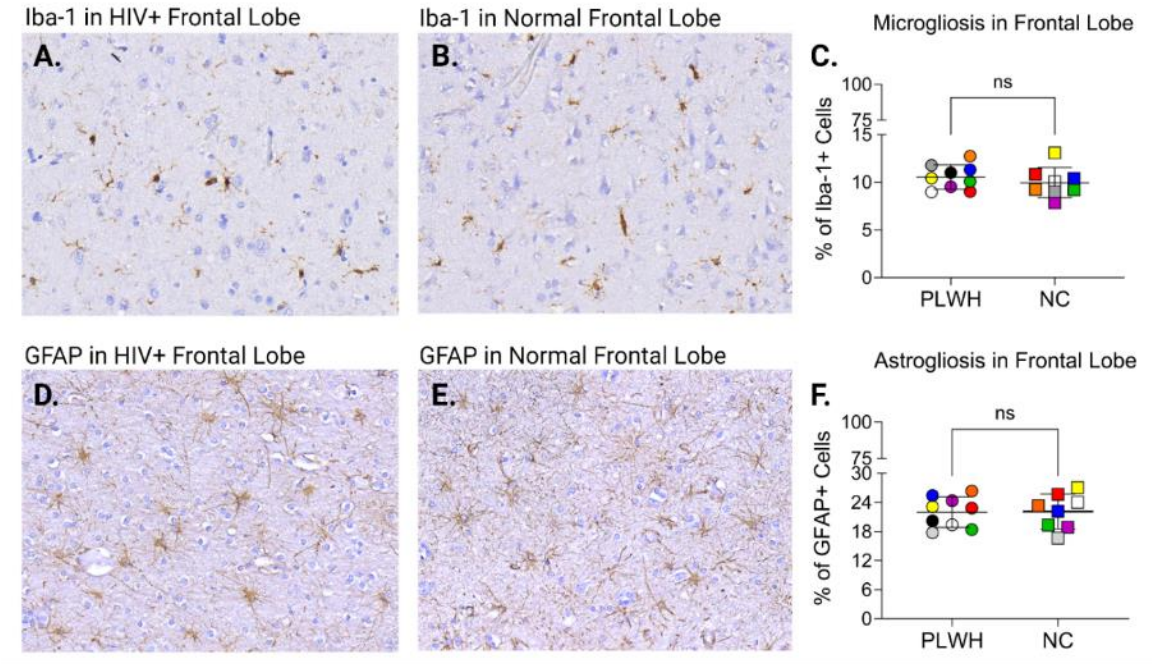

Figure 4.3. Similar activation levels of microglia and astrocytes between HIV+ and HIV- frontal lobes. Microglia and astrocytes were labeled in the frontal lobe of HIV+ and HIV- individuals by IHC using anti-Iba-1 and anti-GFAP antibodies, respectively. Quantifications of Iba-1+ and GFAP+ cells were also conducted. (A) Microglia (Iba-1+) staining in the frontal lobe of HIV+ individuals showing almost identical percentages of positive cells. (B) Microglia in the frontal lobe of HIV- individuals. (C) There was no significant difference in the percentage of Iba-1+ cells in the frontal lobes between HIV+ and HIV- groups. (D) Astrocytes (GFAP+) staining in the frontal lobe of HIV+ individuals. (E) Astrocytes in the frontal lobe of

HIV- individuals, once again showing very similar percentages. (F) No significant difference in the proportion of GFAP+ cells in the frontal lobes between HIV+ and HIV- groups. PLWH, people living with HIV; NC, normal control; ns, not significant.

Similar activation levels of microglia and astrocytes between HIV+ and HIV- individuals' basal ganglia tissues

In support of the findings from frontal lobes, there were also no differences in the levels of Iba-1+ and GFAP+ cells between HIV+ and HIV- in the basal ganglia tissues. Specifically, the mean (SD) percentage of Iba-1+ cells in HIV+ basal ganglia tissues were 11.07% (1.49%), which were not significantly different from those in HIV- basal ganglia tissues [10.78% (1.50%)] (**Figure 4.4A-C**). Moreover, the mean (SD) percentages of GFAP+ cells between HIV+ [20.74% (3.26%)] and HIV- basal ganglia tissues [21.14% (3.01%)] were also similar (**Figure 4.4D-F**).

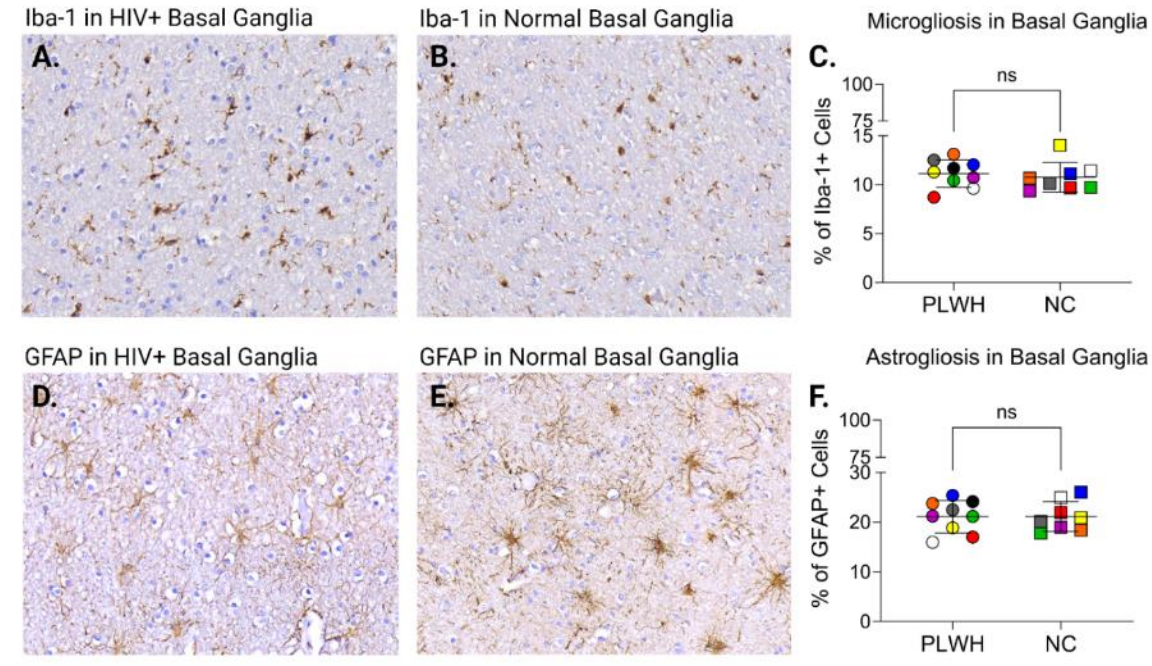

Figure 4.4. Similar activation levels of microglia and astrocytes between HIV+ and HIV- basal ganglia tissues. Microglia and astrocytes were immunohistochemically labeled and quantified in the basal ganglia tissues of HIV+ and HIV- individuals. (A) Microglia (Iba-1+) staining in the basal ganglia of HIV+ individuals. (B) Microglia in the basal ganglia of HIV- individuals. (C) There was no significant difference in the percentages of Iba-1+ cells in the

basal ganglia tissues between HIV+ and HIV- groups. (D) Astrocytes (GFAP+) staining in the basal ganglia of HIV+ individuals. (E) Astrocytes in the basal ganglia of HIV- individuals. (F) Similar percentages of GFAP+ cells were observed in the basal ganglia tissues between HIV+ and HIV- groups. PLWH, people living with HIV; NC, normal control; ns, not significant.

Similar levels of CD8+ CTL infiltration into the brains between HIV+ and HIV- individuals

Since HIV-1 infection has been shown to lead to an increased in CD8+ CTL infiltration into the brain tissues in subtype B infected individuals, we then determined if there is increased CD8+ CTL infiltration in the HIV+ brain tissues, we performed immunohistochemistry in frontal lobe and basal ganglia from all HIV+ and HIV- individuals using anti-CD8 antibody. Utilizing the same quantification method for microgliosis and astrogliosis evaluation, the proportions of CD8+ cells were compared between HIV+ and HIV- brain tissues. However, we did not observe any significant differences in the levels of CD8+ CTL infiltration between HIV+ and HIV- individuals [0.68% (0.16%) vs 0.66% (0.14%) in the frontal lobe; 0.62% (0.14%) vs 0.61% (0.19%) in the frontal lobe] (**Figure 4.5**).

Taken together, our results suggest that at the late-stage of subtype C HIV-1 infection there were no significant differences in microgliosis or astrogliosis compared to the controls. Moreover, no detectable increased CD8+ CTL infiltration was detected due to HIV-1 infection. In support of the reported low levels of subtype C HIV-1 proviruses detectable in both aviremic and viremic brain tissues, our report on the unremarkable neuropathology findings of the HIV+ brain tissues further substantiate our earlier findings that subtype C HIV-1 has poor neurotropism and that the brain is not a significant reservoir for subtype C HIV-1.

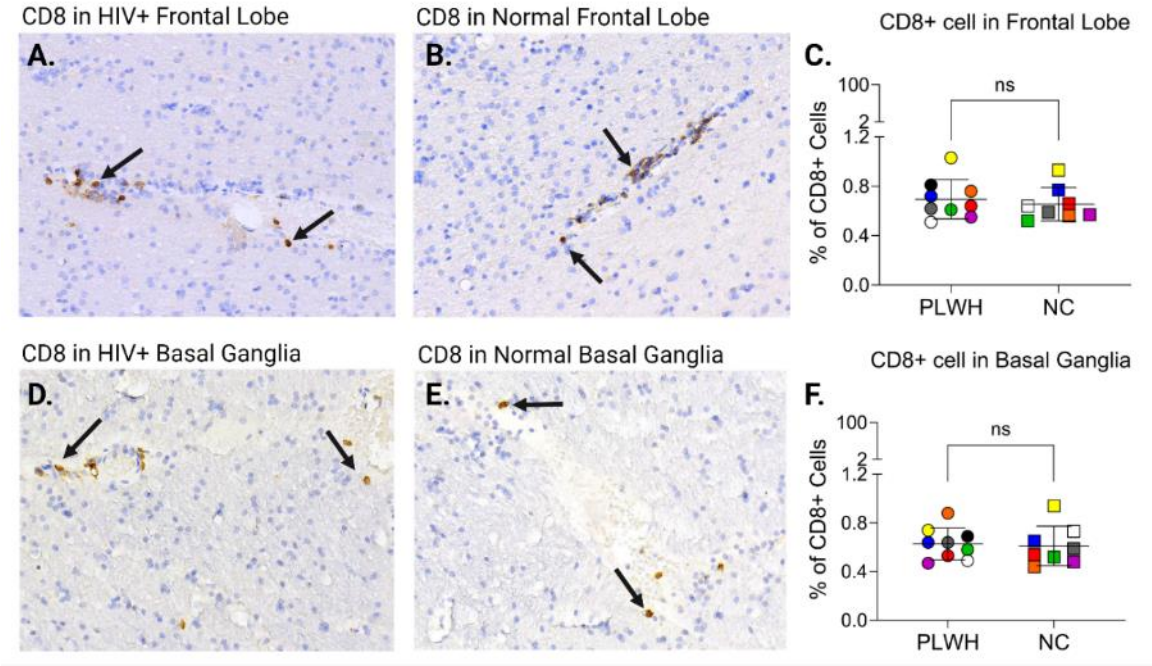

Figure 4.5. Similar levels of CD8+ CTL infiltration into the brain between PLWH and uninfected controls. CD8+ T cells were labeled and quantified in the brain tissues of HIV+ and HIV- individuals. Most CD8+ T cells were observed in perivascular regions in the brain tissues. (A) CD8+ T cells observed in the frontal lobe of HIV+ individuals. (B) CD8+ T cells observed in the frontal lobe of HIV- individuals. (C) No significant difference in the percentage of CD8+ T cells in the frontal lobes between HIV+ and HIV- groups. (D) CD8+ T cells observed in the basal ganglia of HIV+ individuals. (E) CD8+ T cells observed in the basal ganglia of HIV- individuals. (F) Similar levels of CD8+ T cell infiltration was observed in the basal ganglia tissues between HIV+ and HIV- groups. PLWH, people living with HIV; NC, normal control; ns, not significant. Arrows indicate representative CD8+ cells.

Discussion

Although ART has enabled PLWH to live a normal lifespan, the development of HAND in 30-50% PLWH still severely affects the quality of life for these individuals (300, 301). The presence of HIV-1 in the brain in ART era poses dual risks to PLWH, as the brain serves not only as an important HIV tissue reservoir for viral reactivation but also for contributing to HAND. Results from subtype B and C HIV-1 studies suggest that subtype C HIV-1 is less neurotropic compared to subtype B. Subtype B proviruses were readily detected in the brain even under ART (93, 105), while subtype C proviruses were

only detected in a minority of brain tissues in viremic individuals (196, 253, 293). However, whether genetic variations among different HIV-1 subtypes affect neurological outcomes remains unresolved. Pre-clinical *in vitro* studies have indicated lower neurotropism and neurotoxicity for the subtype C virus and its viral Tat protein compared to subtype B HIV-1 (302, 303). Moreover, epidemiological studies have reported that subtype C HIV-1 infection in India is associated with reduced severity and rate of HAND (304, 305). In contrast, another study conducted in southern Brazil indicated that subtype B and subtype C HIV-1 infected individuals did not differ significantly in the rate of HAND (306). This discrepancy might be due, at least in part, to differences in geographic conditions of the subtype C HIV-1 infected populations, making it challenging to clearly understand the neuropathogenesis of subtype C HIV-1.

Previous studies suggested that subtype C is present in the brain at lower frequencies with lower viral burden (proviral DNA copies), and likely to be a less robust reservoir for reactivation. The lack of detectable viral p24 protein in the brains of subtype C infected individuals is in significant contrast to subtype B HIV-1 infection, for which studies have consistently reported the presence of viral p24 protein in the brains of both viremic and aviremic individuals (93, 274, 275). This indicates that even at late stages of infection, subtype C HIV-1 may not establish productive infection in the brain, which is promising from a therapeutic perspective as it may limit the potential for viral rebound from the CNS after interruption of ART. However, it is not clear if the presence of subtype C proviruses can either directly or indirectly lead to a similar extent of neuropathology as subtype B HIV-1. Consistent with the absence of viral production, we observed only mild HIV-related brain pathologies, such as perivascular cuffs of

lymphocytes and microglial nodules, in a minority of late-stage subtype C-infected individuals (3 out of 9 individuals). These findings aligned with the notion that subtype C infections may lead to milder neuropathological outcomes compared to subtype B (302, 303).

CD8+ CTLs may play a crucial role in the immune surveillance against viral infections, including HIV-1, by targeting and killing cells presenting viral antigens, thereby limiting viral replication and spread (307, 308). On the other hand, excessive or dysregulated CTL activity in the brain can lead to neuroinflammation and collateral damage to neurons and glial cells, contributing to the pathogenesis of HAND and HIV encephalitis (HIVE) (289, 309, 310). Although increased CD8+ CTL infiltration into the brain could be one of the underlying mechanisms of absence of overt brain pathologies and immune activation, our findings indicated otherwise. No increased CTL infiltration into the brain at late-stage subtype C infection suggested that CTLs are not likely to be involved in subtype C HIV-1 neuropathogenesis. Further understanding of the delicate balance between the beneficial and detrimental effects of CTL infiltration in the context of HIV-1 infection will be important for developing targeted therapeutic strategies that harness the positive aspects of the immune response while mitigating its negative consequences in the CNS.

A caveat of our study is the likely degradation of cellular nucleic acids in the brain tissues during the post-mortem sampling, processing, and storage of the brain tissues into FFPE blocks. The degradation of cellular DNA and RNA has hampered our ability to evaluate subtype C HIV-1 proviral DNA and RNA in the collected brain tissues. Nevertheless, the lack of viral p24 in the brains of those with late-stage subtype C

infection provided important insights into the overall viral burden and the nature of subtype C HIV-1 infection at this stage. It is unlikely that the degradation of cellular nucleic acids affected our detection of cellular and viral proteins by immunohistochemistry (IHC), as other cellular protein (Iba-1/GFAP/CD8) were readily detected on the same brain tissues, suggesting that IHC was effective for our archival FFPE brain tissues. Additionally, the lack of computerized clinical documentation in Zambia meant that detailed clinical information, such as time since diagnosis of HIV infection, was unavailable. Nevertheless, having access to brain tissues from ART-naïve individuals who died from AIDS in the era of ART presents a unique opportunity to evaluate late-disease disease neuropathology. Our results from nine such cases consistently showed that there were no remarkable HIV-related neuropathologies and immune activation compared to normal brains tissues, accompanied by the lack of productive infection in the infected brains tissues even at late-stage subtype C HIV-1 infection.

Taken together, besides shedding light on the distinct neuropathological features of subtype C HIV-1 in SSA, our findings also provided further evidence on the lack of neurotropism for subtype C HIV-1 and emphasized the need for subtype-specific considerations in understanding HIV-associated neurological complications. Future research is needed to further understand how subtype C HIV-1 interacts with the CNS, which could lead to targeted therapeutic interventions and improved management of HIV-related neurological complications in regions where subtype C is predominant.

CHAPTER 5:

CANNABIS USE ASSOCIATES WITH REDUCED PROVIRAL BURDEN AND INFLAMMATORY CYTOKINE EXPRESSION IN TISSUES FROM MEN WITH CLADE C HIV-1 ON SUPPRESSIVE ART

Abstract

HIV-1 tissue reservoirs remain the main obstacle against an HIV cure. Limited information exists regarding cannabis's effects on HIV-1 infections *in vivo*, and the impact of cannabis use on HIV-1 parenchymal tissue reservoirs is unexplored. To investigate whether cannabis use alters HIV-1 tissue reservoirs, we systematically collected 21 postmortem brain and peripheral tissues from 20 men with subtype C HIV-1 and with suppressed viral load enrolled in Zambia, 10 of whom tested positive for cannabis use. The tissue distribution and copies of subtype C HIV-1 *LTR*, *gag*, *env* DNA and RNA, and the relative mRNA levels of cytokines IL1β, IL6, IL10, and TGFβ1 were quantified using PCR-based approaches. Utilizing generalized linear mixed models we compared persons with HIV-1 and suppressed viral load, with and without cannabis use. The odds of tissues harboring HIV-1 DNA, and the viral DNA copies in those tissues were significantly lower in persons using cannabis. Moreover, the transcription levels of pro-inflammatory cytokines IL1β and IL6 in lymphoid tissues of persons using cannabis were also significantly lower. Our findings suggested that cannabis use is associated with reduced sizes and inflammatory cytokine expression of subtype C HIV-1 reservoirs in men with suppressed viral load.

Introduction

Although antiretroviral therapy (ART) can suppress HIV plasma viral load (pVL) to undetectable levels (aviremia) and people living with HIV (PLWH) are living a more normal life (311), it is not a cure as ART cessation will lead to viral rebound (96). This rebound is derived from integrated HIV-1 DNA (provirus) in different tissues - viral reservoirs (203, 312). Most reservoir studies have focused on subtype B HIV-1, and central nervous system (CNS) and multiple peripheral tissues were documented as potential tissue reservoirs (92, 108, 186, 194). Few reservoir studies have focused on subtype C HIV-1 which predominates in sub-Saharan Africa (SSA) and India, and accounts for nearly 50% of global infection with the premise that all HIV-1 subtypes infection would parallel findings from subtype B (196, 313). Utilizing postmortem tissues from people with suppressed pVL enrolled in Zambia, we have demonstrated that subtype C DNA is variably detected in peripheral tissues and unlike subtype B, it poorly accesses the CNS (253).

Currently, little is known about the impact of co-factors, including substance abuse, on the establishment and maintenance of HIV-1 reservoirs. Cannabis (*Cannabis sativa*) is widely consumed in the general population and PLWH (314, 315). Cannabis use prevalence in SSA appears to be approximately 12% for adults and just under 8% for adolescents. Notably, regional differences exist in the prevalence of cannabis use, with a high prevalence of cannabis use was reported in South Africa [16.7% (9.1–26.0%)] and Zambia [36.5% (34.3–38.7%)](138, 145-147). Of the > 100 cannabinoids in *Cannabis sativa*, Δ9-tetrahydrocannabinol (THC) and cannabidiol (CBD) are the primary psychoactive and non-psychoactive ingredients, respectively (148). To date, the effects of

cannabis on HIV-1 have only been evaluated for subtype B infections and remained controversial. Some have reported cannabis either had no effect (149, 150), or detrimental effects (139, 151), or lower pVL in cannabinoid exposure (152), and reduced inflammation in experimental macaques (153-155). Notably, most of these studies utilized subtype B infected blood samples to study cellular reservoirs, whether cannabis use impacts the size of tissue reservoirs is unknown. Moreover, the impact of cannabis use in subtype C reservoirs is unexplored.

In this study, we systematically quantified HIV-1 *LTR*, *gag*, *env* DNA and RNA in 21 postmortem CNS and peripheral tissues from 20 men with subtype C HIV-1 and with suppressed pVL, 10 of whom were identified as persons using cannabis (THC+). We evaluated the effects of cannabis use on subtype C HIV-1 reservoir distribution, viral burden and expression. Compared to men without cannabis use (THC-), THC+ men have significantly lower odds of a given tissue harboring subtype C HIV-1 proviral DNA, and lower proviral DNA burdens in tissues. Viral RNA was also expressed in fewer tissues in THC+ men. Moreover, in THC+ men, the relative mRNA levels of pro-inflammatory cytokines IL1β and IL6 were also significantly lower in the tissues analyzed. Our findings suggest that there are potential beneficial effects of cannabinoids in reducing the subtype C HIV-1 tissue reservoir size and expression of pro-inflammatory mediators in men with suppressed pVL.

Materials and methods

Study cohort and tissue collections

Deceased persons were consented by the next-of-kin for the postmortem collection of tissue specimens at the mortuary of the University Teaching Hospital (UTH)

in Zambia. Sociodemographic information as well as available medical history were collected whenever possible. Eventually, 381 deceased Zambians were enrolled and autopsied within 48 hours of their deaths. Different brain and peripheral tissues of these 381 persons were collected and cryopreserved at -80°C or processed to formalin-fixed, paraffin-embedded (FFPE) blocks. During autopsy, blood samples were also obtained from the carotids or the hearts of all persons. In cases of severe anemia, blood samples were obtained from the femoral vessels.

Screening of persons with suppressed pVL and with cannabis use

Postmortem plasma samples of the deceased were first utilized to determine HIV-1 serological status using HIV Rapid Test. For HIV-1 seropositive persons, plasma VL were quantified in triplicates using the RNA UltraSense One-Step RT-qPCR System (Invitrogen, Waltham, MA) with AcroMetrix HIV-1 standard (Thermo Fisher Scientific, Fremont, CA) with HIV-1 *LTR* primers and probe (Supplementary Table 1). The cutoff of HIV-1 *LTR* RNA detection in our system was 70 copies/ml. In this study, HIV+ persons with pLV lower than 70 copies/ml were identified as persons with suppressed pVL. Plasma samples were also used in laboratory testing for 11-nor-9-carboxy-Δ9-tetrahydrocannabinol (THC-COOH), a stable main secondary metabolite of THC, using the Cannabinoid (THCA/CTHC) Direct ELISA Kit (Immunalysis, Pomona, CA) to validate the information about cannabis use from surrogate interviewees (next-of-kin). Eventually, ten men with suppressed pVL were determined with cannabis use (HIV+/THC+) according to both ELISA and next-of-kin reports. To investigate the potential impacts of cannabis use on HIV-1 tissue reservoirs in persons with suppressed

pVL, ten age-matched men with suppressed pVL who tested negative and were not next-of-kin-reported for cannabis use (HIV+/THC-) were included in this study as controls.

Quantifications of HIV-1 DNA/RNA in different tissues

For HIV-1 DNA quantification, 100 ng genomic DNA were used as templates utilizing QuantStudio™ 3 Real-Time PCR System (Thermo Fisher Scientific, Fremont, CA). Genomic 8E5 cellular DNA, containing single proviral HIV-1 genome/cell, was used as standards. To determine viral RNA loads, 500 ng total RNA and AcroMetrix HIV-1 standards were used with the UltraSense One-Step RT-qPCR System (Invitrogen, Waltham, MA). Amplicons against HIV-1 *LTR*, *gag*, and *env* genes used for DNA copy determination were also used for viral cDNA (RNA) quantification.

Quantification of inflammatory cytokine mRNA levels by SYBR Green qPCR

To identify the relative transcription levels of inflammatory cytokines in tissues, total RNA extracted from frozen tissues were used to synthesize first-strand cDNA using Invitrogen™ SuperScript™ III First-Strand Synthesis System (ThermoFisher, Carlsbad, CA), with 25 ng of cDNA as template in subsequent SYBR Green qPCR. PrimePCR™ SYBR Green Assays, using Bio-Rad primer pairs against inflammatory cytokine cDNAs (IL1β, Assay ID: qHsaCID0022272; IL6, Assay ID: qHsaCID0020314; IL10, Assay ID: qHsaCED0003369; TGFβ1, Assay ID: qHsaCID0017026). Primers against the internal reference, *GAPDH* mRNA were also used (Supplementary Table 1). The ΔCT value was calculated (cytokine CT value – *GAPDH* CT value), and when the cytokine mRNA level CT value was over 40, the ΔCT value was set as 99.

Statistical analysis

Generalized linear mixed models (GLMMs) were used to compare THC+ and THC- persons. Fixed effects were included for cannabis use and tissue location, while random effects were used for each participant. Negative binomial families were assumed for predicting the copies of viral DNA and RNA, while binomial families were assumed for predicting the presence of any viral DNA or RNA. The functions glmer.nb and glmer from the lme4 package in R statistical software were used for the analyses. Confidence intervals (CIs) and associated p-values were Wald-based, and no multiple correction adjustment was used. To tests whether there were THC differences within each specific tissue (no repeated measures), Firth's corrected logistic regression (via the logistf function) was used for testing presence of any viral DNA/RNA while negative binomial (via the nb.glm function) was used for analyzing the counts directly. Firth's correction was used here to correct for the separation that was observed in several tissue locations. The Mann-Whitney test was utilized in cytokine ΔCT comparisons. All tests were 2-tailed and P-values < 0.05 were considered as significant.

Results

Identification of THC+ persons with subtype C HIV-1 and suppressed pVL

Figure 5.1A shows the experimental design and postmortem sampling. In this study, 381 deceased Zambians were enrolled and autopsied within 48 hours of their deaths. Among those persons, 82 persons with 'undetectable' pVL (< 70 copies/ml) were identified. Among them 10 men (U1-U10) were identified as persons using cannabis via plasma THC metabolite detection (THC+), and 10 age-matched men with suppressed pVL (N1-N10) from the other 72 THC- persons with suppressed pVL were used as controls

(253). Eight CNS tissues [frontal lobe, parietal lobe, temporal lobe, occipital lobe, hippocampus, cerebellum, basal ganglia, and choroid plexus (CPx)], and 13 peripheral tissues, as well as plasma sample, were collected from each person (**Figure 5.1B**).

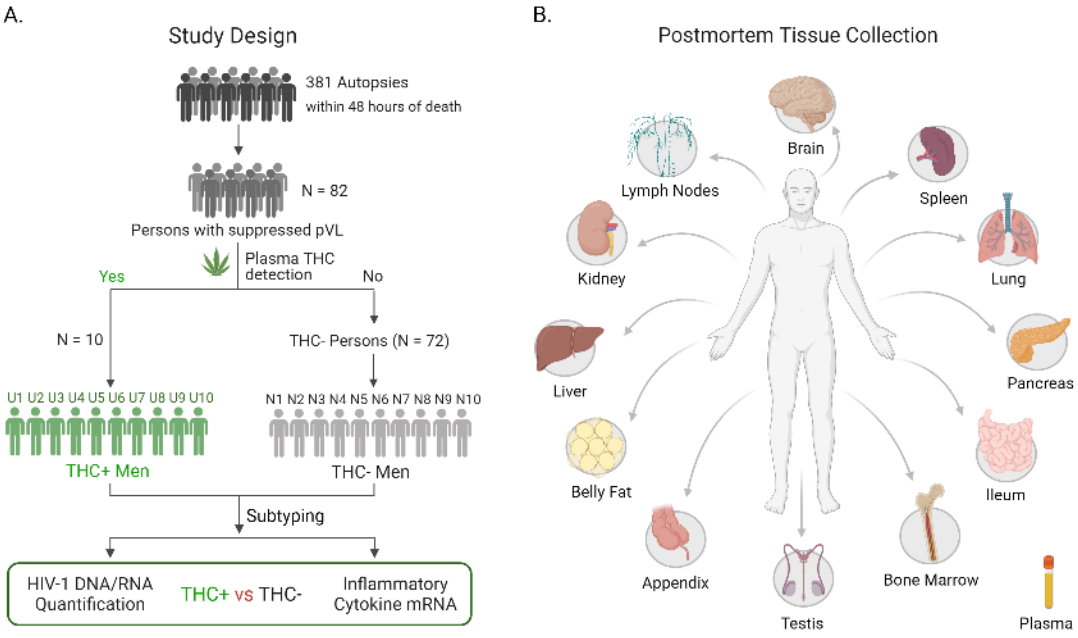

Figure 5.1. Postmortem sampling of persons with suppressed pVL, with or without cannabis use. (A) The flow diagram showed the screening of postmortem persons with/without cannabis use. Plasma RNA preparations from HIV-1 seropositive persons were subjected to standard RT-qPCR to identify persons with suppressed pVL (< 70 copies/ml). The detection of THC-COOH by ELISA in plasma from persons with suppressed pVL was used as the criteria to group persons with cannabis use (THC+) (U1, U2, U3, U4, U5, U6, U7, U8, U9, U10) and without cannabis use (THC-) (N1, N2, N3, N4, N5, N6, N7, N8, N9, N10). HIV-1 subtyping by sequencing of *env* DNA confirmed subtype C HIV-1 infection. Viral DNA and RNA copies were determined by different PCR-based methods from frozen tissue genomic DNA and total RNA. The relative mRNA levels of different inflammatory cytokines were also measured in different tissues utilizing SYBR Green qPCR. (B) Postmortem samples were collected within 48 hours of persons' death. Multiple cryopreserved brain and peripheral tissues were systematic collected. Frozen plasma samples were also collected.

Information including age, gender, and ART treatment of our cohort are shown in **Table 5.1**. To confirm subtype C HIV-1 infection, genomic DNA was extracted from frozen tissues of each person and subjected to nested PCR to amplify the HIV-1 *env* gene. Amplified HIV-1 *env* products were sequenced to determine the HIV-1 subtypes using

REGA HIV Subtyping Tool. HIV-1 *env* sequences were obtained from 17 persons with suppressed pVL, but not from three THC+ persons U4, U5, and U9 due to exceptionally low viral burden. Those 17 persons with *env* sequences were demonstrated to harbor subtype C HIV-1 (**Table 5.1**). However, given that subtype C is responsible for approximately 99% of HIV infections in Zambia, persons U4, U5, and U9 are likely to be also infected with subtype C HIV-1.

Table 5.1. Clinical information of the cohort analyzed

Person ID	Age	Sex at Birth	THC Status	pVL (copies/ml)	Age of ART Initiation	ART Duration	ART Regimen[A]	Post-mortem Interval	HIV-1 Subtype[B]
U1	28	M	THC+	<70	Unknown	Unknown	Atripla	5 hours	C
U2	60	M	THC+	<70	Unknown	Unknown	Atripla	27 hours	C
U3	59	M	THC+	<70	Unknown	Unknown	Atripla	40 hours	C
U4	28	M	THC+	<70	Unknown	Unknown	Atripla	15 hours	NA
U5	25	M	THC+	<70	Unknown	Unknown	Atripla	45 hours	NA
U6	20	M	THC+	<70	Unknown	Unknown	Atripla	27 hours	C
U7	28	M	THC+	<70	Unknown	Unknown	Atripla	14 hours	C
U8	52	M	THC+	<70	Unknown	Unknown	Atripla	17 hours	C
U9	35	M	THC+	<70	32	3 years	Atripla	12 hours	NA
U10	50	M	THC+	<70	Unknown	Unknown	Atripla	27 hours	C
N1	40	M	THC-	<70	32	8 years	Atripla	30 hours	C
N2	60	M	THC-	<70	52	8 years	Atripla	7 hours	C
N3	45	M	THC-	<70	Unknown	Unknown	Atripla	3 hours	C
N4	50	M	THC-	<70	40	10 years	Atripla	4 hours	C
N5	53	M	THC-	<70	48	5 years	Atripla	< 48 hours	C
N6	40	M	THC-	<70	36	4 years	Atripla	26 hours	C
N7	47	M	THC-	<70	Unknown	Unknown	Atripla	18 hours	C
N8	39	M	THC-	<70	34	5 years	Atripla	33 hours	C
N9	36	M	THC-	<70	Unknown	Unknown	Atripla	18 hours	C
N10	25	M	THC-	<70	Unknown	Unknown	Atripla	6 hours	C

Detectable HIV-1 DNA in various tissues of THC+ persons with suppressed pVL

Eight of 10 THC- persons with suppressed pVL (N1-N8) had already been previously characterized for viral tissue distribution and viral burden (253). To identify the tissue distribution and viral burden of subtype C reservoirs in THC+ persons with suppressed pVL, HIV-1 *LTR* DNA copies in tissues of 10 THC+ men were quantified (**Figure 5.2**). Moreover, to identify which tissues might harbor potentially intact HIV-1 provirus, *gag* and *env* DNA were also quantified in *LTR* DNA+ tissues.

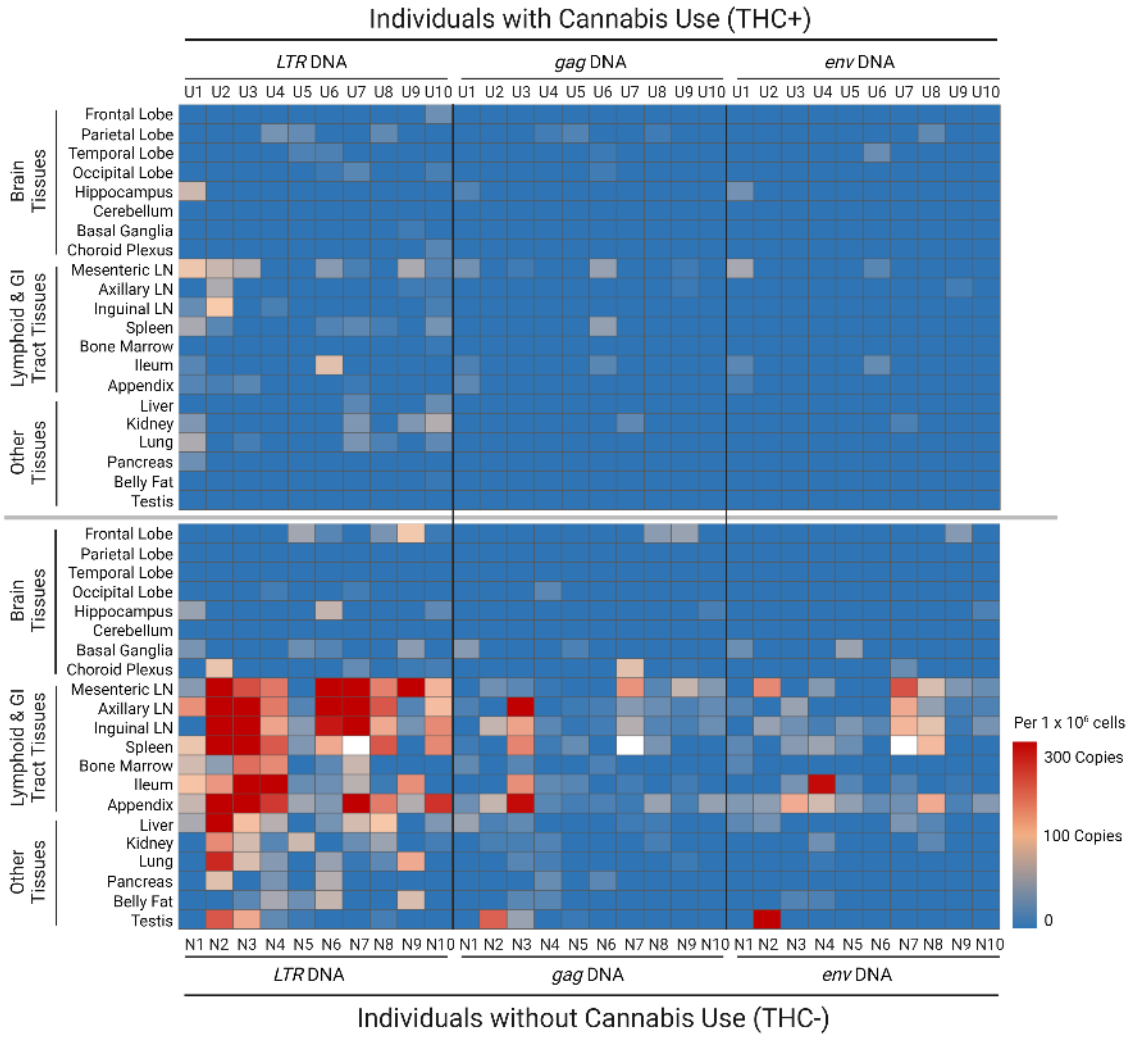

Figure 5.2. Heatmap of subtype C HIV-1 DNA in THC+ and THC- persons with suppressed pVL. The heatmap displays the abundance of three subtype C HIV-1 genes (*LTR*, *gag*, and *env*) DNA in different anatomical locations of 10 THC+ and 10 THC- men with

suppressed pVL based on qPCR analysis. Blocks with color indicate viral copy numbers; undetectable are in blue to highest DNA copies in red (up to 1538 copies/1 x 10^6 cells). The spleen of person N7 failed to be sampled (blank cells). Three subgroups of tissues were also shown. HIV-1 DNA copies were determined by qPCR with 100 ng genomic DNA as template. All samples were analyzed in triplicate qPCR reactions, and viral DNA copy numbers were calculated as the means of triplicate PCR and normalized to 1 million cells.

For the THC+ persons, HIV-1 DNA burden varied among different tissues and persons, and viral DNA was rarely detected in the brain tissues. Specifically, out of 80 total brain tissues from 10 THC+ persons, HIV-1 DNA was only detected in 12 tissues (15%), and only 3 brain tissues harbored *LTR*, *gag*, and *env* DNA (3.8%). Viral burdens in all brain tissues were lower than 100 copies/10^6 cells, supporting our previously finding that brain is not a good reservoir for subtype C HIV-1 [**Figure 5.2**, (253)]. In contrast, HIV-1 DNA was detected in 40 of 130 peripheral tissues (30.8%), and 6 of them harbored all three viral genes (**Figure 5.2**). However, the highest viral *LTR* DNA copy in THC+ tissues were quite low at 100 copies/10^6 cells, as detected in the inguinal lymph node of person U2 (**Figure 5.2**). In addition, the tissue distributions of detectable provirus also varied among the THC+ persons (**Figure 5.2**).

Less tissues harboring subtype C provirus in THC+ persons

To investigate the potential impact of cannabis use on subtype C HIV-1 reservoirs, we compared the tissue distribution of HIV-1 DNA between THC+ and THC- groups using a GLMM. After accounting for individual dependence and tissue location, THC+ persons had significantly lower odds of a tissue harboring HIV-1 DNA (**Figure 5.3A**). Specifically, tissues of THC+ persons showed 0.16 times, or ~6-fold lower odds of harboring HIV-1 *LTR* DNA (95% CI = 0.08-0.32) and 0.07 times or ~14 -fold lower odds of harboring all three *LTR*/*gag*/*env* DNAs (95% CI = 0.03-0.17) (**Figure 5.3A**).

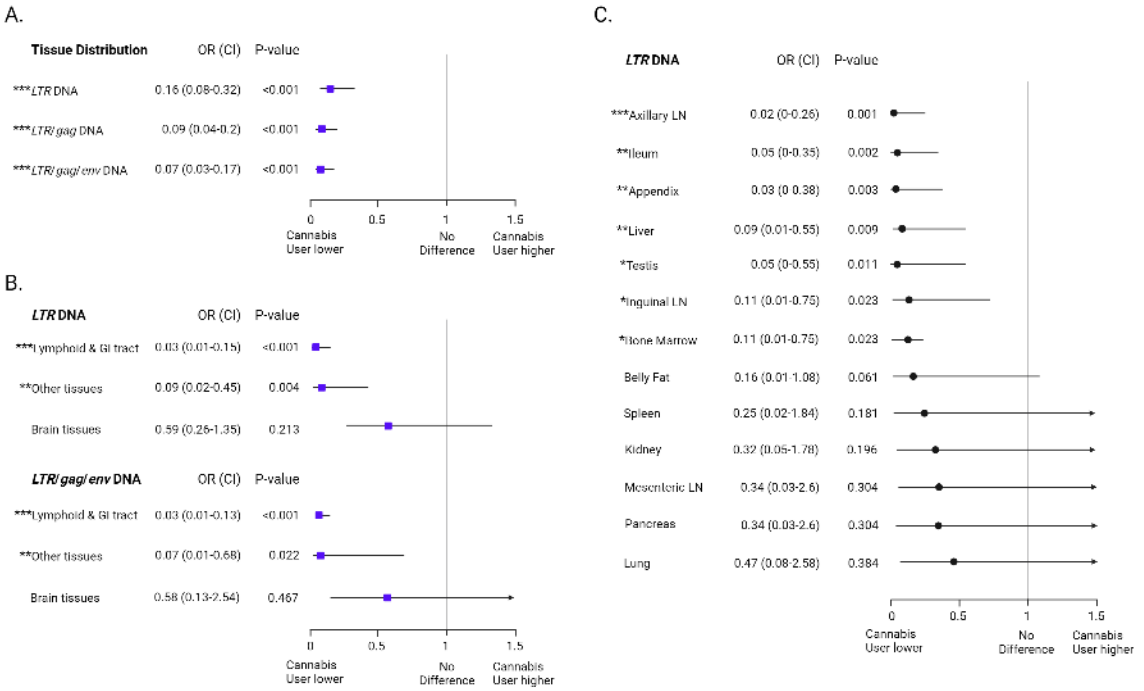

Figure 5.3. Comparisons of tissue distribution of subtype C HIV-1 DNA between THC+ and THC- persons with suppressed pVL. Adjusted odds ratios (OR) of harboring HIV-1 DNA in tissues for THC+ versus THC- groups were calculated from mixed logistic regression models with random effects for person ID and fixed effects for specific locations. (A) **Overall comparisons of THC effects across all tissues:** Significantly lower odds of tissues harboring any proviral DNA (*LTR* DNA) or all three proviruses (*LTR*/*gag*/*env* DNA) in THC+ persons compared to THC- persons. (B) **Comparisons of THC effects within 3 tissue subgroups:** In THC+ persons, tissues from "lymphoid & GI tissues" and "other tissues" subgroups, but not from "brain tissues" subgroup, had significantly lower odds of containing *LTR* DNA and all three viral DNAs compared to their counterparts in THC- persons. (C) **Comparison of THC effects within individual tissues:** Forest plots showing the differences in the odds of presence of *LTR* DNA in tissues in subgroups "lymphoid & GI tissues" and "other tissues" between THC+ and THC- persons. Tissues were shown in order based on their p-values, which were calculated from univariable logistic regression models (no repeated measurements within one tissue type). 95% CI and p-values were shown in all three plots. Significance was labelled when $p < 0.05$ (*), $p < 0.01$ (**), and $p < 0.001$ (***).

To better understand how this difference might be related to different organ/tissue systems, we stratified 21 tissues into 3 subgroups. The eight CNS tissues were classified into "brain tissues" subgroup, three types of lymph nodes (LNs), bone marrow, spleen, ileum, and appendix were divided into "lymphoid & GI tract tissues" subgroup, and the

remaining 6 peripheral tissues were categorized as the "other tissues" subgroup. The GLMM results showed that comparing THC+ to THC- persons, the odds of presence of any proviruses (*LTR* DNA) or potential intact proviruses (*LTR*/*gag*/*env* DNA) were significantly lower in "lymphoid & GI tract tissues" and "other tissues" subgroups, whereas the "brain tissues" subgroup showed no significant differences (**Figure 5.3B**). Furthermore, we also analyzed THC-dependent distribution differences of *LTR* DNA at single tissue level using Firth's corrected logistic regression. Here there was only one observation per patient. Axillary LN, ileum, appendix, liver, testis, inguinal LN, and bone marrow showed significant differences, whereas belly fat, spleen, kidney, mesenteric LN, pancreas, and lung tissues did not (**Figure 5.3C**). For example, the odds of harboring *LTR* DNA in THC+ axillary LNs were 0.02 times or ~50-fold lower than that in THC- axillary LNs, and this difference is significant ($p = 0.001$, ***). Although the odds of harboring *LTR* DNA in THC+ spleen tissues were 0.25 times or ~4-fold lower than that in THC- spleen tissues, this difference is not significant as the p value is 0.181, which is > 0.05 (**Figure 5.3C**).

Lower viral burden of subtype C reservoir in THC+ persons

We also tested for significant magnitude of proviral burden (HIV-1 DNA copies) differentials between THC+ and THC- persons. Detectable DNA copies ranged from 4 to 1538 copies/10^6 cells in THC- persons, and from 4 to 100 copies/10^6 cells in THC+ persons (**Figure 5.2**). The GLMM results showed that THC+ persons had significantly lower copies of viral *LTR*, *gag*, and *env* DNA (**Figure 5.4A**). At the tissue subgroup level, copies of *LTR* DNA or *env* DNA were significantly lower in "lymphoid & GI tract tissues" and "other tissues" subgroups in THC+ persons, while the "brain tissues"

subgroup showed no significant differences (**Figure 5.4B**). However, all peripheral tissues in THC+ persons were shown to harbor a lower level of viral *LTR* DNA compared to the THC- persons (**Figure 5.4C**). Specifically, the copies of *LTR* DNA in THC+ appendix tissues were 0.02 times or ~50-fold lower than that in THC- appendix tissues, and this difference is significant ($p < 0.001$, ***). Moreover, the copies of *LTR* DNA in THC+ ileums were 0.08 times or ~12-fold lower than that in THC- ileums, and this difference is also significant ($p = 0.011$, **) (**Figure 5.4C**).

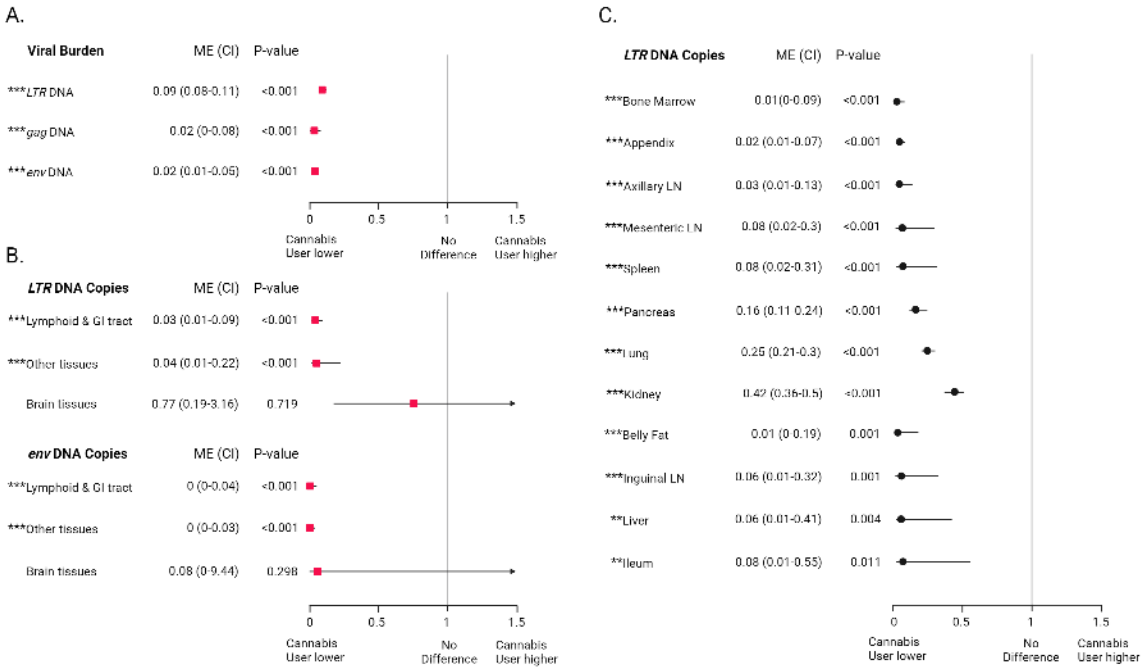

Figure 5.4. Comparisons of the levels of viral burden between THC+ and THC- persons with suppressed pVL. Multiplicative effect (ME) of THC+ versus THC- groups on the copies of viral DNA were calculated from mixed negative binomial regression models with random effects for individual ID and fixed effects for specific locations. (A) **Overall comparisons of THC effects across all tissues:** Significantly lower copies of proviral *LTR* DNA ($p < 0.001$), *gag* DNA ($p < 0.001$), *env* DNA ($p < 0.001$) in THC+ persons compared to THC- persons. (B) **Comparisons of THC effects within 3 tissue subgroups:** In THC+ persons, tissues from "lymphoid & GI tissues" and "other tissues" subgroups, but not from "brain tissues" subgroup, had significantly lower copies of *LTR* DNA and *env* DNA compared to their counterparts in THC- persons. (C) **Comparison of THC effects within individual tissues:** Forest plot showing the differences in the levels of viral burden in tissues from subgroups "lymphoid & GI tissues" and "other tissues" between THC+ and THC- persons. Tissues were

shown in order based on their p-values, which were calculated from univariable negative binomial regression models (no repeated measurements within one tissue type). 95% CI and p-values were shown in all three plots. Significance was labelled when $p < 0.01$ (**) and $p < 0.001$ (***).

Few tissues express viral RNA in THC+ persons

To detect and quantify THC-dependent differences in viral RNA expression in different tissues, HIV-1 *LTR*, *gag*, and *env* RNA copies were quantified. In THC- persons, HIV-1 RNA was detected in 8 out of 10 persons (80%). Viral RNA was detectable primarily in the "lymphoid and GI tract tissues", sporadically in the "other tissues", but not in the "brain tissues" [**Figures 5.5**, (253)]. Specifically, viral *LTR* RNA was detectable in 30.7% proviral DNA+ tissues (35 out of 114 tissues) with copy number ranging from 13 to 1609 copies/500 ng total RNA (**Figure 5.5**). For THC+ persons, *LTR* RNA was only detected in 4 persons, compared to 8 in THC- group. Moreover, viral RNA was only detected in "lymphoid and GI tract tissues" subgroup and only 7 tissues expressed detectable viral RNA (**Figure 5.5**) with the copy number ranging from 52 to 278 copies/500 ng total RNA, suggesting a decrease in RNA expression compared to THC- group (**Figure 5.5**).

Although the GLMM results revealed that the odds of tissues expressing *LTR* RNA in THC+ persons were significantly lower than that in THC- persons ($p = 0.041$) (data not shown), the odds of tissues expressing *gag* or *env* RNA could not be analyzed because they were undetectable for the THC+ group (**Figure 5.5**).

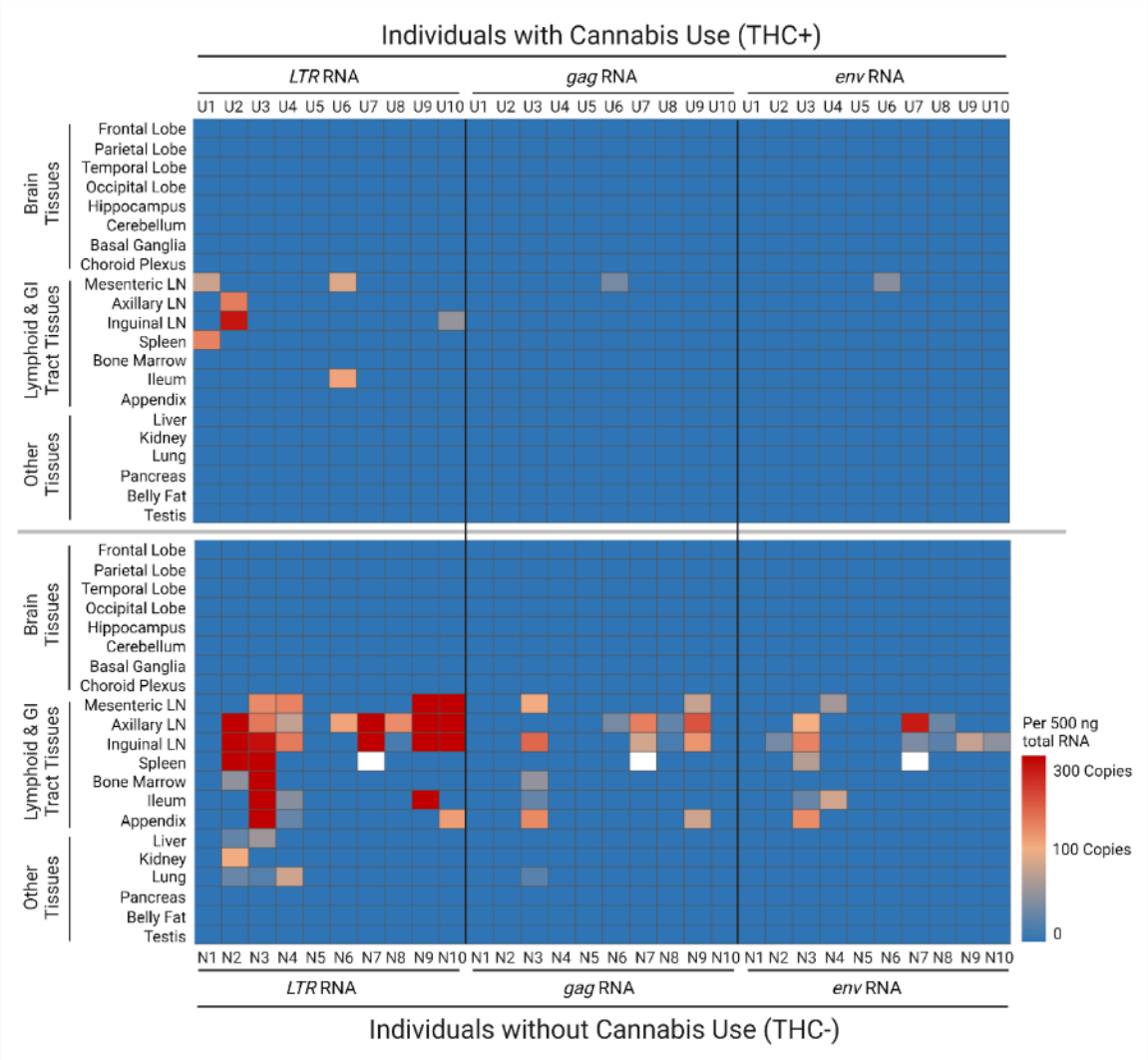

Figure 5.5. Heatmap of subtype C HIV-1 RNA in THC+ and THC- persons with suppressed pVL. A heatmap displaying viral RNA transcripts (*LTR*, *gag*, and *env*) abundance as determined by RT-qPCR analysis in 10 THC+ and 10 THC- persons with suppressed pVL. Blocks with color indicate viral copy numbers; undetectable are in blue to highest DNA copies in red (up to 1566 copies/500 ng total RNA). Blank indicates sample was not available. HIV-1 RNA copies were identified by RT-qPCR with 500 ng input RNA as template. All samples were analyzed in duplicate RT-qPCR reactions.

Lower levels of relative mRNA of pro-inflammatory cytokines in the lymph node and appendix tissues of THC+ persons

We then investigated the expressions of pro-inflammatory cytokines, IL1β and IL6, and anti-inflammatory cytokines, IL-10 and TGFβ1 in HIV+/THC- and HIV+/THC+

groups. Ten HIV-/THC- people were also used as normal controls. Cytokine mRNA levels were quantified from axillary lymph node and appendix, two tissues which showed lower viral burden in THC+ persons than in THC- persons (**Figure 5.4**). Relative mRNA levels of the four cytokines in axillary lymph node showed no significant differences between HIV-/THC- controls and HIV+/THC- persons. However, the axillary lymph nodes from HIV+/THC+ group had significantly lower IL1β and IL6, but equivalent IL10 and TGFβ1 relative mRNA levels (**Figure 5.6A**) when compared to HIV+/THC- group. Similarly for appendix tissues, there were also significantly lower relative mRNA levels of IL1β and IL6, but similar mRNA levels of IL10 and TGFβ1 in the HIV+/THC+ group (**Figure 5.6B**).

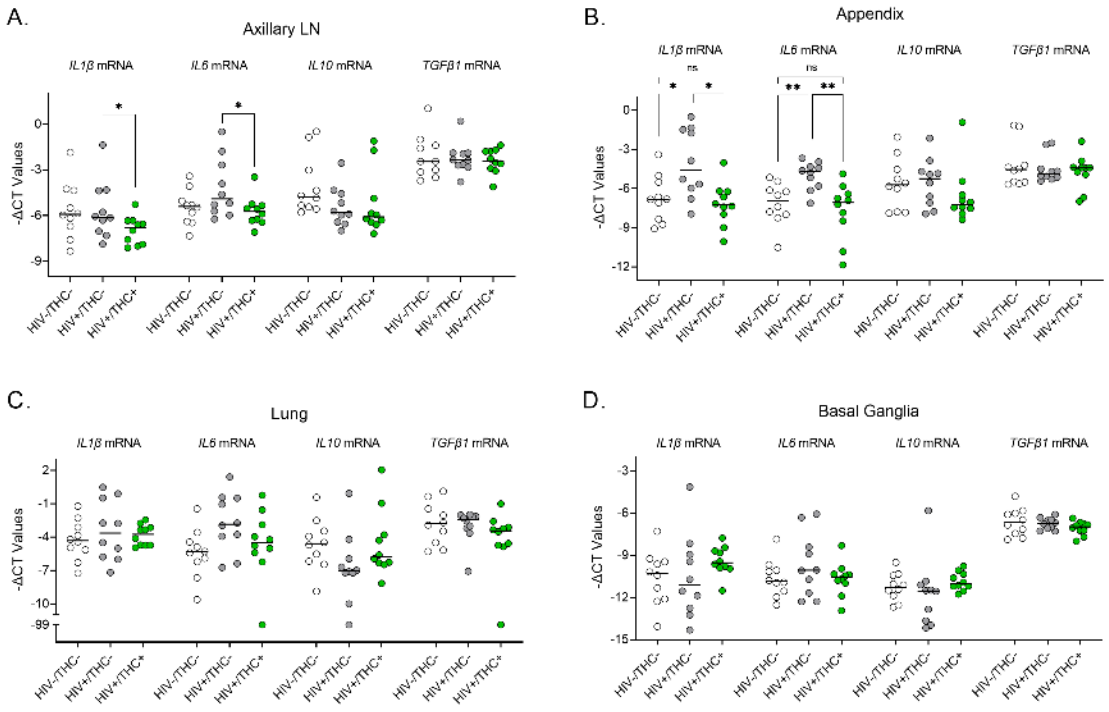

Figure 5.6. Transcription levels of inflammatory cytokines in subtype C HIV-1 tissue reservoirs between THC+ and THC- persons with suppressed pVL. The relative mRNA levels of pro-inflammatory cytokines IL1β and IL6, and anti-inflammatory cytokines IL10 and TGFβ1 were measured in axillary LN, appendix, lung, and basal ganglia among HIV-/THC-, HIV+/THC-, and HIV+/THC+ persons. (A) Significantly lower relative transcription levels of

pro-inflammatory cytokines IL1β and IL6 in axillary LN in HIV+/THC+ persons compared to HIV+/THC- persons ($p < 0.05$). (B) Lower relative mRNA levels of pro-inflammatory cytokines IL1β ($p < 0.05$) and IL6 ($p < 0.01$) in appendix tissues in HIV+/THC+ persons compared to HIV+/THC- persons. (C) There was no significant difference in inflammatory cytokine levels in lung tissues among the three groups. (D) No significant difference in cytokine levels was observed in basal ganglia between any groups. The mRNA level of GAPDH was used as internal reference. Each data point represents a single tissue. -ΔCT value was used to have a better visualization (a higher Y axes location reflect a higher relative mRNA level). Significance was labelled when and $p < 0.05$ (*) and $p < 0.01$ (**), and 'ns' means 'not significant'.

We also analyzed the cytokine mRNA levels in tissues (Lung and basal ganglia) with very low levels of viral DNA and RNA. We did not observe any significant differences in any cytokine mRNA in either tissue among the groups (**Figure 5.6C&D**). Taken together, these results indicated that cannabis use associated with reduced pro-inflammatory cytokine expression but did not alter anti-inflammatory cytokine expression in subtype C HIV-1 lymphoid tissue reservoirs that harbored most of proviruses.

Discussion

Despite the common use of cannabis by PLWH its potential effects on HIV-1 have not been extensively evaluated, even for subtype B HIV-1. Studies using blood samples from persons with subtype B HIV-1 showed that cannabis use is associated with lower pVLs (152), reduced frequency of activated immune cells (154), and accelerated viral DNA decay in peripheral blood mononuclear cells (PBMCs) (155). Whether cannabis use affect proviral DNA burden in parenchymal tissue reservoirs of people with subtype B HIV-1 requires further investigation. More importantly, whether cannabis use has any effects on non-B subtypes need to be explored. In this study we showed that the odds of tissue harboring subtype C HIV-1 DNA, and proviral burden in peripheral tissues were significantly lower in THC+ men with suppressed pVL when compared to THC- men

(Figures 3 and 4). Our findings suggest that cannabis use has a beneficial effect on reducing size and the distribution of subtype C HIV-1 tissue reservoirs in men with suppressed pVL.

At this point it is not clear whether any of our identified subtype C tissue reservoirs harbor replication-competent proviruses. However, we are not able to perform quantitative viral outgrowth assay (QVOA) (220-222, 316), or two-probe intact proviral DNA assay (IPDA) or near full length (nfl) Q4PCR (317, 318), to determine whether there are full length proviral DNA because of the postmortem tissue sampling and the low copies of detectable viral DNA in the tissues. Given that the majority (> 90%) of HIV-1 proviruses were shown to be defective in subtype B reservoirs (203, 319), it is likely a similar proportion of intact proviruses may exist in subtype C infected tissues.

Subtype B HIV-1 studies have shown that cannabis use associates with reduced inflammatory cytokine production in cerebrospinal fluid (CSF) and blood (320). Consistent with that, the proinflammatory cytokines IL1β and IL6 transcript levels in tissues with relatively high subtype C proviral DNA burden (axillary lymph node and appendix) was reduced in THC+ persons whereas anti-inflammatory cytokine expression was not differential. Our findings with subtype C HIV-1 tissue reservoirs suggest cannabinoid negative regulation of inflammatory mediators in tissues reservoirs without concomitant positive regulation of anti-inflammatory pathways. Previous studies have indicated that cannabinoids might modulate inflammatory responses via endocannabinoid system with interactions with NF-κB or toll-like receptor (TLR) pathways (321-323). The findings presented here suggest that the specific mechanisms may be involved in

cannabinoid modulation of inflammation in subtype C HIV-1 infection and will need further investigation.

One of the limitations in this study is the number of persons with suppressed pVL and with cannabis use available for postmortem sampling and comparison. We were readily able to identify and recruit THC+/HIV- persons but even though we have screened through 381 autopsied persons, we were only able to identify 29 deceased THC+/HIV+ persons, and only 10 of whom were virally suppressed (ART-treated aviremic). This is due to common practices in Zambia where health care providers encourage PLWH to cease drinking alcohol and smoking (including cannabis) due to their potential detrimental effects. Additionally, although all participants were autopsied within 48 hours of their deaths, there were variations of postmortem intervals among persons and possible degradation of nucleic acid. Nevertheless, our results clearly demonstrate significant differentials in subtype C HIV-1 tissue reservoirs with cannabis use in the cases analyzed. A further caveat of our study is that we were only able to identify people using cannabis by measuring the presence of THC metabolite in the deceased plasma using commercially available ELISA test. The test was not designed to be quantitative and can only provide a positive or negative result from recent cannabis use. We have been using it as confirmation of the report from next-of-kin. Similarly, given the limited resources we have on site we were not able to quantify the levels of cannabidiol (CBD) even though CBD was reported to have more significant anti-inflammatory effect than THC. Future similar study in a resource rich setting will be needed to confirm our observations. In addition, due to lack of computerized clinical documentation in Zambia, and linkage to HIV/ART databases, information such as time

since diagnosis of HIV infection, duration and adherence to ART treatment, were also not available.

In summary, our work demonstrates that cannabis use is associated with reduced distribution and size of subtype C HIV-1 reservoirs in men who received ART and achieved pVL suppression. Our findings also have clinical implications; cannabinoids could have therapeutic benefit in conjunction with ART to further reduce viral burden and inflammation in HIV-1 proviral tissue reservoirs and mitigate susceptibility to a variety of chronic inflammation-associated conditions that disproportionately impact PLWH. Our study also suggests that cannabis use should be further evaluated in the future randomized studies with larger PLWH cohorts to study its potential effects.

CHAPTER 6:

CONCLUDING REMARKS

The Joint United Nations Programme on HIV/AIDS (UNAIDS) has taken a lead on the HIV cure agenda to achieve its vision of zero new HIV infections, zero discrimination and zero AIDS-related deaths by 2030. However, substantial challenges still remain. First is the existence of HIV-1 reservoirs being a major hurdle for the cure of HIV-1 infection even with ART. Second, is the lack of information on other HIV-1 subtypes besides subtype B, which have presented challenges to our overall understanding of HIV-1 reservoirs and the development of effective cure strategies. Much of the knowledge on HIV-1 reservoirs accumulated has been on the subtype B because of the available of resources and infrastructure to conduct such HIV-1 studies in North America and Europe where this subtype is prevalent, and still little is known about HIV-1 reservoirs for other non-B subtypes, including the most widespread subtype C HIV-1. Consequently, the overall objectives of this dissertation research were to better understand subtype C HIV-1 reservoirs in virally suppressed PLWH and evaluate the impact of cannabis use on subtype C HIV-1 reservoirs. We hypothesize that the viral burden and distributions of the subtype C HIV-1 reservoirs are distinct from the subtype B's, and cannabis use associates with reduced size of the reservoirs.

Subtype C HIV-1 is predominant in resource-limited SSA and India, and accounts for approximately 47% of the global HIV-1 pandemic. A major challenge is the collection and analyses of biopsy tissues from PLWH in the resource limiting settings. Therefore, to accomplish the specific aim 1 of this study, which was to identify all potential subtype C HIV-1 tissue reservoirs in ART-treated aviremic individuals using autopsy cases, our

strategy was to collect post-mortem HIV-1 infected human specimens and conduct systematic molecular investigations in HIV-1 endemic area where subtype C HIV-1 is predominant in an effort to identify all potential subtype C HIV-1 reservoirs as described in Chapter 2. Our study represents the first detail characterization of subtype C HIV-1 tissue reservoirs via full body autopsies and systematic collections of tissues from ART-suppressed aviremic bodies, employing detailed characterization and molecular analyses of the postmortem tissues. The presence of subtype C HIV-1 proviral DNA varies significantly across different tissues, they were detected predominantly in the lymphoid and GI tract tissues but rarely detectable in the CNS. Interestingly, subtype C HIV-1 proviruses were readily detected in the appendix tissues, which has never been investigated and reported as an HIV-1 tissue reservoir. This discovery underscores the critical need for a comprehensive reservoir analysis and the need to develop HIV-1 subtype specific strategies to target potentially different reservoirs in PLWH infected with different HIV-1 subtypes. Future studies should also be conducted with a larger cohort of subtype C HIV-1 infected individuals to confirm our findings. In addition, given that more than 90% of subtype B HIV-1 proviruses were found to be defective, to determine whether it is similar for subtype C proviruses will require detection and analyses of full-length proviruses, and isolation of infectious viral particles from these tissue reservoirs, which unfortunately cannot be readily carried out with our autopsied tissues.

Our findings in Chapter 2 that human appendix might serve as a novel HIV-1 tissue reservoir, had accomplished part of the aim 2, which was to identify and characterize novel tissue reservoirs for subtype C HIV-1 infected ART treated aviremic individuals and determine the extent of infection and infected cell types in these tissue

reservoirs. To fully accomplish the aim 2, Chapter 3 extended the findings in Chapter 2 and further characterized the viral genetics and cellular tropism of the infected appendix tissues. The HIV-1 *env* DNA from both appendix and intestine-draining mesenteric LN tissues of aviremic PLWH were analyzed in parallel utilizing SGA. We observed substantial viral homogeneities within the appendix tissues when compared to LNs, which suggests that the appendix tissues can provide a unique tissue environment, possibly due to different immunological or therapeutic selective pressures. Further investigations utilizing single cell genomics and spatial multi-omics to evaluate the potential impact of the appendix's unique tissue environment for viral latency and reactivation, the interactions between infected or bystander FDCs and CD4+ T cells, as well as the role of gut associated microbiome perturbations and microbial translocation on the HIV-1 persisting in the appendix will be warranted.

The IF triple staining in this Chapter revealed that the FDCs are the most plausible cell lineage harboring subtype C HIV-1 whereas only a minor population of CD4+ T follicle helper cells and macrophages were found to be infected by subtype C HIV-1. Future studies, with single-cell RNA sequencing on FDCs and CD4+ T cells isolated from the appendix tissues or with spatial multi-omics on appendix tissues, should be conducted to uncover specific cellular mechanisms and molecular pathways that render FDCs more susceptible to subtype C HIV-1 infection in the appendix. The identification and characterization of this novel HIV-1 tissue and cellular reservoir for subtype C HIV-1 will need to be followed up with studies to determine whether the human appendix can also serve as reservoirs for other HIV-1 subtypes. Further investigation will also be needed to determine whether there are additional unrecognized

tissues reservoirs for different HIV-1 subtypes so that tailored therapeutic approaches can be developed to target those tissue reservoirs. At this point it is not clear whether the appendix tissues harbor any potential infectious proviral DNA even though there were detectable *env* genes in the appendix. Unfortunately, such analyses also will not be possible with autopsied tissues.

It has been well-documented that the brain could also be a crucial reservoir for subtype B HIV-1. The presence of HIV-1 in the brain in ART era poses dual risks to PLWH, as the brain serves not only as an important HIV tissue reservoir for viral reactivation, but infection of the brain can contribute to a spectrum of HAND, from asymptomatic neurocognitive impairment (ANI) to severe HAD or HIVE. The specific aim 3 of my dissertation research is to determine whether brain tissues can serve as HIV reservoir in subtype C infected individuals, and the extent of neuropathology, viral burden, CD8+ lymphocyte infiltration, and immune activation. However, our findings in Chapter 2 and Chapter 4 indicated that HIV proviral DNA was rarely detectable in the brain tissues for subtype C HIV-1, even in late-stage HIV disease individuals. This suggests that there could be differences in neurotropism between different HIV-1 subtypes, future characterization of HIV-1 reservoirs for these other subtypes, such as subtype A (the third most widespread which accounts for 10% of all infections), should be carried out in order to gain a better understanding of potential differences in HIV-1 reservoirs and tissue tropism of different HIV-1 subtypes. Moreover, the penetration efficacy of ART for the brain and other immune privileged sites, such as testicular tissue may play a crucial role in the persistence of HIV-1 reservoirs. These sites can harbor viral reservoirs that escape the full antiviral effects of ART, allowing HIV-1 to persist and

potentially rebound if therapy is interrupted. Future studies to understand the dynamics of ART penetration into these sites will be critical for developing strategies that can effectively target these hidden reservoirs and achieve a more comprehensive suppression of the virus.

Although studies with subtype B HIV-1 have suggested that proviruses in the brain are associated with physiological changes and immune activation accompanied with microgliosis and astrogliosis, the natural courses of neuropathogenesis of other HIV-1 subtypes, especially the most widespread subtype C in SSA, have not been adequately investigated. Thus, in Chapter 4, postmortem brain tissues from ART-naïve individuals with late-stage subtype C HIV-1 infection, and from uninfected normal controls were characterized for evaluating HIV-1 associated neuropathology. The comparative analysis utilizing H&E and IHC results demonstrated only limited neuropathology and brain immune activation (microgliosis or astrogliosis) associated with subtype C HIV-1 infection, which contrasts with the findings from late disease stage subtype B HIV-1 infected brain tissues. Our observations from this study not only broaden our understanding of subtype C HIV-1's impact on the CNS but also emphasizes that future subtype-specific studies on potential CNS pathogenesis will be needed. Moreover, future studies on the molecular and cellular mechanisms such as the role of cellular factors in contributing to the distinct neuropathological outcomes by different HIV-1 subtypes will be needed. Overall, the lack of neuropathogenesis coupled to apparent lack of CNS reservoirs have provided useful insights for strategies in curing subtype C infection and improving clinical management for PLWH in SSA.

While co-factors such as ART initiation timing, co-infections, and lifestyle choices (e.g., substance use, diet) have been investigated for their impacts on subtype B HIV-1 infection, most studies focused on their impact on host immune responses, ART efficacy, disease progression, and comorbidities. Their potential impacts on HIV-1 reservoirs have not been investigated. Cannabis use is increasingly prevalent in PLWH due to shifting legal and societal norms, and emerges as a critical co-factor in HIV-1 infection with its proposed immunomodulatory effects. To date, the effects of cannabis on HIV-1 have only been evaluated for subtype B infections and remained controversial. Few studies evaluated its impacts on HIV-1 cellular reservoirs in peripheral blood in vitro, but its impacts on parenchymal tissue reservoirs remain unexplored. The last aim of this study is to determine whether cannabis use impacts the size, distribution as well as inflammatory cytokine expression in subtype C HIV-1 reservoirs. In our ART-suppressed African cohort, we compared the distribution and viral burden in different subtype C HIV-1 tissue reservoirs between PWLH with and without cannabis use. Interestingly, our findings indicated that cannabis use is associated with reduced sizes of subtype C HIV-1 tissue reservoirs and the expression inflammatory cytokine in the tissues, and presented a compelling case for considering lifestyle factors in therapeutic strategy development. These findings not only provided support on medicinal cannabis use, but also has implications on its legalization and usage for PLWH. Future studies will be needed to understand the mechanism on how it can affect the HIV proviruses and latent tissue reservoirs, whether there are dosage effects of the cannabinoids (CBD or THC) on the HIV proviruses in different tissue reservoirs, such as in human appendix tissues. Future studies with more detailed information about cannabis use, including the frequency and

types of cannabis used, the route of cannabis consumption, should be done to evaluate whether it can be used as novel adjunct therapies to target and reduce HIV-1 persistence. Moreover, longitudinal studies assessing the long-term impact of cannabis use on HIV-1 progression and reservoir dynamics are also warranted. This could involve monitoring changes in reservoir dynamics over time relative to cannabis use patterns, ART adherence, and clinical outcomes.

Overall, this dissertation research has enhanced our understanding of subtype C HIV-1, particularly subtype C reservoirs, and the impact of cannabis use on these reservoirs. An interesting finding in this research is the identification of the appendix as a novel HIV-1 tissue reservoir. This finding highlights the importance for healthcare providers to look beyond the usual locations when managing HIV-1 infection. This knowledge encourages a more comprehensive approach to targeting viral persistence, beyond the traditionally recognized sites. Insights from this thesis, coupled with recent advances in technology such as advance imaging and molecular characterization techniques, single-cell RNA sequencing and spatial multi-omics will present powerful tools for further detail mapping of reservoir locations and quantifying viral RNA expression with unparalleled detail. These tools would help us to have a better understand about the distribution and dynamics of viral reservoirs, which is crucial for efforts to eliminate HIV from the body.

The research on how cannabis affects HIV-1 reservoirs also opens new pathways for both scientific study and healthcare. The findings in my dissertation research suggest that incorporating lifestyle choices, such as cannabis use, into HIV treatment plans could improve health outcomes for PLWH. This study also contributes to ongoing discussions

about the legal and medical use of cannabis, especially for PLWH. As policies around cannabis evolve, this research supports the need for policies based on solid evidence, considering both the potential benefits and risks of cannabis use in HIV-1 management.

While the present study has concentrated on the impact of cannabis use on HIV-1 reservoirs, a broader exploration of the roles of other co-factors is warranted. Future studies should consider a wide array of other factors that could influence HIV-1 reservoirs, including but not limited to other lifestyle factors (diet, alcohol use) and co-infections (HBV, TB, or HPV). Understanding the multifaceted interactions between these co-factors and ART, and their collective impact on reservoir dynamics, is crucial. This knowledge could drive the development of personalized treatment strategies, tailored to meet the specific needs and situations of PLWH.

In conclusion, this dissertation research has deepened our understanding of HIV-1 infection, particularly for subtype C, and laid the groundwork for new research and treatment strategies. By delving into the complexities of HIV-1 reservoirs and the impact of cannabis use, this dissertation paved the way for future innovative approaches on HIV/AIDS management, which ultimately will inch us closer to the ultimate goal of a cure for HIV-1 infection.

REFERENCES

1. Zhu T, Korber BT, Nahmias AJ, Hooper E, Sharp PM, and Ho DD. An African HIV-1 sequence from 1959 and implications for the origin of the epidemic. *Nature.* 1998;391(6667):594-7.
2. Centers for Disease C. Pneumocystis pneumonia--Los Angeles. *MMWR Morb Mortal Wkly Rep.* 1981;30(21):250-2.
3. Centers for Disease C. Kaposi's sarcoma and Pneumocystis pneumonia among homosexual men--New York City and California. *MMWR Morb Mortal Wkly Rep.* 1981;30(25):305-8.
4. Centers for Disease C. Update on acquired immune deficiency syndrome (AIDS)--United States. *MMWR Morb Mortal Wkly Rep.* 1982;31(37):507-8, 13-4.
5. Barre-Sinoussi F, Chermann JC, Rey F, Nugeyre MT, Chamaret S, Gruest J, et al. Isolation of a T-lymphotropic retrovirus from a patient at risk for acquired immune deficiency syndrome (AIDS). *Science.* 1983;220(4599):868-71.
6. Gallo RC, Salahuddin SZ, Popovic M, Shearer GM, Kaplan M, Haynes BF, et al. Frequent detection and isolation of cytopathic retroviruses (HTLV-III) from patients with AIDS and at risk for AIDS. *Science.* 1984;224(4648):500-3.
7. Popovic M, Sarngadharan MG, Read E, and Gallo RC. Detection, isolation, and continuous production of cytopathic retroviruses (HTLV-III) from patients with AIDS and pre-AIDS. *Science.* 1984;224(4648):497-500.
8. Sarngadharan MG, Popovic M, Bruch L, Schupbach J, and Gallo RC. Antibodies reactive with human T-lymphotropic retroviruses (HTLV-III) in the serum of patients with AIDS. *Science.* 1984;224(4648):506-8.
9. Schupbach J, Popovic M, Gilden RV, Gonda MA, Sarngadharan MG, and Gallo RC. Serological analysis of a subgroup of human T-lymphotropic retroviruses (HTLV-III) associated with AIDS. *Science.* 1984;224(4648):503-5.

10. Coffin J, Haase A, Levy JA, Montagnier L, Oroszlan S, Teich N, et al. Human immunodeficiency viruses. *Science.* 1986;232(4751):697.

11. Zhao G, Perilla JR, Yufenyuy EL, Meng X, Chen B, Ning J, et al. Mature HIV-1 capsid structure by cryo-electron microscopy and all-atom molecular dynamics. *Nature.* 2013;497(7451):643-6.

12. Payne D, Wadonda-Kabondo N, Wang A, Smith-Sreen J, Kabaghe A, Bello G, et al. Trends in HIV prevalence, incidence, and progress towards the UNAIDS 95-95-95 targets in Malawi among individuals aged 15-64 years: population-based HIV impact assessments, 2015-16 and 2020-21. *Lancet HIV.* 2023;10(9):e597-e605.

13. Disease GBD, Injury I, and Prevalence C. Global, regional, and national incidence, prevalence, and years lived with disability for 354 diseases and injuries for 195 countries and territories, 1990-2017: a systematic analysis for the Global Burden of Disease Study 2017. *Lancet.* 2018;392(10159):1789-858.

14. Dwyer-Lindgren L, Cork MA, Sligar A, Steuben KM, Wilson KF, Provost NR, et al. Mapping HIV prevalence in sub-Saharan Africa between 2000 and 2017. *Nature.* 2019;570(7760):189-+.

15. Williams A, Menon S, Crowe M, Agarwal N, Biccler J, Bbosa N, et al. Geographic and Population Distributions of Human Immunodeficiency Virus (HIV)-1 and HIV-2 Circulating Subtypes: A Systematic Literature Review and Meta-analysis (2010-2021). *J Infect Dis.* 2023;228(11):1583-91.

16. Peeters M, Piot P, and van der Groen G. Variability among HIV and SIV strains of African origin. *AIDS.* 1991;5 Suppl 1:S29-36.

17. Sharp PM, and Hahn BH. Origins of HIV and the AIDS pandemic. *Cold Spring Harb Perspect Med.* 2011;1(1):a006841.

18. Mourez T, Simon F, and Plantier JC. Non-M variants of human immunodeficiency virus type 1. *Clin Microbiol Rev.* 2013;26(3):448-61.

19. Olabode AS, Ng GT, Wade KE, Salnikov M, Grant HE, Dick DW, et al. Revisiting the recombinant history of HIV-1 group M with dynamic network community detection. *Proc Natl Acad Sci U S A.* 2022;119(19):e2108815119.

20. Visseaux B, Bertine M, Le Hingrat Q, Ferre V, Charpentier C, Collin F, et al. HIV-2 diversity displays two clades within group A with distinct geographical distribution and evolution. *Virus Evol.* 2021;7(1):veab024.

21. Drylewicz J, Matheron S, Lazaro E, Damond F, Bonnet F, Simon F, et al. Comparison of viro-immunological marker changes between HIV-1 and HIV-2-infected patients in France. *AIDS.* 2008;22(4):457-68.

22. Carvalho AC, Valadas E, Franca L, Carvalho C, Aleixo MJ, Mendez J, et al. Population mobility and the changing epidemics of HIV-2 in Portugal. *HIV Med.* 2012;13(4):219-25.

23. Nyamweya S, Hegedus A, Jaye A, Rowland-Jones S, Flanagan KL, and Macallan DC. Comparing HIV-1 and HIV-2 infection: Lessons for viral immunopathogenesis. *Rev Med Virol.* 2013;23(4):221-40.

24. Korber B, Muldoon M, Theiler J, Gao F, Gupta R, Lapedes A, et al. Timing the ancestor of the HIV-1 pandemic strains. *Science.* 2000;288(5472):1789-96.

25. Worobey M, Gemmel M, Teuwen DE, Haselkorn T, Kunstman K, Bunce M, et al. Direct evidence of extensive diversity of HIV-1 in Kinshasa by 1960. *Nature.* 2008;455(7213):661-4.

26. Hemelaar J, Elangovan R, Yun J, Dickson-Tetteh L, Fleminger I, Kirtley S, et al. Global and regional molecular epidemiology of HIV-1, 1990-2015: a systematic review, global survey, and trend analysis. *Lancet Infect Dis.* 2019;19(2):143-55.

27. Desire N, Cerutti L, Le Hingrat Q, Perrier M, Emler S, Calvez V, et al. Characterization update of HIV-1 M subtypes diversity and proposal for subtypes A and D sub-subtypes reclassification. *Retrovirology.* 2018;15(1):80.

28. Frankel AD, and Young JA. HIV-1: fifteen proteins and an RNA. *Annu Rev Biochem.* 1998;67:1-25.

29. Naghavi MH, Schwartz S, Sonnerborg A, and Vahlne A. Long terminal repeat promoter/enhancer activity of different subtypes of HIV type 1. *AIDS Res Hum Retroviruses.* 1999;15(14):1293-303.

30. Brown PH, Tiley LS, and Cullen BR. Efficient Polyadenylation within the Human-Immunodeficiency-Virus Type-1 Long Terminal Repeat Requires Flanking U3-Specific Sequences. *J Virol.* 1991;65(6):3340-3.

31. Klaver B, and Berkhout B. Comparison of 5' and 3' Long Terminal Repeat Promoter Function in Human-Immunodeficiency-Virus. *J Virol.* 1994;68(6):3830-40.

32. Vicenzi E, Dimitrov DS, Engelman A, Migone TS, Purcell DFJ, Leonard J, et al. An Integration-Defective U5 Deletion Mutant of Human-Immunodeficiency-Virus Type-1 Reverts by Eliminating Additional Long Terminal Repeat Sequences. *J Virol.* 1994;68(12):7879-90.

33. Dutilleul A, Rodari A, and Van Lint C. Depicting HIV-1 Transcriptional Mechanisms: A Summary of What We Know. *Viruses.* 2020;12(12).

34. Freed EO. HIV-1 assembly, release and maturation. *Nat Rev Microbiol.* 2015;13(8):484-96.

35. Rhee SY, Sankaran K, Varghese V, Winters MA, Hurt CB, Eron JJ, et al. HIV-1 Protease, Reverse Transcriptase, and Integrase Variation. *J Virol.* 2016;90(13):6058-70.

36. Bergeron L, Sullivan N, and Sodroski J. Target cell-specific determinants of membrane fusion within the human immunodeficiency virus type 1 gp120 third variable region and gp41 amino terminus. *J Virol.* 1992;66(4):2389-97.

37. Ali A, Mishra R, Kaur H, and Chandra Banerjea A. HIV-1 Tat: An update on transcriptional and non-transcriptional functions. *Biochimie.* 2021;190:24-35.

38. Li YL, Langley CA, Azumaya CM, Echeverria I, Chesarino NM, Emerman M, et al. The structural basis for HIV-1 Vif antagonism of human APOBEC3G. *Nature.* 2023;615(7953):728-33.

39. Waheed AA, Swiderski M, Khan A, Gitzen A, Majadly A, and Freed EO. The viral protein U (Vpu)-interacting host protein ATP6V0C down-regulates cell-surface expression of tetherin and thereby contributes to HIV-1 release. *J Biol Chem.* 2020;295(21):7327-40.

40. Khan H, Sumner RP, Rasaiyaah J, Tan CP, Rodriguez-Plata MT, Van Tulleken C, et al. HIV-1 Vpr antagonizes innate immune activation by targeting karyopherin-mediated NF-kappaB/IRF3 nuclear transport. *Elife.* 2020;9.

41. Geyer M, Fackler OT, and Peterlin BM. Structure--function relationships in HIV-1 Nef. *EMBO Rep.* 2001;2(7):580-5.

42. Spach DH, Wood BR, Karpenko A, Unruh KT, Kinney RG, Roscoe C, et al. Creating a National HIV Curriculum. *J Assoc Nurses AIDS Care.* 2016;27(3):261-73.

43. Larsen KP, Mathiharan YK, Kappel K, Coey AT, Chen DH, Barrero D, et al. Architecture of an HIV-1 reverse transcriptase initiation complex. *Nature.* 2018;557(7703):118-22.

44. Kuniholm J, Coote C, and Henderson AJ. Defective HIV-1 genomes and their potential impact on HIV pathogenesis. *Retrovirology.* 2022;19(1).

45. Sabo Y, Walsh D, Barry DS, Tinaztepe S, de Los Santos K, Goff SP, et al. HIV-1 induces the formation of stable microtubules to enhance early infection. *Cell Host Microbe.* 2013;14(5):535-46.

46. Dharan A, and Campbell EM. Role of Microtubules and Microtubule-Associated Proteins in HIV-1 Infection. *J Virol.* 2018;92(16).

47. Pawlica P, and Berthoux L. Cytoplasmic dynein promotes HIV-1 uncoating. *Viruses.* 2014;6(11):4195-211.

48. Carnes SK, Zhou J, and Aiken C. HIV-1 Engages a Dynein-Dynactin-BICD2 Complex for Infection and Transport to the Nucleus. *J Virol.* 2018;92(20).

49. Xue GG, Yu HJ, Buffone C, Huang SW, Lee K, Goh SL, et al. The HIV-1 capsid core is an opportunistic nuclear import receptor. *Nat Commun.* 2023;14(1).

50. Fu LR, Weiskopf EN, Akkermans O, Swanson NA, Cheng SY, Schwartz TU, et al. HIV-1 capsids enter the FG phase of nuclear pores like a transport receptor. *Nature.* 2024;626(8000).

51. Müller TG, Zila V, Peters K, Schifferdecker S, Stanic M, Lucic B, et al. HIV-1 uncoating by release of viral cDNA from capsid-like structures in the nucleus of infected cells. *Elife.* 2021;10.

52. Astiazaran P, Bueno MTD, Morales E, Kugelman JR, Garcia-Rivera JA, and Llano M. HIV-1 integrase modulates the interaction of the HIV-1 cellular cofactor LEDGF/p75 with chromatin. *Retrovirology.* 2011;8.

53. Vansant G, Chen HC, Zorita E, Trejbalova K, Miklik D, Filion G, et al. The chromatin landscape at the HIV-1 provirus integration site determines viral expression. *Nucleic Acids Res.* 2020;48(14):7801-17.

54. Patro SC, Brandt LD, Bale MJ, Halvas EK, Joseph KW, Shao W, et al. Combined HIV-1 sequence and integration site analysis informs viral dynamics and allows reconstruction of replicating viral ancestors. *Proc Natl Acad Sci U S A.* 2019;116(51):25891-9.

55. Imamichi H, Smith M, Adelsberger JW, Izumi T, Scrimieri F, Sherman BT, et al. Defective HIV-1 proviruses produce viral proteins. *Proc Natl Acad Sci U S A.* 2020;117(7):3704-10.

56. Li C, Mori LP, Lyu S, Bronson R, Getzler AJ, Pipkin ME, et al. The chaperone protein p32 stabilizes HIV-1 Tat and strengthens the p-TEFb/RNAPII/TAR complex promoting HIV transcription elongation. *Proc Natl Acad Sci U S A.* 2023;120(1):e2217476120.

57. Emery A, and Swanstrom R. HIV-1: To Splice or Not to Splice, That Is the Question. *Viruses.* 2021;13(2).

58. Malim MH, Hauber J, Le SY, Maizel JV, and Cullen BR. The HIV-1 rev trans-activator acts through a structured target sequence to activate nuclear export of unspliced viral mRNA. *Nature.* 1989;338(6212):254-7.

59. Nikolaitchik OA, and Hu WS. Deciphering the role of the Gag-Pol ribosomal frameshift signal in HIV-1 RNA genome packaging. *J Virol.* 2014;88(8):4040-6.

60. Jacks T, Power MD, Masiarz FR, Luciw PA, Barr PJ, and Varmus HE. Characterization of ribosomal frameshifting in HIV-1 gag-pol expression. *Nature.* 1988;331(6153):280-3.

61. Lerner G, Weaver N, Anokhin B, and Spearman P. Advances in HIV-1 Assembly. *Viruses.* 2022;14(3).

62. Johnson DS, Bleck M, and Simon SM. Timing of ESCRT-III protein recruitment and membrane scission during HIV-1 assembly. *Elife.* 2018;7.

63. Tough RH, and McLaren PJ. Interaction of the Host and Viral Genome and Their Influence on HIV Disease. *Front Genet.* 2018;9:720.

64. Burger H, and Hoover D. HIV-1 tropism, disease progression, and clinical management. *J Infect Dis.* 2008;198(8):1095-7.

65. Cohen MS, Shaw GM, McMichael AJ, and Haynes BF. Acute HIV-1 Infection. *N Engl J Med.* 2011;364(20):1943-54.

66. Lange CG, Lederman MM, Medvik K, Asaad R, Wild M, Kalayjian R, et al. Nadir CD4+ T-cell count and numbers of CD28+ CD4+ T-cells predict functional responses to immunizations in chronic HIV-1 infection. *AIDS.* 2003;17(14):2015-23.

67. Lederman MM, and Margolis L. The lymph node in HIV pathogenesis. *Semin Immunol.* 2008;20(3):187-95.

68. Lee E, von Stockenstrom S, Morcilla V, Odevall L, Hiener B, Shao W, et al. Impact of Antiretroviral Therapy Duration on HIV-1 Infection of T Cells within Anatomic Sites. *J Virol.* 2020;94(3).

69. de Wolf F, Spijkerman I, Schellekens PT, Langendam M, Kuiken C, Bakker M, et al. AIDS prognosis based on HIV-1 RNA, CD4+ T-cell count and function: markers with reciprocal predictive value over time after seroconversion. *AIDS.* 1997;11(15):1799-806.

70. Stebbing J, Powles T, and Bower M. AIDS-associated Kaposi's sarcoma associated with a low viral load and a high CD4 cell count. *AIDS.* 2008;22(4):551-2.

71. Menendez-Arias L, and Delgado R. Update and latest advances in antiretroviral therapy. *Trends Pharmacol Sci.* 2022;43(1):16-29.

72. Yarchoan R, and Broder S. Development of antiretroviral therapy for the acquired immunodeficiency syndrome and related disorders. A progress report. *N Engl J Med.* 1987;316(9):557-64.

73. Stambuk D, Youle M, Hawkins D, Farthing C, Shanson D, Farmer R, et al. The efficacy and toxicity of azidothymidine (AZT) in the treatment of patients with AIDS and AIDS-related complex (ARC): an open uncontrolled treatment study. *Q J Med.* 1989;70(262):161-74.

74. De Simone C, Tzantzoglou S, Santini G, Vullo V, di Orio F, Leuter C, et al. Clinical and immunologic effects of combination therapy with intravenous immunoglobulins and AZT in HIV-infected patients. *Immunopharmacol Immunotoxicol.* 1991;13(3):447-58.

75. Drug cocktail restores partial immunity. *AIDS Alert.* 1997;12(4):48.

76. Schmit JC, and Weber B. Recent advances in antiretroviral therapy and HIV infection monitoring. *Intervirology.* 1997;40(5-6):304-21.

77. Langmann P, Klinker H, Schirmer D, Zilly M, Bienert A, and Richter E. High-performance liquid chromatographic method for the simultaneous determination of HIV-1

protease inhibitors indinavir, saquinavir and ritonavir in plasma of patients during highly active antiretroviral therapy. *J Chromatogr B Biomed Sci Appl.* 1999;735(1):41-50.

78. de Bethune MP. Non-nucleoside reverse transcriptase inhibitors (NNRTIs), their discovery, development, and use in the treatment of HIV-1 infection: a review of the last 20 years (1989-2009). *Antiviral Res.* 2010;85(1):75-90.
79. Dow DE, and Bartlett JA. Dolutegravir, the Second-Generation of Integrase Strand Transfer Inhibitors (INSTIs) for the Treatment of HIV. *Infect Dis Ther.* 2014;3(2):83-102.
80. Este JA, and Telenti A. HIV entry inhibitors. *Lancet.* 2007;370(9581):81-8.
81. Graham NM. Metabolic disorders among HIV-infected patients treated with protease inhibitors: a review. *J Acquir Immune Defic Syndr.* 2000;25 Suppl 1:S4-11.
82. Tsiodras S, Mantzoros C, Hammer S, and Samore M. Effects of protease inhibitors on hyperglycemia, hyperlipidemia, and lipodystrophy: a 5-year cohort study. *Arch Intern Med.* 2000;160(13):2050-6.
83. Kolakowska A, Maresca AF, Collins IJ, and Cailhol J. Update on Adverse Effects of HIV Integrase Inhibitors. *Curr Treat Options Infect Dis.* 2019;11(4):372-87.
84. Clutter DS, Jordan MR, Bertagnolio S, and Shafer RW. HIV-1 drug resistance and resistance testing. *Infect Genet Evol.* 2016;46:292-307.
85. Hemkens LG, and Bucher HC. HIV infection and cardiovascular disease. *Eur Heart J.* 2014;35(21):1373-81.
86. Dirajlal-Fargo S, and Funderburg N. HIV and cardiovascular disease: the role of inflammation. *Curr Opin HIV AIDS.* 2022;17(5):286-92.
87. Swanepoel CR, Atta MG, D'Agati VD, Estrella MM, Fogo AB, Naicker S, et al. Kidney disease in the setting of HIV infection: conclusions from a Kidney Disease: Improving Global Outcomes (KDIGO) Controversies Conference. *Kidney Int.* 2018;93(3):545-59.

88. Dominguez-Molina B, Leon A, Rodriguez C, Benito JM, Lopez-Galindez C, Garcia F, et al. Analysis of Non-AIDS-Defining Events in HIV Controllers. *Clin Infect Dis.* 2016;62(10):1304-9.

89. Cattelan AM, Mazzitelli M, Presa N, Cozzolino C, Sasset L, Leoni D, et al. Changing Prevalence of AIDS and Non-AIDS-Defining Cancers in an Incident Cohort of People Living with HIV over 28 Years. *Cancers (Basel).* 2023;16(1).

90. Wei F, Gaisa MM, D'Souza G, Xia N, Giuliano AR, Hawes SE, et al. Epidemiology of anal human papillomavirus infection and high-grade squamous intraepithelial lesions in 29 900 men according to HIV status, sexuality, and age: a collaborative pooled analysis of 64 studies. *Lancet HIV.* 2021;8(9):e531-e43.

91. Eggers C, Arendt G, Hahn K, Husstedt IW, Maschke M, Neuen-Jacob E, et al. HIV-1-associated neurocognitive disorder: epidemiology, pathogenesis, diagnosis, and treatment. *J Neurol.* 2017;264(8):1715-27.

92. Lamers SL, Rose R, Maidji E, Agsalda-Garcia M, Nolan DJ, Fogel GB, et al. HIV DNA Is Frequently Present within Pathologic Tissues Evaluated at Autopsy from Combined Antiretroviral Therapy-Treated Patients with Undetectable Viral Loads. *J Virol.* 2016;90(20):8968-83.

93. Donoso M, D'Amico D, Valdebenito S, Hernandez CA, Prideaux B, and Eugenin EA. Identification, Quantification, and Characterization of HIV-1 Reservoirs in the Human Brain. *Cells.* 2022;11(15).

94. Lu SM, Tremblay ME, King IL, Qi J, Reynolds HM, Marker DF, et al. HIV-1 Tat-induced microgliosis and synaptic damage via interactions between peripheral and central myeloid cells. *PLoS One.* 2011;6(9):e23915.

95. Liu X, Bae C, Gelman BB, Chung JM, and Tang SJ. A neuron-to-astrocyte Wnt5a signal governs astrogliosis during HIV-associated pain pathogenesis. *Brain.* 2022;145(11):4108-23.

96. Henderson LJ, Reoma LB, Kovacs JA, and Nath A. Advances toward Curing HIV-1 Infection in Tissue Reservoirs. *J Virol.* 2020;94(3).

97. Bitnun A, Ransy DG, Brophy J, Kakkar F, Hawkes M, Samson L, et al. Clinical Correlates of Human Immunodeficiency Virus-1 (HIV-1) DNA and Inducible HIV-1 RNA Reservoirs in Peripheral Blood in Children With Perinatally Acquired HIV-1 Infection With Sustained Virologic Suppression for at Least 5 Years. *Clin Infect Dis.* 2020;70(5):859-66.

98. Schnittman SM, Psallidopoulos MC, Lane HC, Thompson L, Baseler M, Massari F, et al. The reservoir for HIV-1 in human peripheral blood is a T cell that maintains expression of CD4. *Science.* 1989;245(4915):305-8.

99. Banga R, Procopio FA, Lana E, Gladkov GT, Roseto I, Parsons EM, et al. Lymph node dendritic cells harbor inducible replication-competent HIV despite years of suppressive ART. *Cell Host Microbe.* 2023;31(10):1714-31 e9.

100. Vibholm LK, Lorenzi JCC, Pai JA, Cohen YZ, Oliveira TY, Barton JP, et al. Characterization of Intact Proviruses in Blood and Lymph Node from HIV-Infected Individuals Undergoing Analytical Treatment Interruption. *J Virol.* 2019;93(8).

101. Zeng M, Southern PJ, Reilly CS, Beilman GJ, Chipman JG, Schacker TW, et al. Lymphoid tissue damage in HIV-1 infection depletes naive T cells and limits T cell reconstitution after antiretroviral therapy. *PLoS Pathog.* 2012;8(1):e1002437.

102. Hogan LE, Vasquez J, Hobbs KS, Hanhauser E, Aguilar-Rodriguez B, Hussien R, et al. Increased HIV-1 transcriptional activity and infectious burden in peripheral blood and gut-associated CD4+ T cells expressing CD30. *PLoS Pathog.* 2018;14(2):e1006856.

103. Ladinsky MS, Kieffer C, Olson G, Deruaz M, Vrbanac V, Tager AM, et al. Electron tomography of HIV-1 infection in gut-associated lymphoid tissue. *PLoS Pathog.* 2014;10(1):e1003899.

104. Imaz A, Tiraboschi JM, Niubo J, Martinez-Picado J, Cottrell ML, Domingo P, et al. Dynamics of the Decay of Human Immunodeficiency Virus (HIV) RNA and Distribution of Bictegravir in the Genital Tract and Rectum in Antiretroviral-naive Adults Living With HIV-1 Treated With Bictegravir/Emtricitabine/Tenofovir Alafenamide (Spanish HIV/AIDS Research Network, PreEC/RIS 58). *Clin Infect Dis.* 2021;73(7):e1991-e9.

105. Chung HK, Hattler JB, Narola J, Babbar H, Cai Y, Abdel-Mohsen M, et al. Development of Droplet Digital PCR-Based Assays to Quantify HIV Proviral and Integrated DNA in Brain Tissues from Viremic Individuals with Encephalitis and Virally Suppressed Aviremic Individuals. *Microbiol Spectr.* 2022;10(1):e0085321.

106. Gabuzda D, Yin J, Misra V, Chettimada S, and Gelman BB. Intact Proviral DNA Analysis of the Brain Viral Reservoir and Relationship to Neuroinflammation in People with HIV on Suppressive Antiretroviral Therapy. *Viruses.* 2023;15(4).

107. Oliveira MF, Pankow A, Vollbrecht T, Kumar NM, Cabalero G, Ignacio C, et al. Evaluation of Archival HIV DNA in Brain and Lymphoid Tissues. *J Virol.* 2023;97(6):e0054323.

108. Ganor Y, Real F, Sennepin A, Dutertre CA, Prevedel L, Xu L, et al. HIV-1 reservoirs in urethral macrophages of patients under suppressive antiretroviral therapy. *Nat Microbiol.* 2019;4(4):633-44.

109. Kandathil AJ, Sugawara S, Goyal A, Durand CM, Quinn J, Sachithanandham J, et al. No recovery of replication-competent HIV-1 from human liver macrophages. *J Clin Invest.* 2018;128(10):4501-9.

110. Costiniuk CT, Salahuddin S, Farnos O, Olivenstein R, Pagliuzza A, Orlova M, et al. HIV persistence in mucosal CD4+ T cells within the lungs of adults receiving long-term suppressive antiretroviral therapy. *AIDS.* 2018;32(16):2279-89.

111. Hughes K, Akturk G, Gnjatic S, Chen B, Klotman M, and Blasi M. Proliferation of HIV-infected renal epithelial cells following virus acquisition from infected macrophages. *Aids.* 2020;34(11):1581-91.

112. Chaillon A, Gianella S, Dellicour S, Rawlings SA, Schlub TE, De Oliveira MF, et al. HIV persists throughout deep tissues with repopulation from multiple anatomical sources. *J Clin Invest.* 2020;130(4):1699-712.

113. Smith DM, Kingery JD, Wong JK, Ignacio CC, Richman DD, and Little SJ. The prostate as a reservoir for HIV-1. *Aids.* 2004;18(11):1600-2.

114. Couturier J, Suliburk JW, Brown JM, Luke DJ, Agarwal N, Yu X, et al. Human adipose tissue as a reservoir for memory CD4+ T cells and HIV. *AIDS.* 2015;29(6):667-74.

115. Gantner P, Buranapraditkun S, Pagliuzza A, Dufour C, Pardons M, Mitchell JL, et al. HIV rapidly targets a diverse pool of CD4+T cells to establish productive and latent infections. *Immunity.* 2023;56(3):653-+.

116. Morcilla V, Bacchus-Souffan C, Fisher K, Horsburgh BA, Hiener B, Wang XQ, et al. HIV-1 Genomes Are Enriched in Memory CD4+ T Cells with Short Half-Lives. *Mbio.* 2021;12(5).

117. Tang YY, Chaillon A, Gianella S, Wong LM, Li DJ, Simermeyer TL, et al. Brain microglia serve as a persistent HIV reservoir despite durable antiretroviral therapy. *J Clin Invest.* 2023;133(12).

118. Lu F, Zankharia U, Vladimirova O, Yi YJ, Collman RG, and Lieberman PM. Epigenetic Landscape of HIV-1 Infection in Primary Human Macrophage. *J Virol.* 2022;96(7).

119. Dickey LL, Martins LJ, Planelles V, and Hanley TM. HIV-1-induced type I IFNs promote viral latency in macrophages. *J Leukocyte Biol.* 2022;112(5):1343-56.

120. Pena-Cruz V, Agosto LM, Akiyama H, Olson A, Moreau Y, Larrieux JR, et al. HIV-1 replicates and persists in vaginal epithelial dendritic cells. *J Clin Invest.* 2018;128(8):3439-44.

121. Hsia K, Tsai V, Zvaifler NJ, and Spector SA. Low-Prevalence of Hiv-1 Proviral DNA in Peripheral-Blood Monocytes and Dendritic Cells from Hiv-1-Infected Individuals. *Aids.* 1995;9(4):398-9.

122. Hiener B, Horsburgh BA, Eden JS, Barton K, Schlub TE, Lee E, et al. Identification of Genetically Intact HIV-1 Proviruses in Specific CD4(+) T Cells from Effectively Treated Participants. *Cell Rep.* 2017;21(3):813-22.

123. Kim Y, Anderson JL, and Lewin SR. Getting the "Kill" into "Shock and Kill": Strategies to Eliminate Latent HIV. *Cell Host Microbe.* 2018;23(1):14-26.

124. Yeh YJ, and Ho YC. Shock-and-kill versus block-and-lock: Targeting the fluctuating and heterogeneous HIV-1 gene expression. *Proc Natl Acad Sci U S A.* 2021;118(16).

125. Arcia D, Acevedo-Saenz L, Rugeles MT, and Velilla PA. Role of CD8(+) T Cells in the Selection of HIV-1 Immune Escape Mutations. *Viral Immunol.* 2017;30(1):3-12.

126. Yim LY, Lam KS, Luk TY, Mo Y, Lu X, Wang J, et al. Transforming Growth Factor beta Signaling Promotes HIV-1 Infection in Activated and Resting Memory CD4(+) T Cells. *J Virol.* 2023;97(5):e0027023.

127. Brumme ZL, Chopera DR, and Brockman MA. Modulation of HIV reservoirs by host HLA: bridging the gap between vaccine and cure. *Curr Opin Virol.* 2012;2(5):599-605.

128. Ananworanich J, Chomont N, Eller LA, Kroon E, Tovanabutra S, Bose M, et al. HIV DNA Set Point is Rapidly Established in Acute HIV Infection and Dramatically Reduced by Early ART. *EBioMedicine.* 2016;11:68-72.

129. Siliciano RF, and Greene WC. HIV latency. *Cold Spring Harb Perspect Med.* 2011;1(1):a007096.

130. Mohammadi A, Etemad B, Zhang X, Li Y, Bedwell GJ, Sharaf R, et al. Viral and host mediators of non-suppressible HIV-1 viremia. *Nat Med.* 2023;29(12):3212-23.

131. Olson A, Ragan EJ, Nakiyingi L, Lin N, Jacobson KR, Ellner JJ, et al. Brief Report: Pulmonary Tuberculosis Is Associated With Persistent Systemic Inflammation and

Decreased HIV-1 Reservoir Markers in Coinfected Ugandans. *J Acquir Immune Defic Syndr.* 2018;79(3):407-11.

132. Moreno E, Ron R, and Serrano-Villar S. The microbiota as a modulator of mucosal inflammation and HIV/HPV pathogenesis: From association to causation. *Front Immunol.* 2023;14:1072655.

133. Zerbato JM, Avihingsanon A, Singh KP, Zhao W, Deleage C, Rosen E, et al. HIV DNA persists in hepatocytes in people with HIV-hepatitis B co-infection on antiretroviral therapy. *EBioMedicine.* 2023;87:104391.

134. Langkilde A, Petersen J, Klausen HH, Henriksen JH, Eugen-Olsen J, and Andersen O. Inflammation in HIV-infected patients: impact of HIV, lifestyle, body composition, and demography - a cross sectional cohort study. *PLoS One.* 2012;7(12):e51698.

135. Riley ED, Kizer JR, Tien PC, Vittinghoff E, Lynch KL, Wu AHB, et al. Multiple substance use, inflammation and cardiac stretch in women living with HIV. *Drug Alcohol Depend.* 2022;238:109564.

136. Kirk GD, Astemborski J, Mehta SH, Ritter KD, Laird GM, Bordi R, et al. Nonstructured Treatment Interruptions Are Associated With Higher Human Immunodeficiency Virus Reservoir Size Measured by Intact Proviral DNA Assay in People Who Inject Drugs. *J Infect Dis.* 2021;223(11):1905-13.

137. Basukala B, Rossi S, Bendiks S, Gnatienko N, Patts G, Krupitsky E, et al. Virally Suppressed People Living with HIV Who Use Opioids Have Diminished Latency Reversal. *Viruses.* 2023;15(2).

138. Belete H, Mekonen T, Espinosa DC, Ambaw F, Connor J, Chan G, et al. Cannabis use in sub-Saharan Africa: A systematic review and meta-analysis. *Addiction.* 2023;118(7):1201-15.

139. Lee JT, Saag LA, Kipp AM, Logan J, Shepherd BE, Koethe JR, et al. Self-reported Cannabis Use and Changes in Body Mass Index, CD4 T-Cell Counts, and HIV-1 RNA Suppression in Treated Persons with HIV. *AIDS Behav.* 2020;24(4):1275-80.

140. Aletraris L, Graves BD, and Ndung'u JJ. Assessing the Impact of Recreational Cannabis Legalization on Cannabis Use Disorder and Admissions to Treatment in the United States. *Curr Addict Rep.* 2023;10(2):198-209.

141. Carvalho AF, Stubbs B, Vancampfort D, Kloiber S, Maes M, Firth J, et al. Cannabis use and suicide attempts among 86,254 adolescents aged 12-15 years from 21 low- and middle-income countries. *Eur Psychiatry.* 2019;56:8-13.

142. Patel SM, Thames AD, Arbid N, Panos SE, Castellon S, and Hinkin CH. The aggregate effects of multiple comorbid risk factors on cognition among HIV-infected individuals. *J Clin Exp Neuropsychol.* 2013;35(4):421-34.

143. Lorkiewicz SA, Ventura AS, Heeren TC, Winter MR, Walley AY, Sullivan M, et al. Lifetime marijuana and alcohol use, and cognitive dysfunction in people with human immunodeficiency virus infection. *Subst Abus.* 2018;39(1):116-23.

144. Manthey J, Freeman TP, Kilian C, Lopez-Pelayo H, and Rehm J. Public health monitoring of cannabis use in Europe: prevalence of use, cannabis potency, and treatment rates. *Lancet Reg Health Eur.* 2021;10:100227.

145. Siziya S, Muula AS, Besa C, Babaniyi O, Songolo P, Kankiza N, et al. Cannabis use and its socio-demographic correlates among in-school adolescents in Zambia. *Ital J Pediatr.* 2013;39:13.

146. Haworth A. A preliminary report on self-reported drug use among students in Zambia. *Bull Narc.* 1982;34(3-4):45-60.

147. Kowalski AJ, Addo OY, Kramer MR, Martorell R, Norris SA, Waford RN, et al. Initial engagement and persistence of health risk behaviors through adolescence: longitudinal findings from urban South Africa. *BMC Pediatr.* 2021;21(1):31.

148. Rock EM, and Parker LA. Constituents of Cannabis Sativa. *Adv Exp Med Biol.* 2021;1264:1-13.

149. Okafor CN, Zhou Z, Burrell LE, 2nd, Kelso NE, Whitehead NE, Harman JS, et al. Marijuana use and viral suppression in persons receiving medical care for HIV-infection. *Am J Drug Alcohol Abuse.* 2017;43(1):103-10.

150. Lake S, Kerr T, Capler R, Shoveller J, Montaner J, and Milloy MJ. High-intensity cannabis use and HIV clinical outcomes among HIV-positive people who use illicit drugs in Vancouver, Canada. *Int J Drug Policy.* 2017;42:63-70.

151. Kipp AM, Rebeiro PF, Shepherd BE, Brinkley-Rubinstein L, Turner M, Bebawy S, et al. Daily Marijuana Use is Associated with Missed Clinic Appointments Among HIV-Infected Persons Engaged in HIV Care. *AIDS Behav.* 2017;21(7):1996-2004.

152. Milloy MJ, Marshall B, Kerr T, Richardson L, Hogg R, Guillemi S, et al. High-intensity cannabis use associated with lower plasma human immunodeficiency virus-1 RNA viral load among recently infected people who use injection drugs. *Drug Alcohol Rev.* 2015;34(2):135-40.

153. Amedee AM, Nichols WA, LeCapitaine NJ, Stouwe CV, Birke LL, Lacour N, et al. Chronic Delta(9)-tetrahydrocannabinol administration may not attenuate simian immunodeficiency virus disease progression in female rhesus macaques. *AIDS Res Hum Retroviruses.* 2014;30(12):1216-25.

154. Manuzak JA, Gott TM, Kirkwood JS, Coronado E, Hensley-McBain T, Miller C, et al. Heavy Cannabis Use Associated With Reduction in Activated and Inflammatory Immune Cell Frequencies in Antiretroviral Therapy-Treated Human Immunodeficiency Virus-Infected Individuals. *Clin Infect Dis.* 2018;66(12):1872-82.

155. Chaillon A, Nakazawa M, Anderson C, Christensen-Quick A, Ellis RJ, Franklin D, et al. Effect of Cannabis Use on Human Immunodeficiency Virus DNA During Suppressive Antiretroviral Therapy. *Clin Infect Dis.* 2020;70(1):140-3.

156. Claiborne DT, Prince JL, Scully E, Macharia G, Micci L, Lawson B, et al. Replicative fitness of transmitted HIV-1 drives acute immune activation, proviral load in memory CD4+ T cells, and disease progression. *Proc Natl Acad Sci U S A.* 2015;112(12):E1480-9.

157. Archary D, Gordon ML, Green TN, Coovadia HM, Goulder PJ, and Ndung'u T. HIV-1 subtype C envelope characteristics associated with divergent rates of chronic disease progression. *Retrovirology.* 2010;7:92.

158. Coetzer M, Nedellec R, Cilliers T, Meyers T, Morris L, and Mosier DE. Extreme genetic divergence is required for coreceptor switching in HIV-1 subtype C. *J Acquir Immune Defic Syndr.* 2011;56(1):9-15.

159. Clifford DB, and Ances BM. HIV-associated neurocognitive disorder. *Lancet Infect Dis.* 2013;13(11):976-86.

160. Saylor D, Dickens AM, Sacktor N, Haughey N, Slusher B, Pletnikov M, et al. HIV-associated neurocognitive disorder--pathogenesis and prospects for treatment. *Nat Rev Neurol.* 2016;12(4):234-48.

161. Esser S, Helbig D, Hillen U, Dissemond J, and Grabbe S. Side effects of HIV therapy. *J Dtsch Dermatol Ges.* 2007;5(9):745-54.

162. Simon V, Ho DD, and Abdool Karim Q. HIV/AIDS epidemiology, pathogenesis, prevention, and treatment. *The Lancet.* 2006;368(9534):489-504.

163. Martinez-Bonet M, Puertas MC, Fortuny C, Ouchi D, Mellado MJ, Rojo P, et al. Establishment and Replenishment of the Viral Reservoir in Perinatally HIV-1-infected Children Initiating Very Early Antiretroviral Therapy. *Clin Infect Dis.* 2015;61(7):1169-78.

164. Osborne O, Peyravian N, Nair M, Daunert S, and Toborek M. The Paradox of HIV Blood-Brain Barrier Penetrance and Antiretroviral Drug Delivery Deficiencies. *Trends Neurosci.* 2020;43(9):695-708.

165. Jilg N, Hunt PW, and Gandhi RT. HIV DNA decay during antiretroviral therapy: lessons from a clinic-based cohort study. *AIDS.* 2018;32(15):2255-7.

166. Sgadari C, Monini P, Tripiciano A, Picconi O, Casabianca A, Orlandi C, et al. Continued Decay of HIV Proviral DNA Upon Vaccination With HIV-1 Tat of Subjects on Long-Term ART: An 8-Year Follow-Up Study. *Front Immunol.* 2019;10:233.

167. Besson GJ, Lalama CM, Bosch RJ, Gandhi RT, Bedison MA, Aga E, et al. HIV-1 DNA decay dynamics in blood during more than a decade of suppressive antiretroviral therapy. *Clin Infect Dis.* 2014;59(9):1312-21.

168. Liu PT, Keele BF, Abbink P, Mercado NB, Liu J, Bondzie EA, et al. Origin of rebound virus in chronically SIV-infected Rhesus monkeys following treatment discontinuation. *Nat Commun.* 2020;11(1):5412.

169. Kuo HH, Banga R, Lee GQ, Gao C, Cavassini M, Corpataux JM, et al. Blood and Lymph Node Dissemination of Clonal Genome-Intact Human Immunodeficiency Virus 1 DNA Sequences During Suppressive Antiretroviral Therapy. *J Infect Dis.* 2020;222(4):655-60.

170. McManus WR, Bale MJ, Spindler J, Wiegand A, Musick A, Patro SC, et al. HIV-1 in lymph nodes is maintained by cellular proliferation during antiretroviral therapy. *J Clin Invest.* 2019;129(11):4629-42.

171. Avalos CR, Abreu CM, Queen SE, Li M, Price S, Shirk EN, et al. Brain Macrophages in Simian Immunodeficiency Virus-Infected, Antiretroviral-Suppressed Macaques: a Functional Latent Reservoir. *Mbio.* 2017;8(4).

172. Hatziioannou T, Ambrose Z, Chung NP, Piatak M, Jr., Yuan F, Trubey CM, et al. A macaque model of HIV-1 infection. *Proc Natl Acad Sci U S A.* 2009;106(11):4425-9.

173. Dash PK, Kaminski R, Bella R, Su H, Mathews S, Ahooyi TM, et al. Sequential LASER ART and CRISPR Treatments Eliminate HIV-1 in a Subset of Infected Humanized Mice. *Nat Commun.* 2019;10(1):2753.

174. Honeycutt JB, Thayer WO, Baker CE, Ribeiro RM, Lada SM, Cao Y, et al. HIV persistence in tissue macrophages of humanized myeloid-only mice during antiretroviral therapy. *Nat Med.* 2017;23(5):638-43.

175. Pahar B, Kuebler D, Rasmussen T, Wang X, Srivastav SK, Das A, et al. Quantification of Viral RNA and DNA Positive Cells in Tissues From Simian Immunodeficiency Virus/Simian Human Immunodeficiency Virus Infected Controller and Progressor Rhesus Macaques. *Front Microbiol.* 2019;10:2933.

176. Bertrand L, Cho HJ, and Toborek M. Blood-brain barrier pericytes as a target for HIV-1 infection. *Brain.* 2019;142(3):502-11.

177. Abassi M, Morawski BM, Nakigozi G, Nakasujja N, Kong X, Meya DB, et al. Cerebrospinal fluid biomarkers and HIV-associated neurocognitive disorders in HIV-infected individuals in Rakai, Uganda. *J Neurovirol.* 2017;23(3):369-75.

178. Kelschenbach J, He H, Kim BH, Borjabad A, Gu CJ, Chao W, et al. Efficient Expression of HIV in Immunocompetent Mouse Brain Reveals a Novel Nonneurotoxic Viral Function in Hippocampal Synaptodendritic Injury and Memory Impairment. *Mbio.* 2019;10(4).

179. Leon-Rivera R, Veenstra M, Donoso M, Tell E, Eugenin EA, Morgello S, et al. Central Nervous System (CNS) Viral Seeding by Mature Monocytes and Potential Therapies To Reduce CNS Viral Reservoirs in the cART Era. *Mbio.* 2021;12(2).

180. Veenstra M, Leon-Rivera R, Li M, Gama L, Clements JE, and Berman JW. Mechanisms of CNS Viral Seeding by HIV(+) CD14(+) CD16(+) Monocytes: Establishment and Reseeding of Viral Reservoirs Contributing to HIV-Associated Neurocognitive Disorders. *Mbio.* 2017;8(5).

181. Folks TM, Kessler SW, Orenstein JM, Justement JS, Jaffe ES, and Fauci AS. Infection and replication of HIV-1 in purified progenitor cells of normal human bone marrow. *Science.* 1988;242(4880):919-22.

182. Ladinsky MS, Khamaikawin W, Jung Y, Lin S, Lam J, An DS, et al. Mechanisms of virus dissemination in bone marrow of HIV-1-infected humanized BLT mice. *Elife.* 2019;8.

183. Alexaki A, and Wigdahl B. HIV-1 infection of bone marrow hematopoietic progenitor cells and their role in trafficking and viral dissemination. *PLoS Pathog.* 2008;4(12):e1000215.

184. Sebastian NT, Zaikos TD, Terry V, Taschuk F, McNamara LA, Onafuwa-Nuga A, et al. CD4 is expressed on a heterogeneous subset of hematopoietic progenitors, which persistently harbor CXCR4 and CCR5-tropic HIV proviral genomes in vivo. *PLoS Pathog.* 2017;13(7):e1006509.

185. Costiniuk CT, and Jenabian MA. The lungs as anatomical reservoirs of HIV infection. *Rev Med Virol.* 2014;24(1):35-54.

186. Chaillon A, Gianella S, Dellicour S, Rawlings SA, Schlub TE, De Oliveira MF, et al. HIV persists throughout deep tissues with repopulation from multiple anatomical sources. *J Clin Invest.* 2020;130(4):1699-712.

187. Le Tortorec A, Satie AP, Denis H, Rioux-Leclercq N, Havard L, Ruffault A, et al. Human prostate supports more efficient replication of HIV-1 R5 than X4 strains ex vivo. *Retrovirology.* 2008;5:119.

188. Smith DM, Kingery JD, Wong JK, Ignacio CC, Richman DD, and Little SJ. The prostate as a reservoir for HIV-1. *AIDS.* 2004;18(11):1600-2.

189. Telwatte S, Lee S, Somsouk M, Hatano H, Baker C, Kaiser P, et al. Gut and blood differ in constitutive blocks to HIV transcription, suggesting tissue-specific differences in the mechanisms that govern HIV latency. *PLoS Pathog.* 2018;14(11):e1007357.

190. Gosselin A, Wiche Salinas TR, Planas D, Wacleche VS, Zhang Y, Fromentin R, et al. HIV persists in CCR6+CD4+ T cells from colon and blood during antiretroviral therapy. *AIDS.* 2017;31(1):35-48.

191. Darcis G, Coombs RW, and Van Lint C. Exploring the anatomical HIV reservoirs: role of the testicular tissue. *AIDS.* 2016;30(18):2891-3.

192. Pena-Cruz V, Agosto LM, Akiyama H, Olson A, Moreau Y, Larrieux JR, et al. HIV-1 replicates and persists in vaginal epithelial dendritic cells. *J Clin Invest.* 2018;128(8):3439-44.

193. Zhou Z, Barry de Longchamps N, Schmitt A, Zerbib M, Vacher-Lavenu MC, Bomsel M, et al. HIV-1 efficient entry in inner foreskin is mediated by elevated CCL5/RANTES that recruits T cells and fuels conjugate formation with Langerhans cells. *PLoS Pathog.* 2011;7(6):e1002100.

194. Damouche A, Lazure T, Avettand-Fenoel V, Huot N, Dejucq-Rainsford N, Satie AP, et al. Adipose Tissue Is a Neglected Viral Reservoir and an Inflammatory Site during Chronic HIV and SIV Infection. *PLoS Pathog.* 2015;11(9):e1005153.

195. Bertoldi A, D'Urbano V, Bon I, Verbon A, Rokx C, Boucher C, et al. Development of C-TILDA: A modified TILDA method for reservoir quantification in long term treated patients infected with subtype C HIV-1. *J Virol Methods.* 2020;276:113778.

196. Tso FY, Kang G, Kwon EH, Julius P, Li Q, West JT, et al. Brain is a potential sanctuary for subtype C HIV-1 irrespective of ART treatment outcome. *PLoS One.* 2018;13(7):e0201325.

197. Nakazwe C, Michelo C, Sandoy IF, and Fylkesnes K. Contrasting HIV prevalence trends among young women and men in Zambia in the past 12 years: data from demographic and health surveys 2002-2014. *BMC Infect Dis.* 2019;19(1):432.

198. Chanda-Kapata P, Kapata N, Klinkenberg E, William N, Mazyanga L, Musukwa K, et al. The adult prevalence of HIV in Zambia: results from a population based mobile testing survey conducted in 2013-2014. *AIDS Res Ther.* 2016;13:4.

199. Swamy M. UN agencies issue new guidelines for HIV testing. *HIV AIDS Policy Law Rev.* 2007;12(2-3):39-40.

200. Deleage C, Wietgrefe SW, Del Prete G, Morcock DR, Hao XP, Piatak M, Jr., et al. Defining HIV and SIV Reservoirs in Lymphoid Tissues. *Pathog Immun.* 2016;1(1):68-106.

201. Einkauf KB, Lee GQ, Gao C, Sharaf R, Sun X, Hua S, et al. Intact HIV-1 proviruses accumulate at distinct chromosomal positions during prolonged antiretroviral therapy. *J Clin Invest.* 2019;129(3):988-98.

202. Bruner KM, Wang Z, Simonetti FR, Bender AM, Kwon KJ, Sengupta S, et al. A quantitative approach for measuring the reservoir of latent HIV-1 proviruses. *Nature.* 2019;566(7742):120-5.

203. Bruner KM, Murray AJ, Pollack RA, Soliman MG, Laskey SB, Capoferri AA, et al. Defective proviruses rapidly accumulate during acute HIV-1 infection. *Nat Med.* 2016;22(9):1043-9.

204. Cattin A, Wiche Salinas TR, Gosselin A, Planas D, Shacklett B, Cohen EA, et al. HIV-1 is rarely detected in blood and colon myeloid cells during viral-suppressive antiretroviral therapy. *AIDS.* 2019;33(8):1293-306.

205. Abreu CM, Veenhuis RT, Avalos CR, Graham S, Queen SE, Shirk EN, et al. Infectious Virus Persists in CD4(+) T Cells and Macrophages in Antiretroviral Therapy-Suppressed Simian Immunodeficiency Virus-Infected Macaques. *J Virol.* 2019;93(15).

206. Lutgen V, Narasipura SD, Barbian HJ, Richards M, Wallace J, Razmpour R, et al. HIV infects astrocytes in vivo and egresses from the brain to the periphery. *PLoS Pathog.* 2020;16(6):e1008381.

207. Rahimy E, Li FY, Hagberg L, Fuchs D, Robertson K, Meyerhoff DJ, et al. Blood-Brain Barrier Disruption Is Initiated During Primary HIV Infection and Not Rapidly Altered by Antiretroviral Therapy. *J Infect Dis.* 2017;215(7):1132-40.

208. Shapshak P, Yoshioka M, Sun NC, Nelson SJ, Rhodes RH, Schiller P, et al. HIV-1 in postmortem brain tissue from patients with AIDS: a comparison of different detection techniques. *AIDS.* 1992;6(9):915-23.

209. Satishchandra P, Nalini A, Gourie-Devi M, Khanna N, Santosh V, Ravi V, et al. Profile of neurologic disorders associated with HIV/AIDS from Bangalore, south India (1989-96). *Indian J Med Res.* 2000;111:14-23.

210. Rao VR, Sas AR, Eugenin EA, Siddappa NB, Bimonte-Nelson H, Berman JW, et al. HIV-1 clade-specific differences in the induction of neuropathogenesis. *J Neurosci.* 2008;28(40):10010-6.

211. Santos da Silva E, Mulinge M, Lemaire M, Masquelier C, Beraud C, Rybicki A, et al. The Envelope Cytoplasmic Tail of HIV-1 Subtype C Contributes to Poor Replication Capacity through Low Viral Infectivity and Cell-to-Cell Transmission. *PLoS One.* 2016;11(9):e0161596.

212. He J, Chen Y, Farzan M, Choe H, Ohagen A, Gartner S, et al. CCR3 and CCR5 are co-receptors for HIV-1 infection of microglia. *Nature.* 1997;385(6617):645-9.

213. Proust A, Barat C, Leboeuf M, Drouin J, Gagnon MT, Vanasse F, et al. HIV-1 infection and latency-reversing agents bryostatin-1 and JQ1 disrupt amyloid beta homeostasis in human astrocytes. *Glia.* 2020;68(11):2212-27.

214. Wiley CA. Detection of HIV-1 DNA in microglia/macrophages, astrocytes and neurons isolated from brain tissue with HIV-1 encephalitis by laser capture microdissection. *Brain Pathol.* 2003;13(3):415; author reply -6.

215. Cadena AM, Ventura JD, Abbink P, Borducchi EN, Tuyishime H, Mercado NB, et al. Persistence of viral RNA in lymph nodes in ART-suppressed SIV/SHIV-infected Rhesus Macaques. *Nat Commun.* 2021;12(1):1474.

216. Gunthard HF, Havlir DV, Fiscus S, Zhang ZQ, Eron J, Mellors J, et al. Residual human immunodeficiency virus (HIV) Type 1 RNA and DNA in lymph nodes and HIV RNA in

genital secretions and in cerebrospinal fluid after suppression of viremia for 2 years. *J Infect Dis.* 2001;183(9):1318-27.

217. Kinloch NN, Ren Y, Conce Alberto WD, Dong W, Khadka P, Huang SH, et al. HIV-1 diversity considerations in the application of the Intact Proviral DNA Assay (IPDA). *Nat Commun.* 2021;12(1):165.

218. Simonetti FR, White JA, Tumiotto C, Ritter KD, Cai M, Gandhi RT, et al. Intact proviral DNA assay analysis of large cohorts of people with HIV provides a benchmark for the frequency and composition of persistent proviral DNA. *Proc Natl Acad Sci U S A.* 2020;117(31):18692-700.

219. Gaebler C, Falcinelli SD, Stoffel E, Read J, Murtagh R, Oliveira TY, et al. Sequence Evaluation and Comparative Analysis of Novel Assays for Intact Proviral HIV-1 DNA. *J Virol.* 2021;95(6).

220. Falcinelli SD, Kilpatrick KW, Read J, Murtagh R, Allard B, Ghofrani S, et al. Longitudinal Dynamics of Intact HIV Proviral DNA and Outgrowth Virus Frequencies in a Cohort of Individuals Receiving Antiretroviral Therapy. *J Infect Dis.* 2021;224(1):92-100.

221. Kiselinova M, De Spiegelaere W, Buzon MJ, Malatinkova E, Lichterfeld M, and Vandekerckhove L. Correction: Integrated and Total HIV-1 DNA Predict Ex Vivo Viral Outgrowth. *PLoS Pathog.* 2016;12(3):e1005532.

222. Prodger JL, Capoferri AA, Yu K, Lai J, Reynolds SJ, Kasule J, et al. Reduced HIV-1 latent reservoir outgrowth and distinct immune correlates among women in Rakai, Uganda. *JCI Insight.* 2020;5(14).

223. Schmitt K, and Akkina R. Ultra-Sensitive HIV-1 Latency Viral Outgrowth Assays Using Humanized Mice. *Front Immunol.* 2018;9:344.

224. Girard-Madoux MJH, Gomez de Aguero M, Ganal-Vonarburg SC, Mooser C, Belz GT, Macpherson AJ, et al. The immunological functions of the Appendix: An example of redundancy? *Semin Immunol.* 2018;36:31-44.

225. Crum-Cianflone N, Weekes J, and Bavaro M. Appendicitis in HIV-infected patients during the era of highly active antiretroviral therapy. *HIV Med.* 2008;9(6):421-6.

226. Schleimann MH, Leth S, Krarup AR, Mortensen J, Barstad B, Zaccarin M, et al. Acute Appendicitis as the Initial Clinical Presentation of Primary HIV-1 Infection. *Open Forum Infect Dis.* 2018;5(2):ofy006.

227. Klein DB, Hurley LB, Horberg MA, Silverberg MJ, Follansbee SE, Flamm JA, et al. Increased rates of appendicitis in HIV-infected men: 1991-2005. *J Acquir Immune Defic Syndr.* 2009;52(1):139-40.

228. Berger EA. Finding Fusin/CXCR4, the First "2nd Receptor" for HIV Entry. *Front Immunol.* 2015;6:283.

229. Tan Q, Zhu Y, Li J, Chen Z, Han GW, Kufareva I, et al. Structure of the CCR5 chemokine receptor-HIV entry inhibitor maraviroc complex. *Science.* 2013;341(6152):1387-90.

230. Ikeogu N, Ajibola O, Zayats R, and Murooka TT. Identifying physiological tissue niches that support the HIV reservoir in T cells. *Mbio.* 2023;14(5):e0205323.

231. Martinez-Roman P, Crespo-Bermejo C, Valle-Millares D, Lara-Aguilar V, Arca-Lafuente S, Martin-Carbonero L, et al. Dynamics of HIV Reservoir and HIV-1 Viral Splicing in HCV-Exposed Individuals after Elimination with DAAs or Spontaneous Clearance. *J Clin Med.* 2022;11(13).

232. Persaud D, Bryson Y, Nelson BS, Tierney C, Cotton MF, Coletti A, et al. HIV-1 reservoir size after neonatal antiretroviral therapy and the potential to evaluate antiretroviral-therapy-free remission (IMPAACT P1115): a phase 1/2 proof-of-concept study. *Lancet HIV.* 2024;11(1):e20-e30.

233. Burdorf R, Zhou S, Amon C, Long N, Hill CS, Adams L, et al. Impact Of Low-Frequency HIV-1 Drug Resistance Mutations On Antiretroviral Therapy Outcomes. *J Infect Dis.* 2024.

234. Fidler S, Stohr W, Pace M, Dorrell L, Lever A, Pett S, et al. Antiretroviral therapy alone versus antiretroviral therapy with a kick and kill approach, on measures of the HIV reservoir in participants with recent HIV infection (the RIVER trial): a phase 2, randomised trial. *Lancet.* 2020;395(10227):888-98.

235. Li JZ, Melberg M, Kittilson A, Abdel-Mohsen M, Li Y, Aga E, et al. Predictors of HIV rebound differ by timing of antiretroviral therapy initiation. *JCI Insight.* 2024;9(3).

236. Liuzzi G, D'Offizi G, Topino S, Zaccarelli M, Amendola A, Capobianchi MR, et al. Dynamics of viral load rebound in plasma and semen after stopping effective antiretroviral therapy. *AIDS.* 2003;17(7):1089-92.

237. Elangovan R, Jenks M, Yun J, Dickson-Tetteh L, Kirtley S, Hemelaar J, et al. Global and Regional Estimates for Subtype-Specific Therapeutic and Prophylactic HIV-1 Vaccines: A Modeling Study. *Front Microbiol.* 2021;12:690647.

238. Costiniuk CT, Salahuddin S, Farnos O, Olivenstein R, Pagliuzza AE, Orlova M, et al. HIV persistence in mucosal CD4+ T cells within the lungs of adults receiving long-term suppressive antiretroviral therapy. *Aids.* 2018;32(16):2279-89.

239. Liu Z, Julius P, Kang GB, West JT, and Wood C. Subtype C HIV-1 reservoirs throughout the body in ART-suppressed individuals. *Jci Insight.* 2022;7(20).

240. Liu Z, Julius P, Himwaze CM, Mucheleng'anga LA, Chapple AG, West JT, et al. Cannabis Use Associates With Reduced Proviral Burden and Inflammatory Cytokine in Tissues From Men With Clade C HIV-1 on Suppressive Antiretroviral Therapy. *Journal of Infectious Diseases.* 2024.

241. van Marle G, Gill MJ, Kolodka D, McManus L, Grant T, and Church DL. Compartmentalization of the gut viral reservoir in HIV-1 infected patients. *Retrovirology.* 2007;4.

242. Vellas C, Nayrac M, Collercandy N, Requena M, Jeanne N, Latour J, et al. Intact proviruses are enriched in the colon and associated with PD-1+TIGIT- mucosal CD4+ T cells of people with HIV-1 on antiretroviral therapy. *Ebiomedicine.* 2024;100.

243. Zalar A, Figueroa MI, Ruibal-Ares B, Baré P, Cahn P, de Bracco MMD, et al. Macrophage HIV-1 infection in duodenal tissue of patients on long term HAART. *Antivir Res.* 2010;87(2):269-71.

244. Horn C, Augustin M, Ercanoglu MS, Heger E, Knops E, Bondet V, et al. HIV DNA reservoir and elevated PD-1 expression of CD4 T-cell subsets particularly persist in the terminal ileum of HIV-positive patients despite cART. *Hiv Medicine.* 2021;22(5):397-408.

245. Avettand-Fenoel V, Hocqueloux L, Müller-Trutwin M, Prazuck T, Melard A, Chaix ML, et al. Greater Diversity of HIV DNA Variants in the Rectum Compared to Variants in the Blood in Patients Without HAART. *J Med Virol.* 2011;83(9):1499-507.

246. Galvez C, Urrea V, Garcia-Guerrero MDC, Bernal S, Benet S, Mothe B, et al. Altered T-cell subset distribution in the viral reservoir in HIV-1-infected individuals with extremely low proviral DNA (LoViReTs). *J Intern Med.* 2022;292(2):308-20.

247. Randal Bollinger R, Barbas AS, Bush EL, Lin SS, and Parker W. Biofilms in the large bowel suggest an apparent function of the human vermiform appendix. *J Theor Biol.* 2007;249(4):826-31.

248. Kooij IA, Sahami S, Meijer SL, Buskens CJ, and Te Velde AA. The immunology of the vermiform appendix: a review of the literature. *Clin Exp Immunol.* 2016;186(1):1-9.

249. Gebbers JO, and Laissue JA. Bacterial translocation in the normal human appendix parallels the development of the local immune system. *Ann N Y Acad Sci.* 2004;1029:337-43.

250. Morbe UM, Jorgensen PB, Fenton TM, von Burg N, Riis LB, Spencer J, et al. Human gut-associated lymphoid tissues (GALT); diversity, structure, and function. *Mucosal Immunol.* 2021;14(4):793-802.

251. Arjomand Fard N, Armstrong H, Perry T, and Wine E. Appendix and Ulcerative Colitis: a Key to Explaining the Pathogenesis and Directing Novel Therapies? *Inflamm Bowel Dis.* 2023;29(1):151-60.

252. Vitetta L. The vermiform cecal appendix, expendable or essential? A narrative review. *Curr Opin Gastroenterol.* 2022;38(6):570-6.

253. Liu Z, Julius P, Kang G, West JT, and Wood C. Subtype C HIV-1 reservoirs throughout the body in ART-suppressed individuals. *JCI Insight.* 2022;7(20).

254. Kanat BH, Solmaz OA, Bozdag P, Dogan S, Kutluer N, Kurt F, et al. Chronic appendicitis: the process from pre-diagnosis to pathology. *Eur Rev Med Pharmacol Sci.* 2021;25(24):7898-902.

255. McMyn NF, Varriale J, Fray EJ, Zitzmann C, MacLeod H, Lai J, et al. The latent reservoir of inducible, infectious HIV-1 does not decrease despite decades of antiretroviral therapy. *J Clin Invest.* 2023;133(17).

256. Keele BF, Tazi L, Gartner S, Liu Y, Burgon TB, Estes JD, et al. Characterization of the follicular dendritic cell reservoir of human immunodeficiency virus type 1. *J Virol.* 2008;82(11):5548-61.

257. Heesters BA, Lindqvist M, Vagefi PA, Scully EP, Schildberg FA, Altfeld M, et al. Follicular Dendritic Cells Retain Infectious HIV in Cycling Endosomes. *PLoS Pathog.* 2015;11(12):e1005285.

258. Dave RS, Jain P, and Byrareddy SN. Follicular Dendritic Cells of Lymph Nodes as Human Immunodeficiency Virus/Simian Immunodeficiency Virus Reservoirs and Insights on Cervical Lymph Node. *Front Immunol.* 2018;9:805.

259. Estes JD, Keele BF, Tenner-Racz K, Racz P, Redd MA, Thacker TC, et al. Follicular dendritic cell-mediated up-regulation of CXCR4 expression on CD4 T cells and HIV pathogenesis. *J Immunol.* 2002;169(5):2313-22.

260. Zhou X, Shapiro L, Fellingham G, Willardson BM, and Burton GF. HIV replication in CD4+ T lymphocytes in the presence and absence of follicular dendritic cells: inhibition of replication mediated by alpha-1-antitrypsin through altered IkappaBalpha ubiquitination. *J Immunol.* 2011;186(5):3148-55.

261. Nazli A, Chan O, Dobson-Belaire WN, Ouellet M, Tremblay MJ, Gray-Owen SD, et al. Exposure to HIV-1 directly impairs mucosal epithelial barrier integrity allowing microbial translocation. *PLoS Pathog.* 2010;6(4):e1000852.

262. Scully E, Lockhart A, Huang L, Robles Y, Becerril C, Romero-Tejeda M, et al. Elevated Levels of Microbial Translocation Markers and CCL2 Among Older HIV-1-Infected Men. *Journal of Infectious Diseases.* 2016;213(5):771-5.

263. Younas M, Psomas C, Reynes C, Cezar R, Kundura L, Portales P, et al. Microbial Translocation Is Linked to a Specific Immune Activation Profile in HIV-1-Infected Adults With Suppressed Viremia. *Frontiers in Immunology.* 2019;10.

264. Klein DB, Hurley LB, Horberg MA, Silverberg MJ, Follansbee SE, Flamm JA, et al. Increased Rates of Appendicitis in HIV-Infected Men: 1991-2005. *Jaids-J Acq Imm Def.* 2009;52(1):139-40.

265. Shiels MS, Landgren O, Costello R, Zingone A, Goedert JJ, and Engels EA. Free light chains and the risk of AIDS-defining opportunistic infections in HIV-infected individuals. *Clin Infect Dis.* 2012;55(10):e103-8.

266. Xie Y, Zhu J, Lan G, and Ruan Y. Benefits of early ART initiation on mortality among people with HIV. *Lancet HIV.* 2022;9(6):e377.

267. Kaufman R. ART and science of keeping HIV out of the blood supply. *Blood.* 2020;136(11):1223-4.

268. Kincer LP, Joseph SB, Gilleece MM, Hauser BM, Sizemore S, Zhou S, et al. Rebound HIV-1 in cerebrospinal fluid after antiviral therapy interruption is mainly clonally amplified R5 T cell-tropic virus. *Nat Microbiol.* 2023;8(2):260-71.

269. Bartsch YC, Loos C, Rossignol E, Fajnzylber JM, Yuan D, Avihingsanon A, et al. Viral Rebound Kinetics Correlate with Distinct HIV Antibody Features. *Mbio.* 2021;12(2).

270. Gianella S, Chaillon A, Chun TW, Sneller MC, Ignacio C, Vargas-Meneses MV, et al. HIV RNA Rebound in Seminal Plasma after Antiretroviral Treatment Interruption. *J Virol.* 2020;94(15).

271. Colby DJ, Trautmann L, Pinyakorn S, Leyre L, Pagliuzza A, Kroon E, et al. Rapid HIV RNA rebound after antiretroviral treatment interruption in persons durably suppressed in Fiebig I acute HIV infection. *Nat Med.* 2018;24(7):923-6.

272. Cochrane CR, Angelovich TA, Byrnes SJ, Waring E, Guanizo AC, Trollope GS, et al. Intact HIV Proviruses Persist in the Brain Despite Viral Suppression with ART. *Ann Neurol.* 2022;92(4):532-44.

273. Angelovich TA, Cochrane CR, Zhou J, Tumpach C, Byrnes SJ, Jamal Eddine J, et al. Regional Analysis of Intact and Defective HIV Proviruses in the Brain of Viremic and Virally Suppressed People with HIV. *Ann Neurol.* 2023;94(4):798-802.

274. Moonim MT, Alarcon L, Freeman J, Mahadeva U, van der Walt JD, and Lucas SB. Identifying HIV infection in diagnostic histopathology tissue samples--the role of HIV-1 p24 immunohistochemistry in identifying clinically unsuspected HIV infection: a 3-year analysis. *Histopathology.* 2010;56(4):530-41.

275. Rom S, Pacifici M, Passiatore G, Aprea S, Waligorska A, Del Valle L, et al. HIV-1 Tat binds to SH3 domains: cellular and viral outcome of Tat/Grb2 interaction. *Biochim Biophys Acta.* 2011;1813(10):1836-44.

276. Lamers SL, Rose R, Maidji E, Agsalda-Garcia M, Nolan DJ, Fogel GB, et al. HIV DNA Is Frequently Present within Pathologic Tissues Evaluated at Autopsy from Combined Antiretroviral Therapy-Treated Patients with Undetectable Viral Loads. *Journal of Virology.* 2016;90(20):8968-83.

277. Albalawi YA, Narasipura SD, Olivares LJ, and Al-Harthi L. CD4(dim) CD8(bright) T Cells Home to the Brain and Mediate HIV Neuroinvasion. *J Virol.* 2022;96(15):e0080422.

278. Suzuki K, Zaunders J, Gates TM, Levert A, Butterly S, Liu Z, et al. Elevation of cell-associated HIV-1 transcripts in CSF CD4+ T cells, despite effective antiretroviral therapy, is linked to brain injury. *Proc Natl Acad Sci U S A.* 2022;119(48):e2210584119.

279. Wu X, Liu L, Cheung KW, Wang H, Lu X, Cheung AK, et al. Brain Invasion by CD4(+) T Cells Infected with a Transmitted/Founder HIV-1BJZS7 During Acute Stage in Humanized Mice. *J Neuroimmune Pharmacol.* 2016;11(3):572-83.

280. Ko A, Kang G, Hattler JB, Galadima HI, Zhang J, Li Q, et al. Macrophages but not Astrocytes Harbor HIV DNA in the Brains of HIV-1-Infected Aviremic Individuals on Suppressive Antiretroviral Therapy. *J Neuroimmune Pharmacol.* 2019;14(1):110-9.

281. Boucher T, Liang SJ, and Brown AM. Advancing basic and translational research to deepen understanding of the molecular immune-mediated mechanisms regulating long-term persistence of HIV-1 in microglia in the adult human brain. *J Leukocyte Biol.* 2022;112(5):1223-31.

282. Thompson KA, Cherry CL, Bell JE, and McLean CA. Brain cell reservoirs of latent virus in presymptomatic HIV-infected individuals. *Am J Pathol.* 2011;179(4):1623-9.

283. Bertrand L, Cho HJ, and Toborek M. Blood-brain barrier pericytes as a target for HIV-1 infection. *Brain.* 2019;142:502-11.

284. Murray J, Meloni G, Cortes EP, KimSilva A, Jacobs M, Ramkissoon A, et al. Frontal lobe microglia, neurodegenerative protein accumulation, and cognitive function in people with HIV. *Acta Neuropathol Commun.* 2022;10(1):69.

285. Bade AN, Gorantla S, Dash PK, Makarov E, Sajja BR, Poluektova LY, et al. Manganese-Enhanced Magnetic Resonance Imaging Reflects Brain Pathology During Progressive HIV-1 Infection of Humanized Mice. *Mol Neurobiol.* 2016;53(5):3286-97.

286. O'Connor EE, Zeffiro TA, and Zeffiro TA. Brain Structural Changes following HIV Infection: Meta-Analysis. *AJNR Am J Neuroradiol.* 2018;39(1):54-62.

287. Subra C, and Trautmann L. Role of T Lymphocytes in HIV Neuropathogenesis. *Curr HIV/AIDS Rep.* 2019;16(3):236-43.

288. Sadagopal S, Lorey SL, Barnett L, Basham R, Lebo L, Erdem H, et al. Enhancement of human immunodeficiency virus (HIV)-specific CD8+ T cells in cerebrospinal fluid compared to those in blood among antiretroviral therapy-naive HIV-positive subjects. *J Virol.* 2008;82(21):10418-28.

289. Gray F, Lescure FX, Adle-Biassette H, Polivka M, Gallien S, Pialoux G, et al. Encephalitis with infiltration by CD8+ lymphocytes in HIV patients receiving combination antiretroviral treatment. *Brain Pathol.* 2013;23(5):525-33.

290. Sreeram S, Ye FC, Garcia-Mesa Y, Nguyen K, El Sayed A, Leskov K, et al. The potential role of HIV-1 latency in promoting neuroinflammation and HIV-1-associated neurocognitive disorder. *Trends Immunol.* 2022;43(8):630-9.

291. Hong SZ, and Banks WA. Role of the immune system in HIV-associated neuroinflammation and neurocognitive implications. *Brain Behav Immun.* 2015;45:1-12.

292. Del Valle L, and Pina-Oviedo S. HIV disorders of the brain: pathology and pathogenesis. *Front Biosci.* 2006;11:718-32.

293. Musumali J, Julius P, Siyumbwa SN, Yalcin D, Kang G, Munsaka S, et al. Systematic post-mortem analysis of brain tissue from an HIV-1 subtype C viremic decedent revealed a paucity of infection and pathology. *J Neurovirol.* 2022;28(4-6):527-36.

294. Liu Z, Julius P, Himwaze CM, Mucheleng'anga LA, Chapple AG, West JT, et al. Cannabis Use Associates With Reduced Proviral Burden and Inflammatory Cytokine in Tissues From Men With Clade C HIV-1 on Suppressive Antiretroviral Therapy. *J Infect Dis.* 2024.

295. Sturdevant CB, Joseph SB, Schnell G, Price RW, Swanstrom R, and Spudich S. Compartmentalized replication of R5 T cell-tropic HIV-1 in the central nervous system early in the course of infection. *PLoS Pathog.* 2015;11(3):e1004720.

296. Sharma V, Creegan M, Tokarev A, Hsu D, Slike BM, Sacdalan C, et al. Cerebrospinal fluid CD4+ T cell infection in humans and macaques during acute HIV-1 and SHIV infection. *PLoS Pathog.* 2021;17(12):e1010105.

297. Killingsworth L, and Spudich S. Neuropathogenesis of HIV-1: insights from across the spectrum of acute through long-term treated infection. *Semin Immunopathol.* 2022;44(5):709-24.

298. Banks WA, Freed EO, Wolf KM, Robinson SM, Franko M, and Kumar VB. Transport of human immunodeficiency virus type 1 pseudoviruses across the blood-brain barrier: Role of envelope proteins and adsorptive endocytosis. *J Virol.* 2001;75(10):4681-91.

299. Dohgu S, and Banks WA. Brain pericytes increase the lipopolysaccharide-enhanced transcytosis of HIV-1 free virus across the in vitro blood-brain barrier: evidence for cytokine-mediated pericyte-endothelial cell crosstalk. *Fluids Barriers CNS.* 2013;10(1):23.

300. Wang YH, Liu MX, Lu QD, Farrell M, Lappin JM, Shi J, et al. Global prevalence and burden of HIV-associated neurocognitive disorder A meta-analysis. *Neurology.* 2020;95(19):E2610-E21.

301. Mastrorosa I, Pinnetti C, Brita AC, Mondi A, Lorenzini P, Del Duca G, et al. Declining Prevalence of Human Immunodeficiency Virus (HIV)-Associated Neurocognitive Disorders in Recent Years and Associated Factors in a Large Cohort of Antiretroviral Therapy-Treated Individuals Living With HIV. *Clinical Infectious Diseases.* 2023;76(3):E629-E37.

302. Mishra M, Vetrivel S, Siddappa NB, Ranga U, and Seth P. Clade-specific differences in neurotoxicity of human immunodeficiency virus-1 B and C tat of human neurons: Significance of dicysteine C30C31 motif. *Annals of Neurology.* 2008;63(3):366-76.

303. Rao VR, Sas AR, Eugenin EA, Siddappa NB, Bimonte-Nelson H, Berman JW, et al. HIV-1 clade-specific differences in the induction of neuropathogenesis. *Journal of Neuroscience.* 2008;28(40):10010-6.

304. Riedel D, Ghate M, Nene M, Paranjape RS, Mehendale SM, Bollinger RC, et al. Screening for human immunodeficiency virus (HIV) dementia in an HIV clade C-infected population in India. *Journal of Neurovirology.* 2006;12(1):34-8.

305. Das Gupta J, Satishchandra P, Gopukumar K, Wilkie F, Waldrop-Valverde D, Ellis R, et al. Neuropsychological deficits in human immunodeficiency virus type 1 clade C-seropositive adults from South India. *Journal of Neurovirology.* 2007;13(3):195-202.

306. de Almeida SM, Ribeiro CE, de Pereira AP, Badiee J, Cherner M, Smith D, et al. Neurocognitive impairment in HIV-1 clade C-versus B-infected individuals in Southern Brazil. *Journal of Neurovirology.* 2013;19(6):550-6.

307. Weekes MP, Wills MR, Sissons JG, and Carmichael AJ. Large HIV-specific CD8 cytotoxic T-lymphocyte (CTL) clones reduce their overall size but maintain high frequencies of memory CTL following highly active antiretroviral therapy. *Immunology.* 2006;118(1):25-38.

308. Rall GF, Mucke L, and Oldstone MB. Consequences of cytotoxic T lymphocyte interaction with major histocompatibility complex class I-expressing neurons in vivo. *J Exp Med.* 1995;182(5):1201-12.

309. Zarkali A, Gorgoraptis N, Miller R, John L, Merve A, Thust S, et al. CD8+ encephalitis: a severe but treatable HIV-related acute encephalopathy. *Pract Neurol.* 2017;17(1):42-6.

310. Shenoy A, Marwaha PK, and Worku DA. CD8 Encephalitis in HIV: A Review of This Emerging Entity. *J Clin Med.* 2023;12(3).

311. Johnson LF, Keiser O, Fox MP, Tanser F, Cornell M, Hoffmann CJ, et al. Life expectancy trends in adults on antiretroviral treatment in South Africa. *AIDS.* 2016;30(16):2545-50.

312. Zhang L, Chung C, Hu BS, He T, Guo Y, Kim AJ, et al. Genetic characterization of rebounding HIV-1 after cessation of highly active antiretroviral therapy. *J Clin Invest.* 2000;106(7):839-45.

313. Lee GQ, Reddy K, Einkauf KB, Gounder K, Chevalier JM, Dong KL, et al. HIV-1 DNA sequence diversity and evolution during acute subtype C infection. *Nat Commun.* 2019;10(1):2737.

314. Yin L, Dinasarapu AR, Borkar SA, Chang KF, De Paris K, Kim-Chang JJ, et al. Anti-inflammatory effects of recreational marijuana in virally suppressed youth with HIV-1 are reversed by use of tobacco products in combination with marijuana. *Retrovirology.* 2022;19(1):10.

315. Parry C, Myers B, and Caulkins J. Decriminalisation of recreational cannabis in South Africa. *Lancet.* 2019;393(10183):1804-5.

316. Enick PN, Brooker JP, Tumiotto CM, Staines BT, Eron JJ, McMahon DK, et al. Comparison of methods to quantify inducible HIV-1 outgrowth. *J Virus Erad.* 2021;7(2):100043.

317. Reeves DB, Gaebler C, Oliveira TY, Peluso MJ, Schiffer JT, Cohn LB, et al. Impact of misclassified defective proviruses on HIV reservoir measurements. *Nat Commun.* 2023;14(1):4186.

318. White JA, Kufera JT, Bachmann N, Dai W, Simonetti FR, Armstrong C, et al. Measuring the latent reservoir for HIV-1: Quantification bias in near full-length genome sequencing methods. *PLoS Pathog.* 2022;18(9):e1010845.

319. Joseph KW, Halvas EK, Brandt LD, Patro SC, Rausch JW, Chopra A, et al. Deep Sequencing Analysis of Individual HIV-1 Proviruses Reveals Frequent Asymmetric Long Terminal Repeats. *J Virol.* 2022;96(13):e0012222.

320. Ellis RJ, Peterson SN, Li Y, Schrier R, Iudicello J, Letendre S, et al. Recent cannabis use in HIV is associated with reduced inflammatory markers in CSF and blood. *Neurol Neuroimmunol Neuroinflamm.* 2020;7(5).

321. Ali AM, El-Tawil OS, Al-Mokaddem AK, and Abd El-Rahman SS. Promoted inhibition of TLR4/miR-155/ NF(k)B p65 signaling by cannabinoid receptor 2 agonist (AM1241), aborts inflammation and progress of hepatic fibrosis induced by thioacetamide. *Chem Biol Interact.* 2021;336:109398.

322. Majdi F, Taheri F, Salehi P, Motaghinejad M, and Safari S. Cannabinoids Delta(9)-tetrahydrocannabinol and cannabidiol may be effective against methamphetamine induced mitochondrial dysfunction and inflammation by modulation of Toll-like type-4(Toll-like 4) receptors and NF-kappaB signaling. *Med Hypotheses.* 2019;133:109371.

323. Ma H, Xu F, Liu C, and Seeram NP. A Network Pharmacology Approach to Identify Potential Molecular Targets for Cannabidiol's Anti-Inflammatory Activity. *Cannabis Cannabinoid Res.* 2021;6(4):288-99.